AAS-JAKOBSEN COWI Multiconsult

JOHS HOLT AkerSolutions entail NGI DISSING+WEITLING architecture a|s mossmaritime

Concept development, floating bridge E39 Bjørnafjorden

Appendix S – Enclosure 1

0205546-11-NOT-092

Analysis of parametric resonance of single-degree-of-freedom systems using Newmark's method and Monte Carlo simulation

AAS-JAKOBSEN COWI Multiconsult

JOHS HOLT AkerSolutions entail NGI DISSING+WEITLING architecture a|s mossmaritime

MEMO

PROJECT	Concept development, floating bridge E39 Bjørnafjorden	DOCUMENT CODE	10205546-11-NOT-092
CLIENT	Statens vegvesen	ACCESSIBILITY	Restricted
SUBJECT	Analysis of parametric resonance of single-degree-of-freedom systems using Newmark's method and Monte Carlo simulation	PROJECT MANAGER	Svein Erik Jakobsen
TO	Statens vegvesen	PREPARED BY	Knut Andreas Kvåle
COPY TO		RESPONSIBLE UNIT	AMC

SUMMARY

This memo contains results from time simulations of simple systems and studies the simulations' efficacy with regard to detecting parametric resonance. The effect of quadratic drag damping is given particular attention. Monte Carlo simulations of stochastic processes are also briefly discussed.

The simulation scheme set up with Newmark's method is able to capture the parametric resonance (dynamic instability), when the system is exposed to harmonic parameter variation, and behaves in agreement with analytical models. Long durations are required to build up response from parametric resonance, both from harmonic and stochastic parameter variation. The stability of a quadratically damped system exposed to harmonic parameter variation is restored when the effective damping gives a new critical amplitude such that the response reaches a terminal maximum response. The simulated terminal response matches the analytically computed level.

The criterion to avoid the expected axial force amplitude to exceed the critical harmonic amplitude for all modes, suggested in the provided background material by the Norwegian Public Roads Administration/NTNU, is concerning the onset of parametric resonance. For certain modes, the damping contribution is dominated by nonlinear sources. Strictly, according to the background material, these damping contributions should not be included when assessing the onset of instability. This memo also aims to contribute to document the possibility of including nonlinear damping contributions in the assessment of parametric excitation.

1	24.05.2019	Final issue	K. A. Kvåle	R. M. Larssen	S. E. Jakobsen
0	29.03.2019	Status 2 issue	K. A. Kvåle	R. M. Larssen	S. E. Jakobsen
REV.	DATE	DESCRIPTION	PREPARED BY	CHECKED BY	APPROVED BY

Analysis of parametric resonance of single-degree-of-freedom systems using Newmark's method and Monte Carlo simulation

1 Mathematical interpretation of parametric resonance

A single-degree-of-freedom (SDOF) homogeneous mechanical system can be characterized by the following equation of motion:

$$\ddot{y} + 2\xi\omega_n\dot{y} + \left(\omega_n^2 + \frac{\hat{k}_g}{m}\cdot N(t)\right)y = \frac{p(t)}{m} \tag{1}$$

Here, y is the generalized response, ξ is the critical damping ratio, ω_n is the undamped natural frequency, $\hat{k}_g N(t)$ describe the generalized geometric stiffness due to a time-varying axial force $N(t)$, m is the modal mass, and $p(t) = 0$ is the external force. This second-order differential equation can be rewritten as two first-order differential equations by introducing $z_1 = y$ and $z_2 = \dot{y} = \frac{\partial y}{\partial t}$, as follows:

$$\begin{Bmatrix}\dot{z}_1\\ \dot{z}_2\end{Bmatrix} = \begin{bmatrix}0 & 1\\ -\left(\omega_n^2 + \frac{\hat{k}_g}{m}\cdot N(t)\right) & -2\xi\omega_n\end{bmatrix}\begin{Bmatrix}z_1\\ z_2\end{Bmatrix}$$

or, on compact form: $\{\dot{z}\} = [A(t)]\{z\}$. Assume that the system matrix $[A(t)]$ is a periodic matrix function of period T, such that $[A(t)] = [A(t+T)]$. A *fundamental matrix* is constructed [1][2], as follows:

$$[Z] = \begin{bmatrix}z_1 & \dot{z}_1\\ z_2 & \dot{z}_2\end{bmatrix}$$

such that the following matrix fully describes the system change over one period:

$$[B] = [Z(0)]^{-1}[Z(T)]$$

By letting $[Z(0)] = [I]$, this gives one convenient example of [B]:

$$[B] = \begin{bmatrix}z_1(T) & \dot{z}_1(T)\\ z_2(T) & \dot{z}_2(T)\end{bmatrix} \tag{2}$$

The eigenvalues of this matrix should be negative or zero for the system to be considered stable [1].

2 Newmark simulations to assess stability

2.1 Single-degree-of-freedom (generalized) system

An SDOF system is defined by the following parameters:

- $m = 5.82 \cdot 10^7$kg
- $\omega_n = 0.2412 rad/s$ ($T_n = 26.05s$)
- $\xi = 0.48\%$
- $\hat{k}_g = 0.0118 N/m/N$
- $c_{quad} = 916 kN/(m/s)$

The equation of motion is given in Equation 1, with axial force variation defined as $N(t) = Ncos(\omega t)$. c_{quad} is the quadratic damping, which is introduced to modify the equation of motion as follows:

$$\ddot{y} + 2\xi\omega_n\dot{y} + \frac{c_{quad}}{m}|\dot{y}|\dot{y} + \left(\omega_n^2 + \frac{\hat{k}_g}{m} \cdot N(t)\right) y = \frac{p(t)}{m}$$

The amplitude of N required to initiate parametric resonance for $\omega = 2\omega_n\sqrt{1-\xi^2}$ (twice the damped natural frequency), according to the criterion stated in [3], is $A_{cr} = \frac{4\xi k}{\hat{k}_g} = 5.45MN$. The system is exposed to axial force amplitude characterized by $N = \gamma A_{cr}$, such that γ represents the ratio of applied axial force amplitude to the critical axial force amplitude. To assess the validity of the analytical critical amplitude, simulations where the axial force amplitude is slightly below ($\gamma = 0.9$) and slightly above ($\gamma = 1.1$) the critical amplitude were conducted. Figure 1 and Figure 2 show that the Newmark's method (with linear acceleration configuration) is able to capture the phenomenon and pinpoint the amplitude where the onset of parametric excitation occurs. These simulations are both conducted with $p(t) = 0$ and an initial displacement of 1mm.

2.2 Consequence of exceeding the critical amplitude

The time required to build up energy from parametric resonance is dependent on the critical damping ratio ξ of the mode, if it is assumed that γ is kept constant. For a ratio of actual to critical amplitude of $\gamma = 2.0$, the resulting displacement with two different damping levels are shown in Figure 3. Both cases are initiated with 1 m displacement. The results seen in the figure implies that the consequence of exceeding the critical amplitude in a low damped mode is smaller than for a more damped mode. Note that this comparison is based on keeping the ratio of applied amplitude to critical amplitude constant; the absolute value of the critical amplitude is larger for the larger damped mode from $A_{cr} = \frac{4\xi k}{\hat{k}_g}$. This effect could be particularly useful in the interpretation of stochastic time simulations, that would render chaotic time series, as the lower damped modes will be more robust against temporarily exceedance of the critical amplitudes compared to higher damped modes. In essence, to capture the dynamic instability of modes with low damping and low natural frequency, long time simulations would be required for harmonic excitation. This is expected to cause very long-time simulations for more realistic (chaotic) excitation. Also, to capture the effect of parametric resonance in a stochastic framework relying on Monte Carlo simulations, very long simulation periods are needed for such cases.

Analysis of parametric resonance of single-degree-of-freedom systems using Newmark's method and Monte Carlo simulation

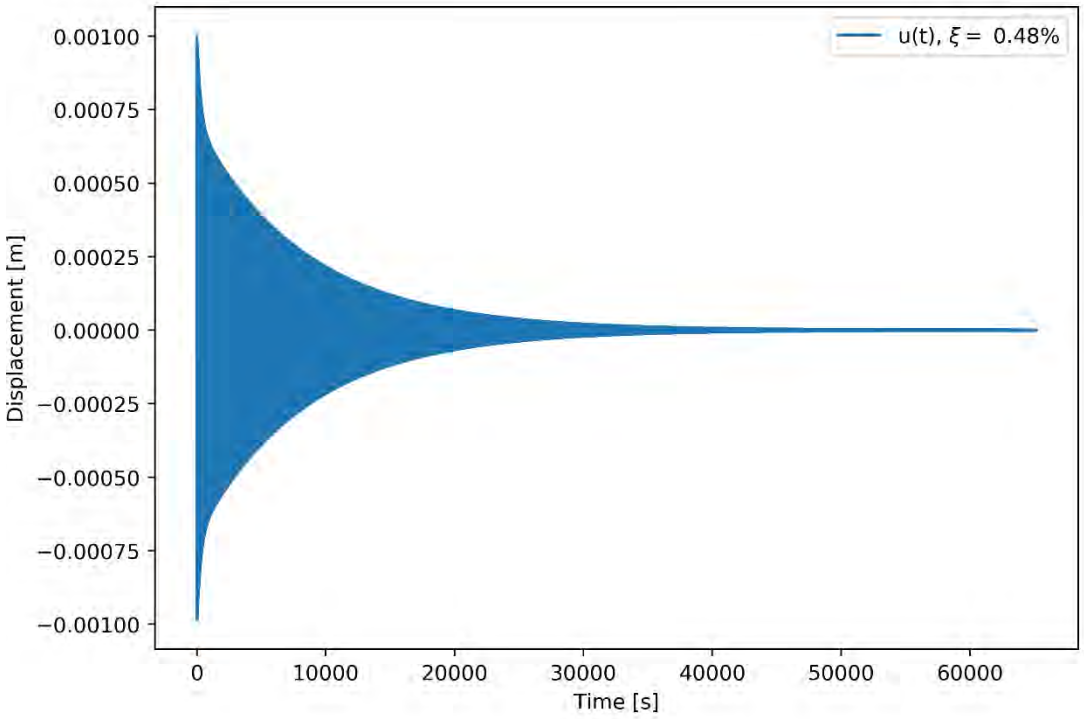

Figure 1. $N = 0.9A_{cr}$.

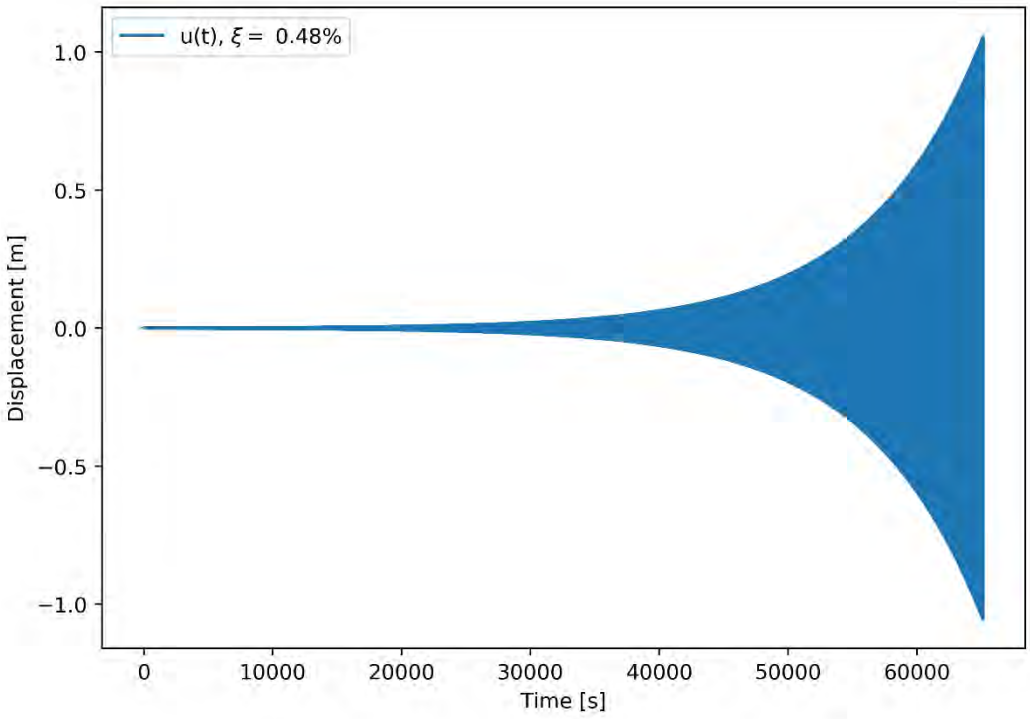

Figure 2. $N = 1.1A_{cr}$.

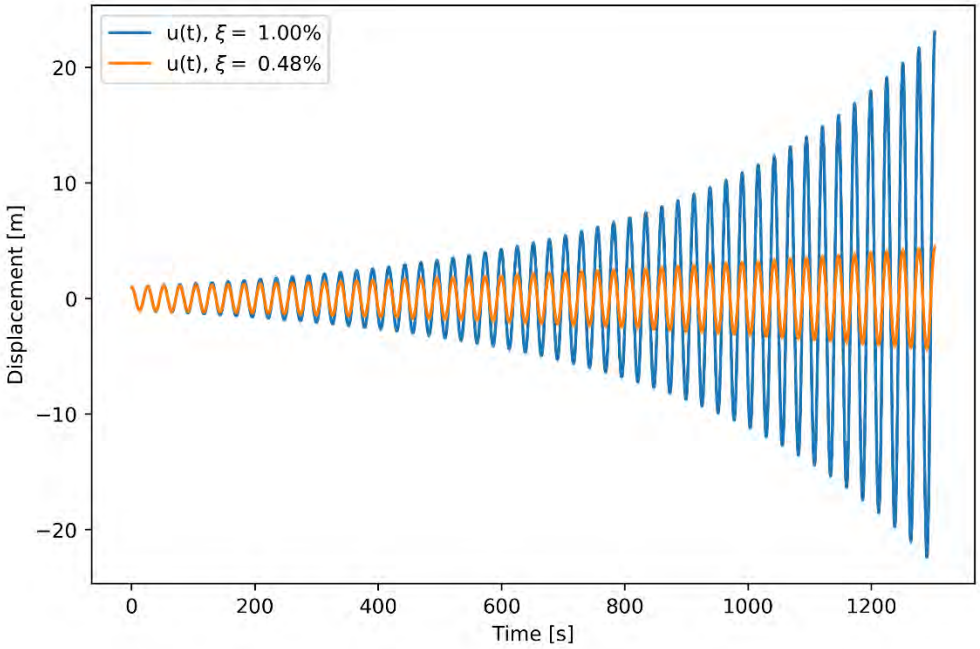

Figure 3. The exponential growth of the higher damped system is much higher than the reference system. Note that the higher damped system is exposed to a larger amplitude because the critical amplitude is increased ($N = 2.0A_{cr}$ for both cases).

2.3 Effect of quadratic drag damping

The interpretation of the critical amplitude given in [3], should be that no parametric excitation should occur, and thus no response-based damping sources could be included (such as drag damping). However, it is evident that the drag damping will contribute in a real-life situation, and the response will converge as the damping increases.

One important scenario to consider, if allowing the drag damping to contribute, is that the mode excited by parametric excitation and is stabilized at an acceptable level due to drag damping, could provide a new parametric variation of the axial force and thus parametrically excite a new mode. This must be more thoroughly investigated at a later stage.

An expression can be established to estimate the *terminal level* (a term chosen to indicate that the level will be reached only in an asymptotical manner) of a parametrically excited SDOF system due to a harmonic axial force variation. The equation of motion is assumed to include linear and quadratic damping as follows:

$$m\ddot{y} + c_{lin}\dot{y} + c_{quad}|\dot{y}|\dot{y} + ky = p(t)$$

For a harmonic motion, the quadratic damping term could be included in a linearized quadratic damping, by assuming the same amount of energy dissipation per cycle, as follows:

$$m\ddot{y} + (c_{lin} + \frac{8}{3\pi}c_{quad}\dot{y}_0)\dot{y} + ky = p(t)$$

Here, $\dot{y}_0$ is the amplitude of the steady-state velocity. To establish the level of the stabilized response, the following total damping is assumed based on the steady-state response level:

$$c = c_{lin} + \frac{8}{3\pi}c_{quad}\dot{y}_0$$

The criterion for the critical amplitude (fundamental stability lobe) is rewritten as:

$$N = A_{cr} = \frac{4\xi k}{\hat{k}_g} = \frac{4c}{2\sqrt{km}} \cdot \frac{k}{\hat{k}_g}$$

$$= 4\frac{c_{lin} + \frac{8}{3\pi}c_{quad}\dot{y}_0}{2\sqrt{km}} \cdot \frac{k}{\hat{k}_g}$$

Solved for the amplitude of the harmonic velocity (at stabilized conditions), this gives:

$$\dot{y}_0 = \frac{\frac{N}{2} \cdot \frac{\hat{k}_g}{k}\sqrt{km} - c_{lin}}{\frac{8}{3\pi}c_{quad}} = \frac{N \cdot \frac{\hat{k}_g}{\omega_n} - 2c_{lin}}{\frac{16}{3\pi}c_{quad}} = 3\pi\frac{N \cdot \frac{\hat{k}_g}{\omega_n} - 2c_{lin}}{16c_{quad}}$$

which further is rewritten to the amplitude of the displacement response, through the relation $\dot{y}_0 = \omega_d y_0$, as follows:

$$y_0 = 3\pi\frac{N \cdot \frac{\hat{k}_g}{\omega_n} - 2c_{lin}}{16c_{quad}} \cdot \frac{1}{\omega_d}$$

Under the assumption that $\omega_n = \omega_d$ (not needed), this can again be rewritten:

$$y_0 = 3\pi\frac{N \cdot \frac{\hat{k}_g}{\omega_n^2} - 2c_{lin} \cdot \frac{1}{\omega_n}}{16c_{quad}} = 3\pi\frac{N \cdot \hat{k}_g - 2c_{lin}\omega_n}{16c_{quad}\omega_n^2} \quad (2)$$

The effect of the quadratic drag damping is visualized in Figure 4, which shows the response of the parametrically excited system with and without this effect included. It is also compared to Equation 2. When the displacements, and thus velocities, grow, they result in larger damping forces which at a certain amplitude level reaches equilibrium with the excess energy caused by the parameter variation. It is noted that the response is converging to a certain level, without overshooting its terminal amplitude.

The effective critical amplitude is recalculated for each time step based on the updated total damping, including both linear and linearized quadratic damping. The result, shown in Figure 5, supports the interpretation of Figure 4; the critical amplitude of the axial force equals the applied axial force when the solution has stabilized, for the case when drag damping is included. The eigenvalues of the fundamental matrix $[B]$, reflected in the *stability indicator,* supports this (stable when below 1).

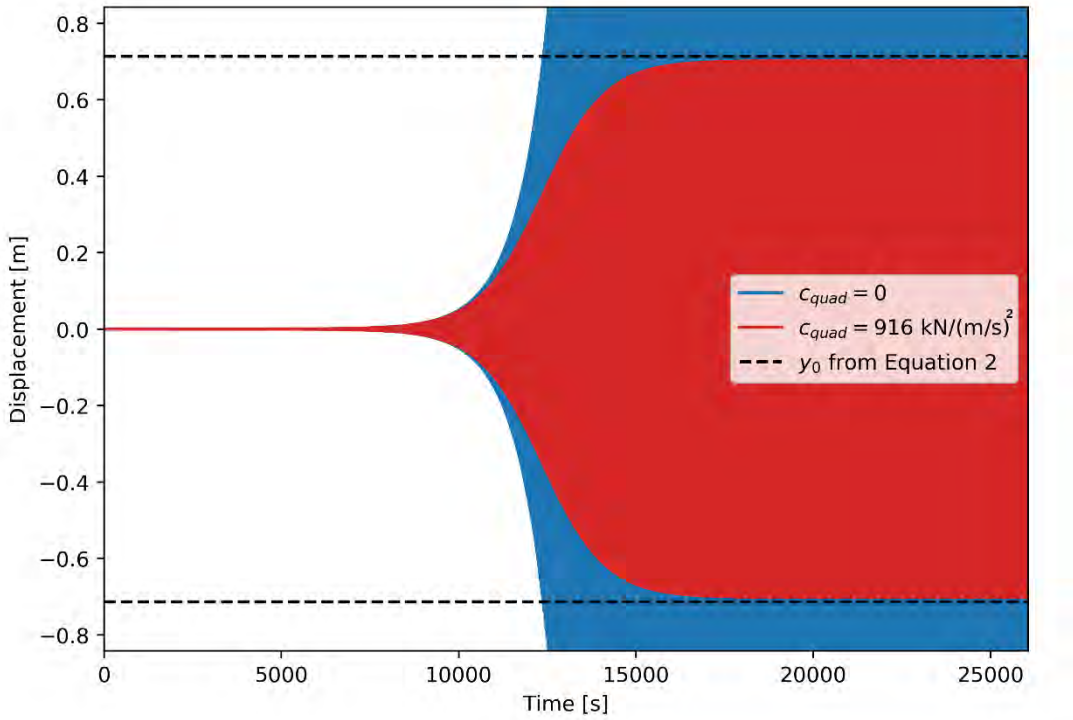

Figure 4. $N = 2.0A_{cr}$. With and without quadratic drag damping.

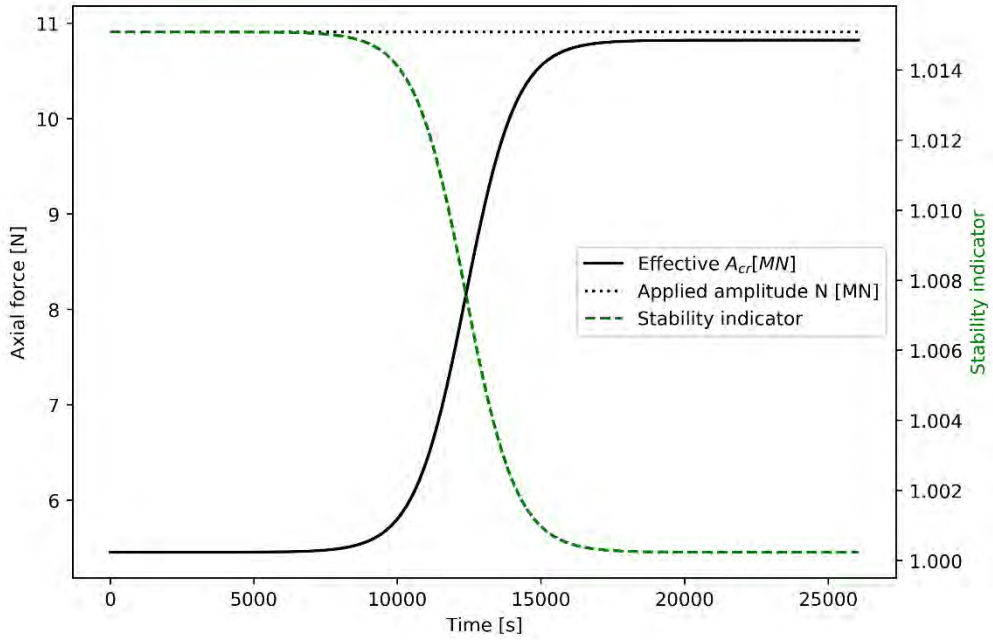

Figure 5. The effect on the effective critical amplitude as the quadratic drag damping increases with increasing amplitude. Initially the amplitude of the axial force is set to $N = 2.0A_{cr}$. The stability indicator is based on the eigenvalues of the matrix $[B]$ found in Equation 2, which indicates stable solutions when at or below 1.0.

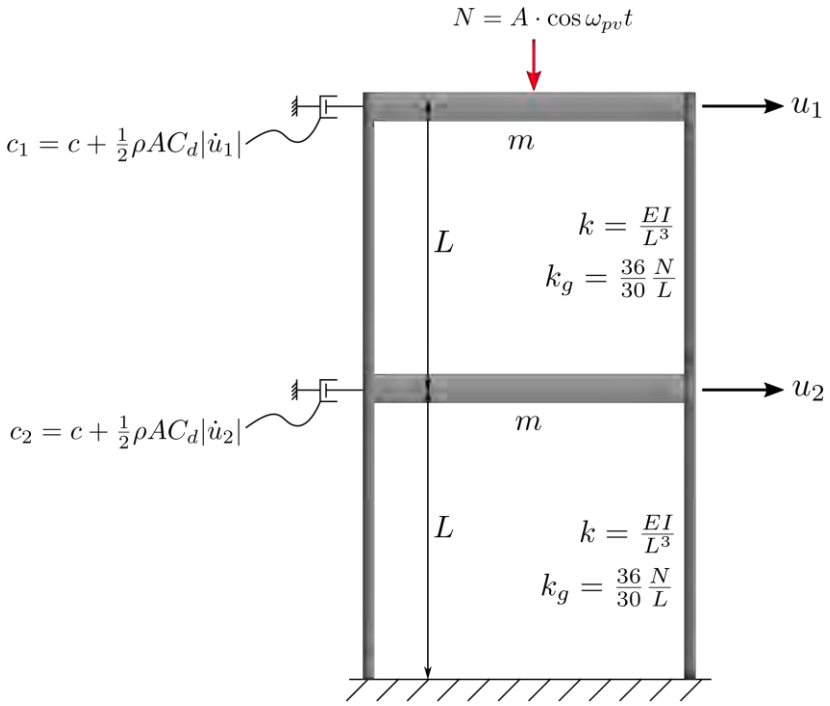

Figure 6. Two-DOF shear frame. The beam material stiffness k applies to beams on both side and are thus included twice for each storey.

2.4 Verification with 2DOF system

To verify the SDOF approach, a 2DOF system, representing a shear frame as shown in Figure 6, is constructed. The system is characterized by the following system parameters:

- $L = 125m$
- $I = 1.0m^4$
- $m = 500$ tonnes
- $c = 1000Ns/m$
- $E = 210MPa$

From the solution of the eigenvalue problem, the two modes of the system are found to be characterized by $T_d = 141.5s$ and $\xi = 1\%$ for mode 1, and $T_d = 54.1s$ and $\xi = 0.4\%$ for mode 2, where T_d is the damped natural period. The mode shapes are depicted in Figure 7.

Drag damping is also introduced in the two DOFs. The drag portion of the dampers are characterized by $\rho = 1000kg/m^3$, $A = 74.5m^2$, and $C_d = 0.5$.

According to the criterion given in [3], the critical amplitude of the applied load N corresponding to the two present modes are 54kN and 20.7kN for modes 1 and 2, respectively.

Newmark time simulations are conducted both with and without the drag contribution, and both slightly above and slightly below the critical amplitude. The results are shown in Figure 8 – Figure 11, which indicate that the onset of instability is correctly identified by the provided formula. It also shows that the response stabilizes at a plateau when drag damping is active, as for the SDOF system, when the equivalent total damping is large enough to ensure that the applied and critical axial force amplitudes are equal. Figure 12 indicates that the system is oscillating purely in the modes correponding to half the frequency of the axial force variation.

Analysis of parametric resonance of single-degree-of-freedom systems using Newmark's method and Monte Carlo simulation

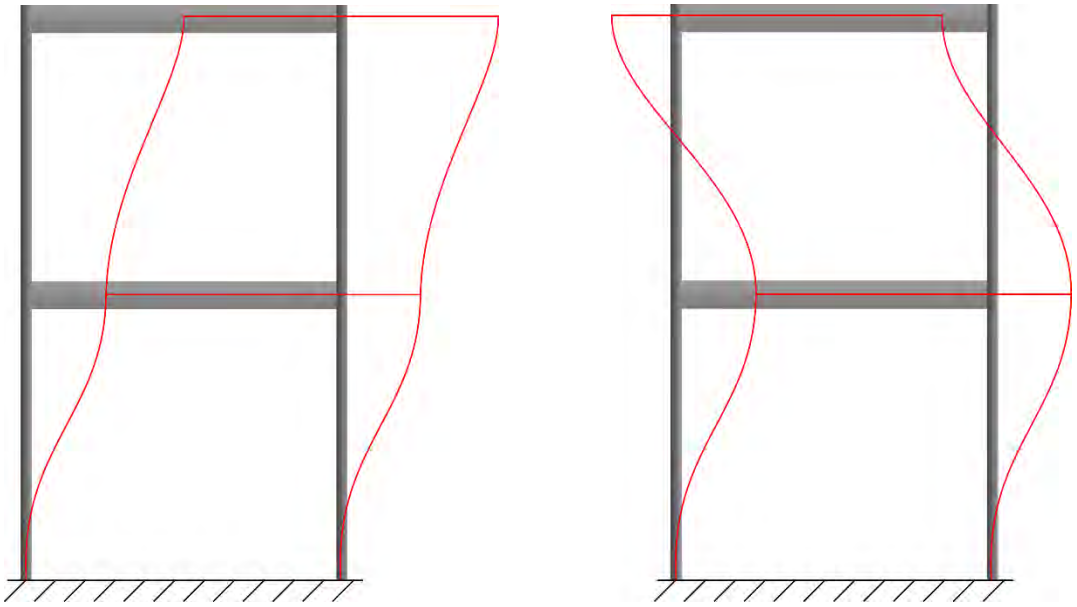

Figure 7. Mode 1 (left) and mode 2 (right).

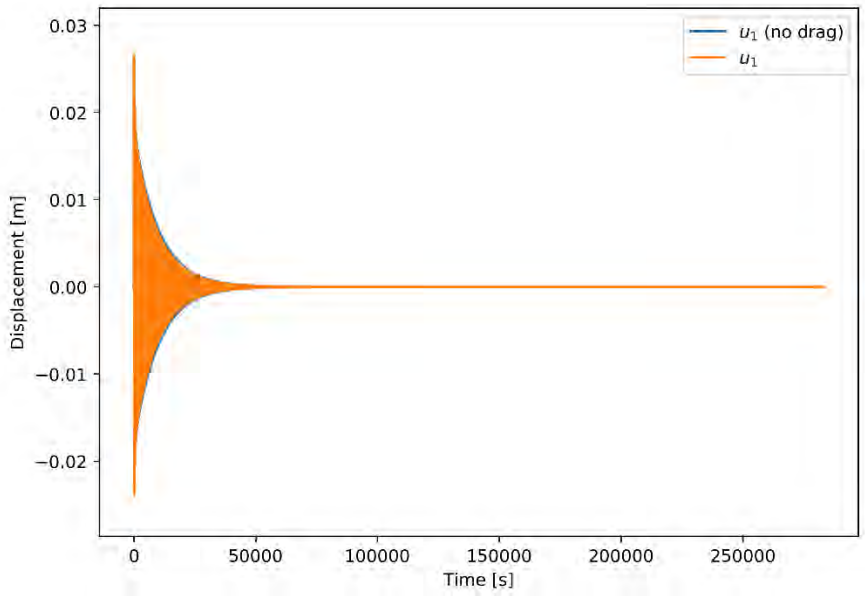

Figure 8. $N = 0.9A_{cr,1} \cdot cos(2\omega_1 t)$. The amplitude of the applied axial force is slightly below the critical amplitude for parametric resonance of mode 1.

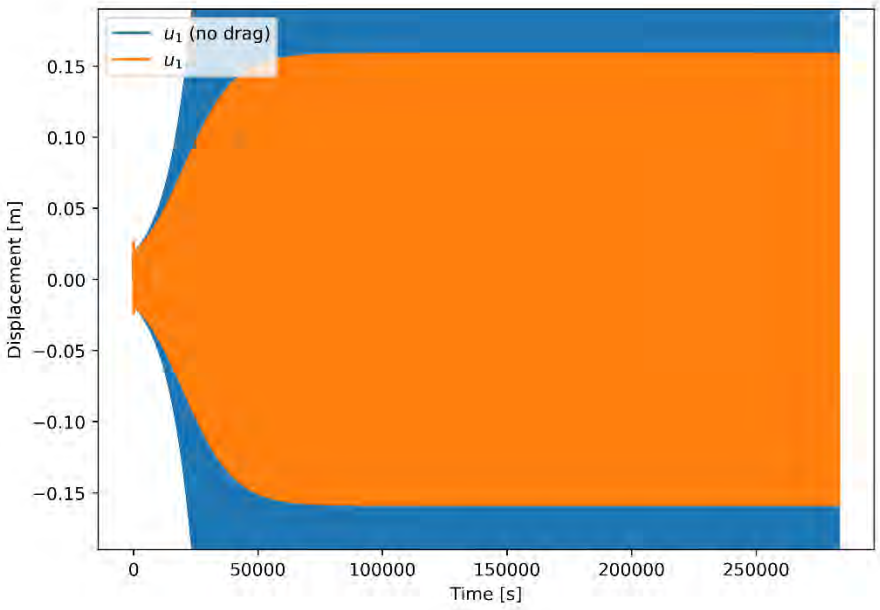

Figure 9. $N = 1.1A_{cr,1} \cdot cos(2\omega_1 t)$. The amplitude of the applied axial force is slightly above the critical amplitude for parametric resonance of mode 1.

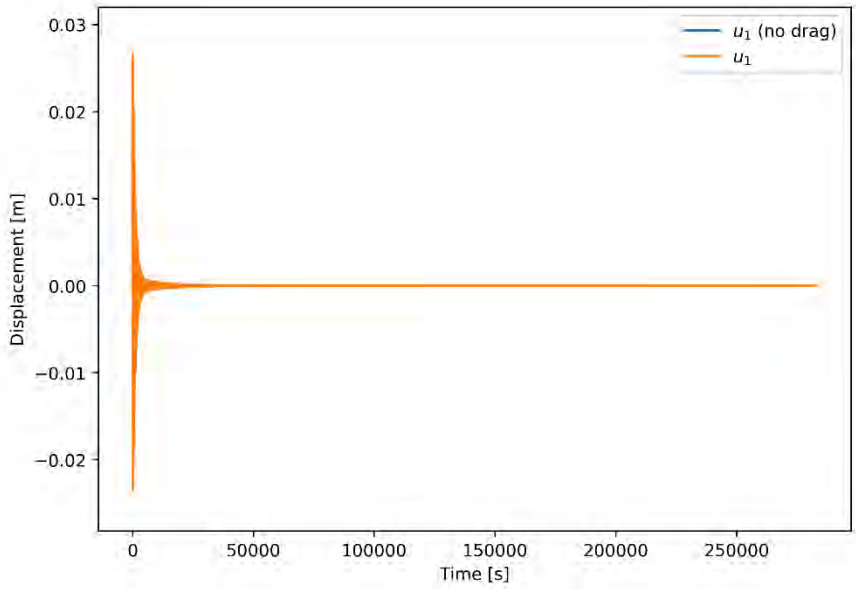

Figure 10. $N = 0.9A_{cr,2} \cdot cos(2\omega_2 t)$. The amplitude of the applied axial force is slightly below the critical amplitude for parametric resonance of mode 2.

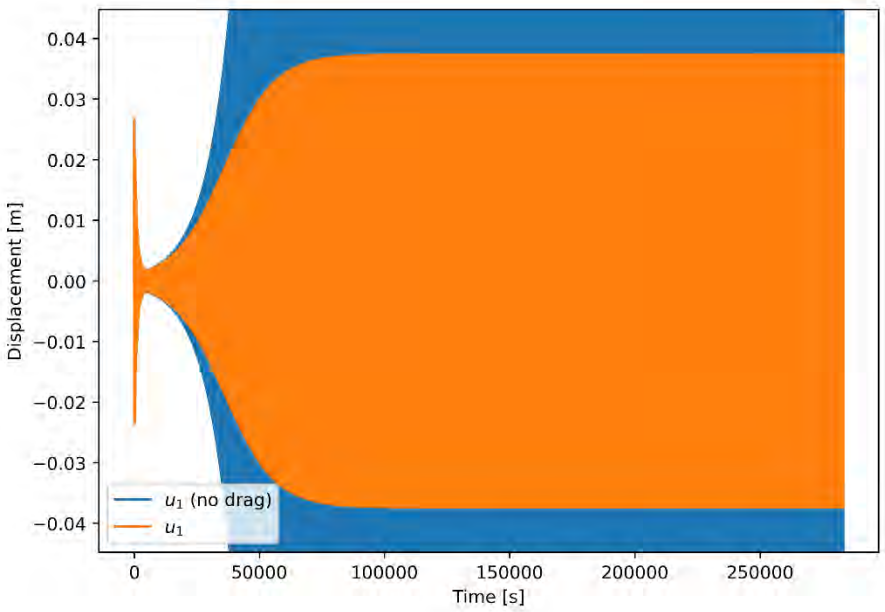

Figure 11. $N = 1.1A_{cr,2} \cdot cos(2\omega_2 t)$. The amplitude of the applied axial force is slightly above the critical amplitude for parametric resonance of mode 2.

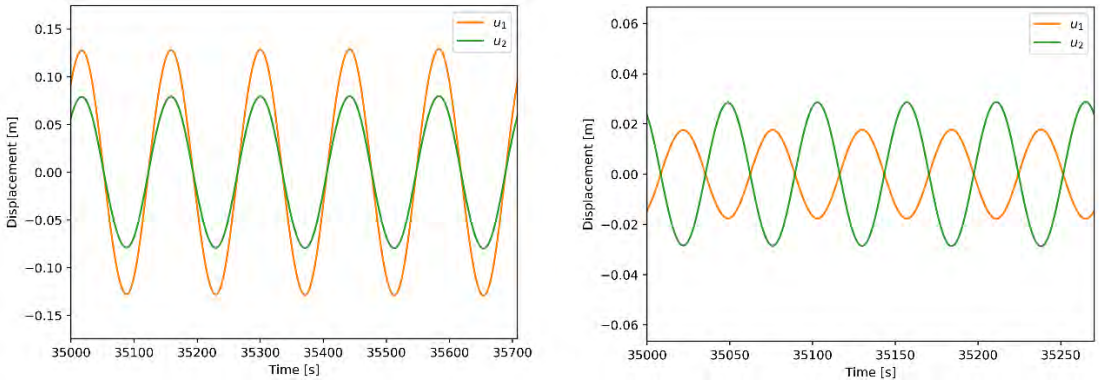

Figure 12. Parametric excitation of mode 1 (left, in-phase DOFs) and mode 2 (right, out-of-phase DOFs) by barely exceeding the critical amplitudes corresponding to the modes. Both modes are exposed to axial force variation at twice the frequency of the damped natural frequencies.

3 Stochastic parameter variation with Monte Carlo simulation

Stochastic parameter variation is characterized by spectral densities of the axial force amplitude. The spatial distribution of the axial force is reflected in the value of the generalized geometric stiffness, $\hat{k}_g$. Here, the spectral density describes the point of maximum axial force. It is assumed that the distribution is independent on the amplitude, but this is of course not necessarily the case. A spatially uniform axial force variation is considered to be conservative, and also representative of the real situation.

The onset of instability in the stochastic cases are ensured by applying a Gaussian white noise load $P(t)$. The amplitude of the white noise is specified by a standard deviation of 1N, unless otherwise specified. The SDOF system considered corresponds to the one defined in Section 2.1. Most response predictions in this section is conducted with quadratic drag damping coefficient $c_{quad} = 916kN/\left(\frac{m}{s}\right)^2$ which is an estimate based on K11 with a large drag factor $C_d = 2.0$. Some results are obtained with quadratic drag damping coefficient $c_{quad} = 458kN/\left(\frac{m}{s}\right)^2$, corresponding to $C_d = 1.0$; these cases are clearly indicated. The main conclusions are similar for other quadratic damping levels as well.

3.1 Bi- and tri-modal cases

3.1.1 Assuming equal maximum amplitudes

The parameter variation was assumed to consist of multiple equally-sized components N_i as follows:

$$N_{tot} = N_1 + N_2 + \cdots + N_n$$

The maximum axial force (when the sum of all components reaches their maximum) was assumed to be equal to 20 times the critical amplitude for the system. The first component was placed at twice the damped natural frequency of the system, whereas the remainder were given frequencies $\omega = 2\omega_d + \Delta\omega \cdot (k-1)$, i.e., placed at higher frequencies with equal spacing $\Delta\omega$. The frequency spacing was varied for both the bi- harmonic and the tri-harmonic cases. Note that the phase angles are drawn randomly from a uniform distribution. Figure 13 – Figure 16 show the resulting maximum realizations for two different frequency spacings for both cases. The effect on the resulting maximum displacement response resulting from varying the frequency spacings are illustrated in Figure 17 and Figure 18. The figures reveal that the total response is converging towards the case with a single harmonic case as the frequency spacing reduces (indicated by a ratio of 1.0 in the figure). The maximum displacements from 10 realizations of the tri-harmonic case are shown in Figure 19, for simulations with and without drag damping. It is evident that the viscous damping term reduces the variability of the resulting response, in addition to reducing the amplitudes dramatically.

Analysis of parametric resonance of single-degree-of-freedom systems using Newmark's method and Monte Carlo simulation

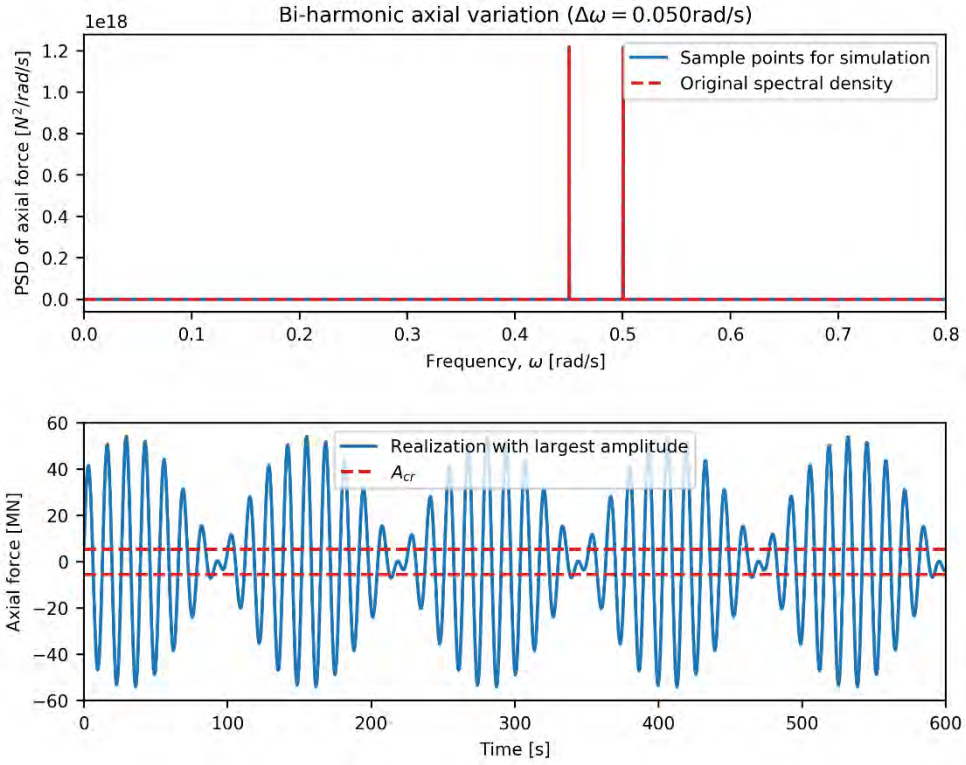

Figure 13. This is showing the bi-harmonic case, where two axial force components at different frequencies with amplitudes N_1 and N_2. Here, $N_1 + N_2 = 10Acr$ (i.e., the sum of the amplitudes is 10 times the critical harmonic amplitude).

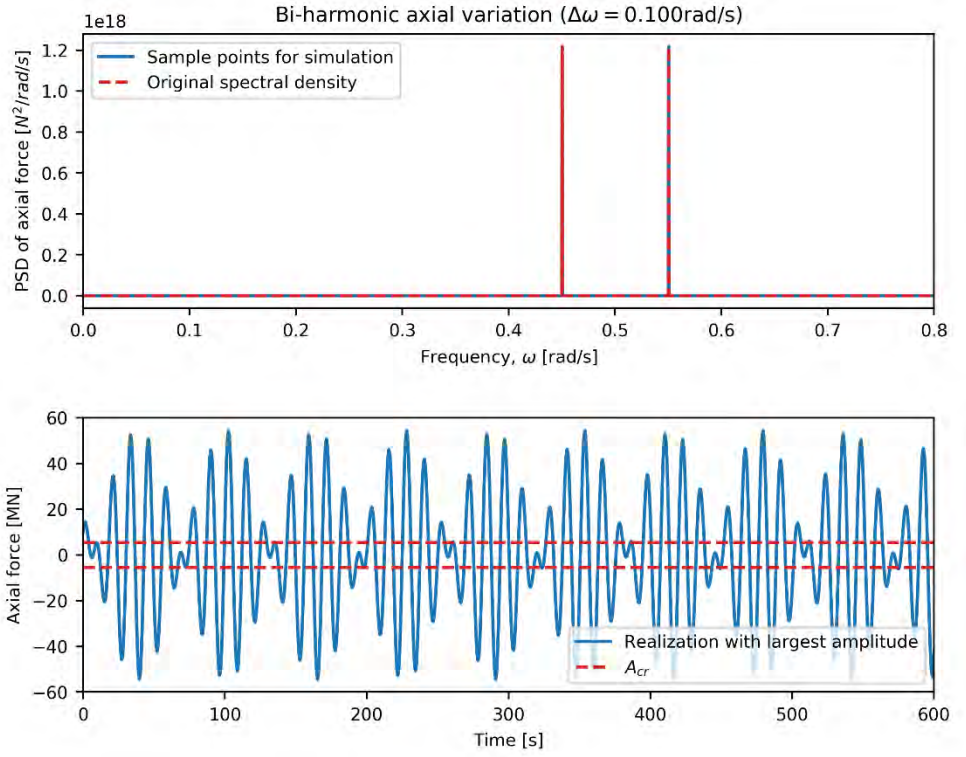

Figure 14. This is showing the bi-harmonic case, where two axial force components at different frequencies with amplitudes N_1 and N_2. Here, $N_1 + N_2 = 10Acr$ (i.e., the sum of the amplitudes is 10 times the critical harmonic amplitude).

Analysis of parametric resonance of single-degree-of-freedom systems using Newmark's method and Monte Carlo simulation

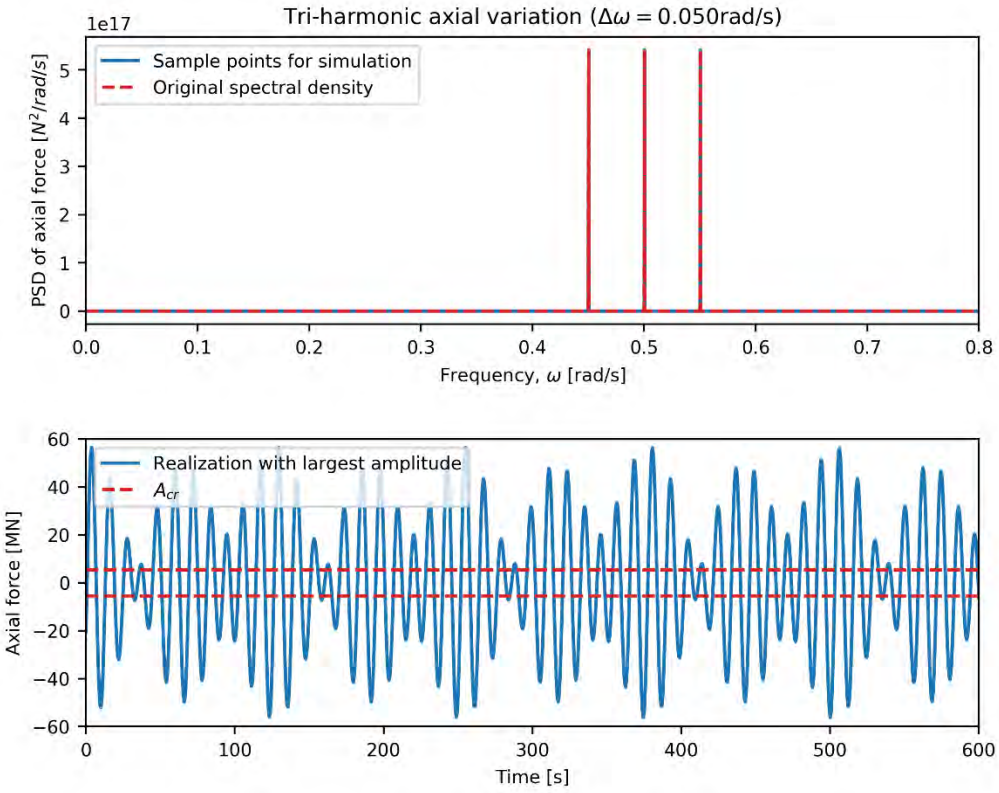

Figure 15. This is showing the tri-harmonic case, where three axial force components at different frequencies with amplitudes N_1, N_2, and N_3. Here, $N_1 + N_2 + N_3 = 10Acr$ (i.e., the sum of the amplitudes is 10 times the critical harmonic amplitude).

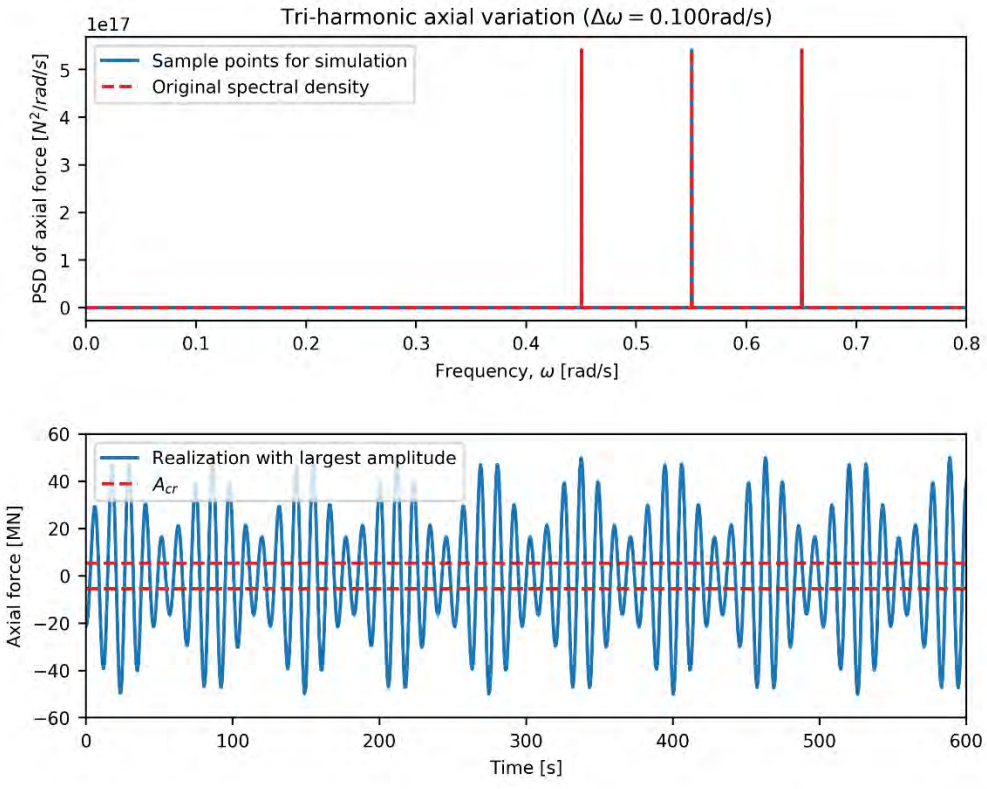

Figure 16. This is showing the tri-harmonic case, where three axial force components at different frequencies with amplitudes N_1, N_2, and N_3. Here, $N_1 + N_2 + N_3 = 10Acr$ (i.e., the sum of the amplitudes is 10 times the critical harmonic amplitude).

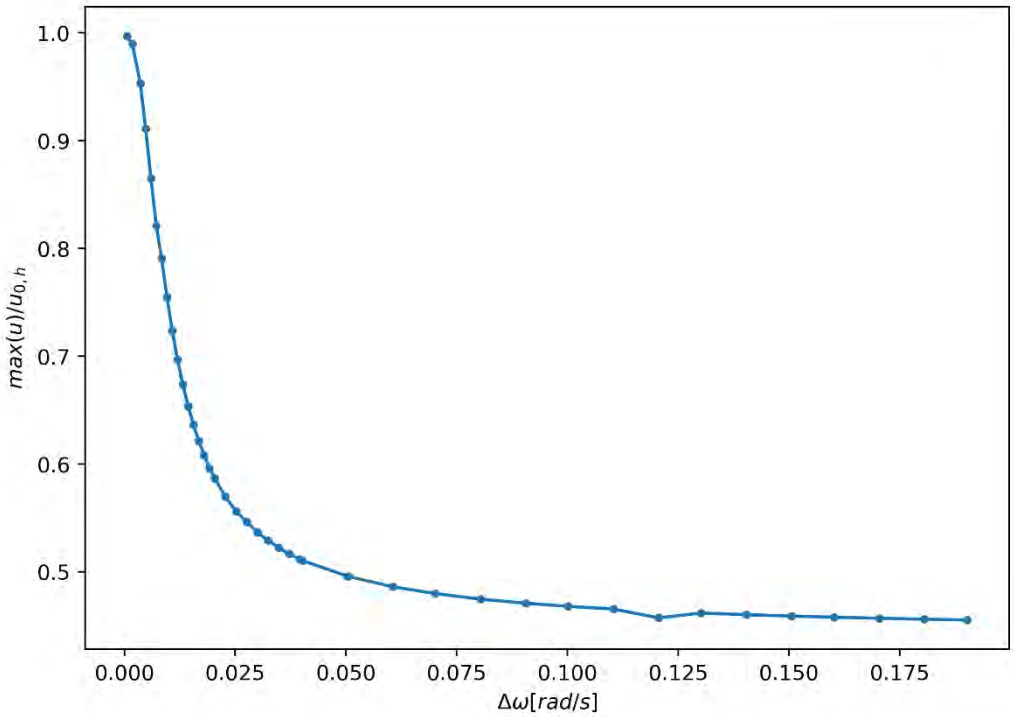

Figure 17. Effect of frequency spacing of the frequency components on the maximum amplitude. Bi-harmonic parameter variation. The maximum amplitude is scaled by the terminal displacement for a harmonic parameter variation with the specified drag damping. $u_{0,h}$ is the maximum displacement from a single harmonic case.

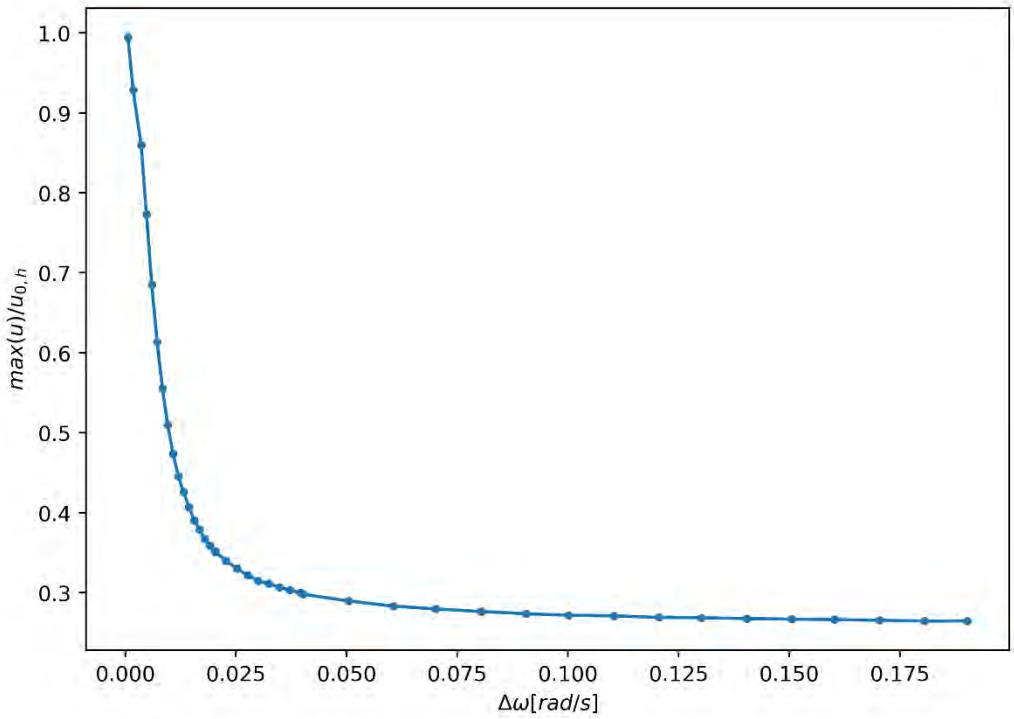

Figure 18. Effect of frequency spacing of the frequency components on the maximum amplitude. Tri-harmonic parameter variation. The maximum amplitude is scaled by the terminal displacement for a harmonic parameter variation with the specified drag damping. $u_{0,h}$ is the maximum displacement from a single harmonic case.

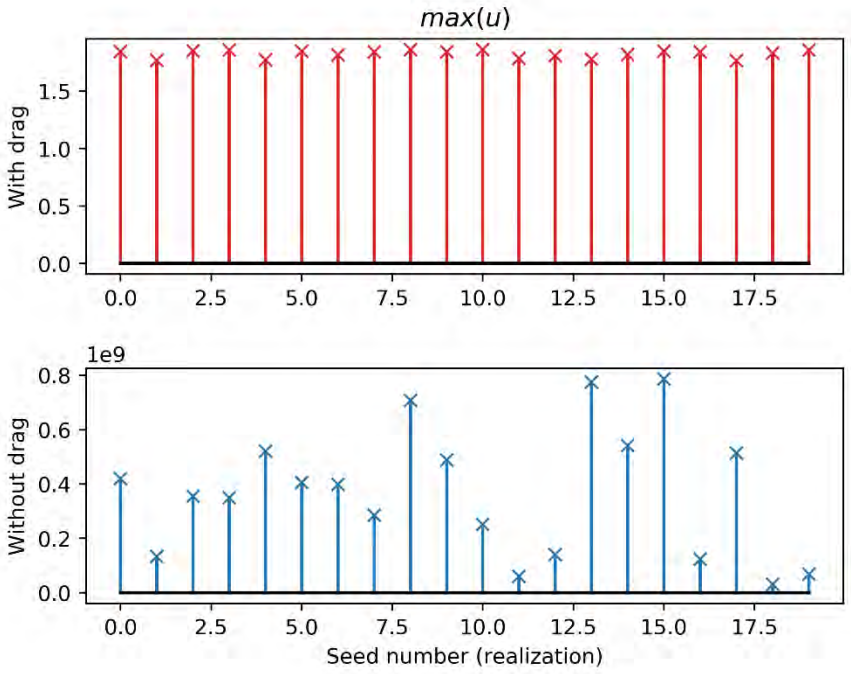

Figure 19. Effect of drag on the variability of the maximum response of an SDOF system exposed to parametric excitation. This is showing the tri-harmonic case, where three axial force components at different frequencies with amplitudes N_1, N_2, and N_3. Here, $N_1 + N_2 + N_3 = 10Acr$ (i.e., the sum of the amplitudes are 20 times the critical harmonic amplitude).

3.1.2 Assuming equal variance

Then, the area under the spectral density was kept constant for the different multi-harmonic cases, ensuring a constant variance. The variance of a harmonic process with amplitude A equals $\frac{A^2}{2}$, such that the total variance can be established as the sum of the variance of the separate components as follows:

$$\sigma_A^2 = \sum \sigma_i^2$$
$$= \frac{A^2}{2} = \Sigma \frac{A_i^2}{2}$$
$$= \sum S(\omega_k)\Delta\omega$$

The most commonly used approach to simulate response from a stochastic excitation is by assuming that the amplitudes of the frequency components are deterministically determined from the spectral density as $c_k = \sqrt{2S(\omega)\Delta\omega}$, whereas the phase angles are drawn random from a uniform distribution. For scenarios where the excitation is built up by numerous frequency components, this works well, by the virtue of the central limit theorem; the resulting amplitude ends up being Gaussian. For special cases, with only a few frequency components, as the bi-harmonic and tri-harmonic cases presented here, the central limit theory fails. Thus, the amplitudes should also be drawn randomly for such cases. The chosen method is by drawing the phase angles from a uniform distribution and the amplitudes c_k from a Rayleigh distribution with variance $\sigma_c = S(\omega)\Delta\omega$.

The amplitude of the applied axial force is chosen as $2A_{cr}$ for a harmonic excitation. This corresponds to a variance $\sigma_N^2 = \frac{N^2}{2} = 2A_{cr}^2$.

For these studies 100 realizations were conducted on each case. Figure 20 and Figure 21 show the spectral densities and corresponding largest simulated realization of the axial force variation for the

applied bi-harmonic and tri-harmonic cases, respectively. They are compared with the harmonic critical amplitude for the system, which indicates that the critical level is often crossed during the simulations. The resulting displacement responses are given Figure 22 and Figure 23, corresponding to bi-harmonic and tri-harmonic excitation, respectively. Both figures show displacement patterns similar to that of a harmonic case when drag is included, stabilizing in a neat manner at a terminal displacement. Because only two or three components are included, this is as expected. The relative phase differences between the various components are constant throughout the simulation, such that each realization represents periodic axial force variations. The maximum axial forces and maximum displacements in each realization for all seeds are depicted in Figure 24 and Figure 25. An important observation is that the variability of the maximum displacement decreases significantly when including drag damping. Also, an obvious observation is that the amplitudes are reduced dramatically when drag damping is included.

Analysis of parametric resonance of single-degree-of-freedom systems using Newmark's method and Monte Carlo simulation

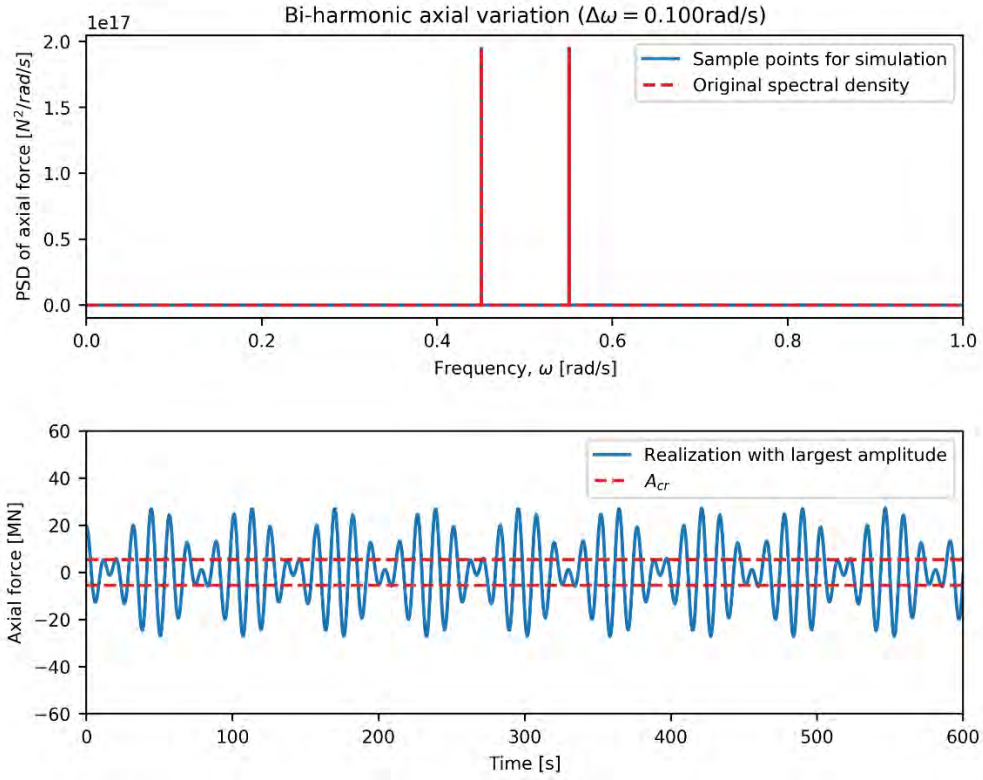

Figure 20. Applied stochastic bi-harmonic axial force and the largest-amplitude realization.

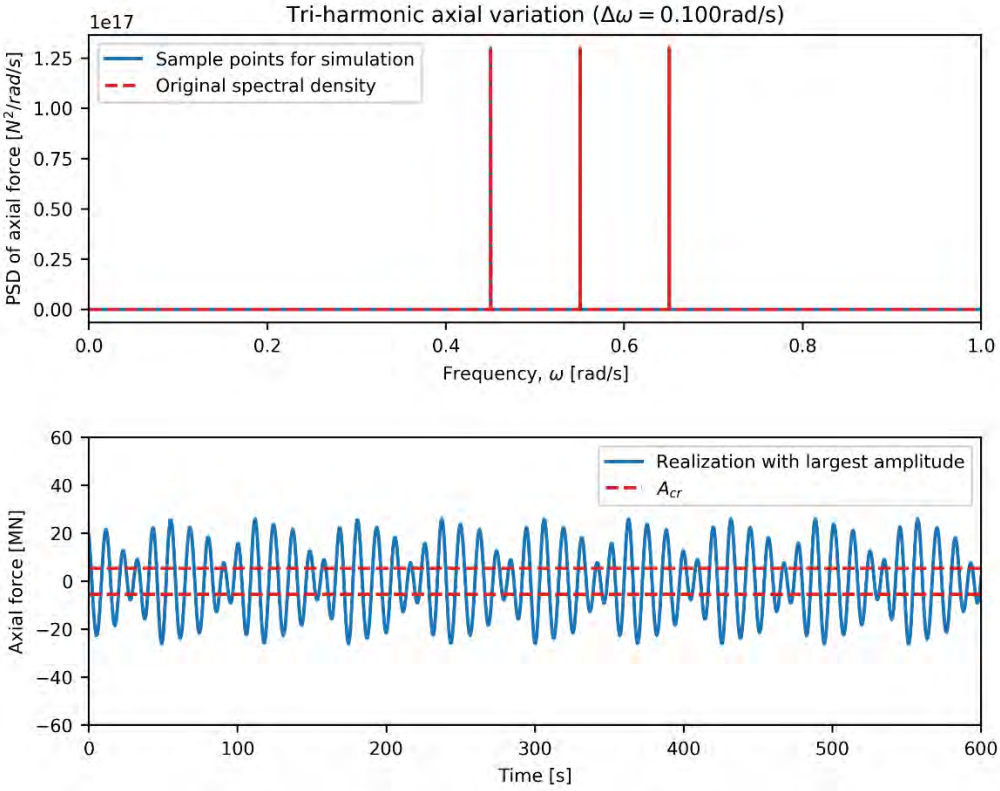

Figure 21. Applied stochastic tri-harmonic axial force and the largest-amplitude realization.

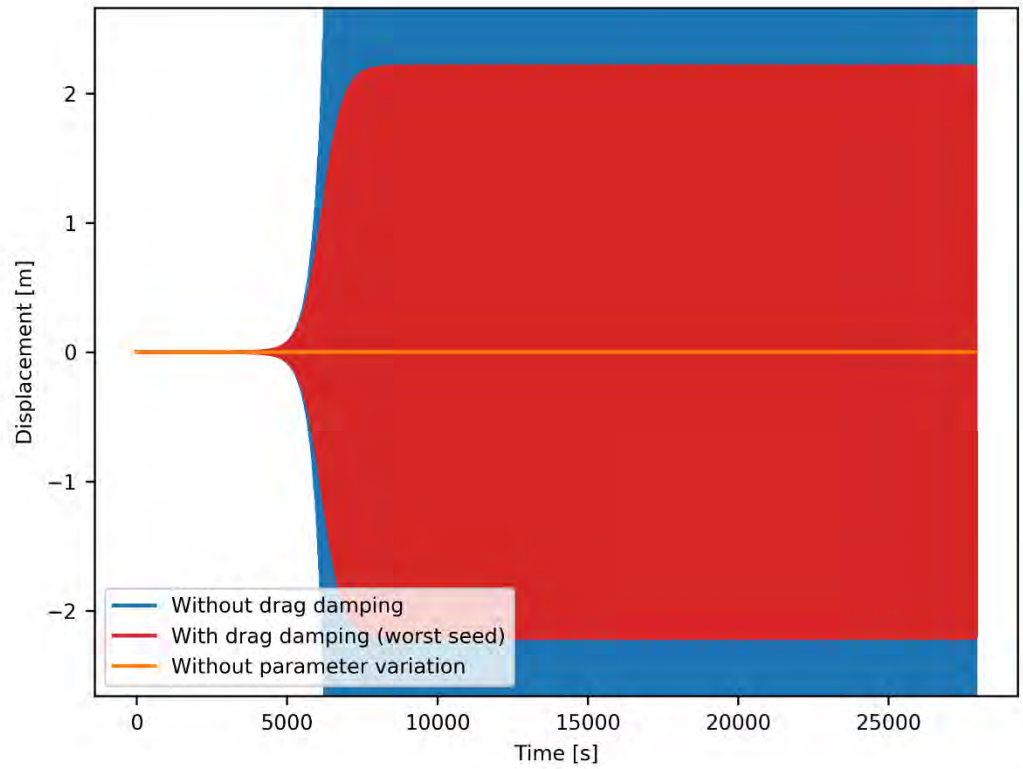

Figure 22. Largest displacement observed from all 100 realizations for stochastic bi-harmonic axial force variation defined in Figure 20.

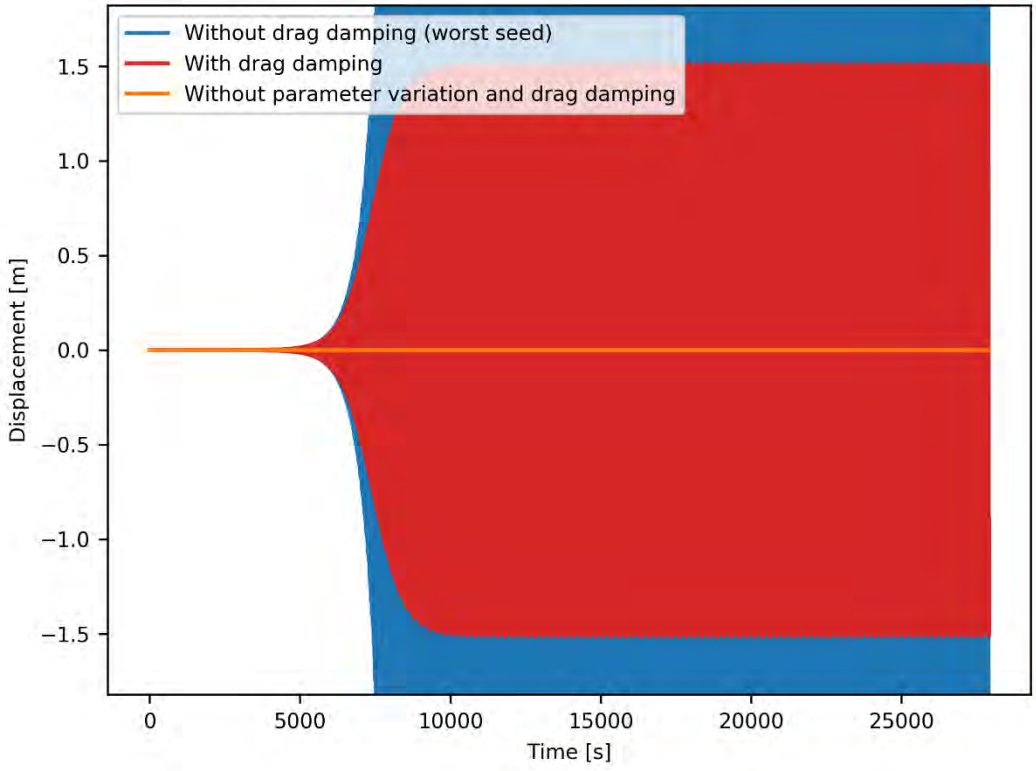

Figure 23. Largest displacement observed from all 100 realizations for stochastic tri-harmonic axial force variation defined in Figure 21.

Analysis of parametric resonance of single-degree-of-freedom systems using Newmark's method and Monte Carlo simulation

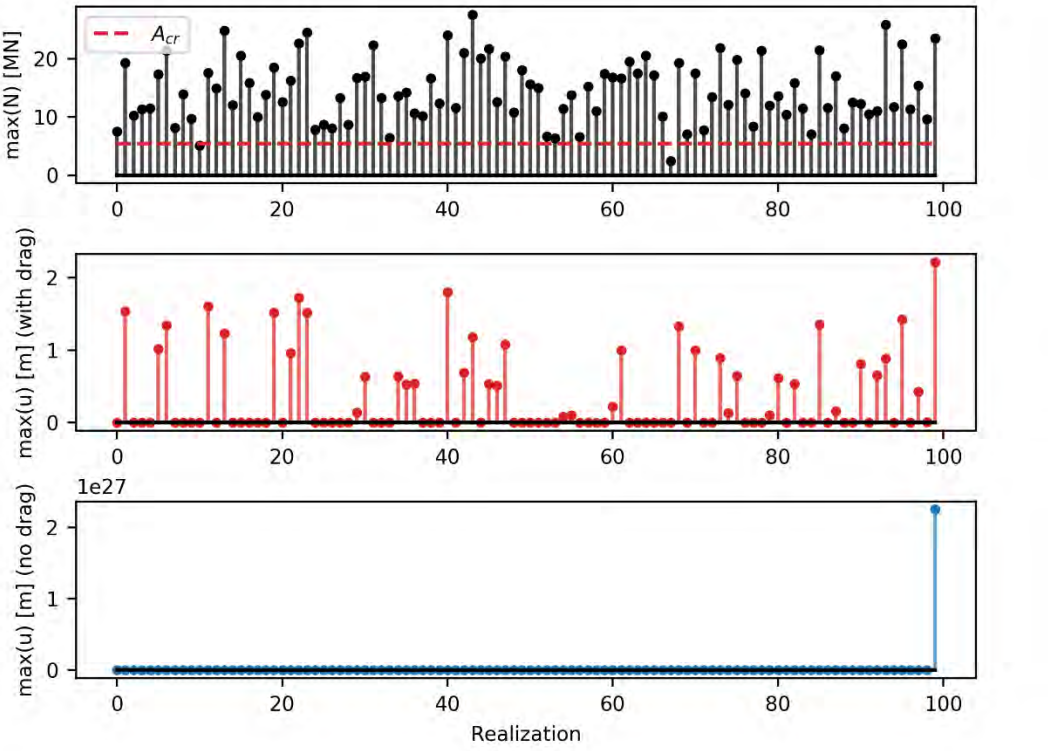

Figure 24. Maxima of axial force and displacement (with and without drag) for 100 realizations, for stochastic bi-harmonic axial force variation.

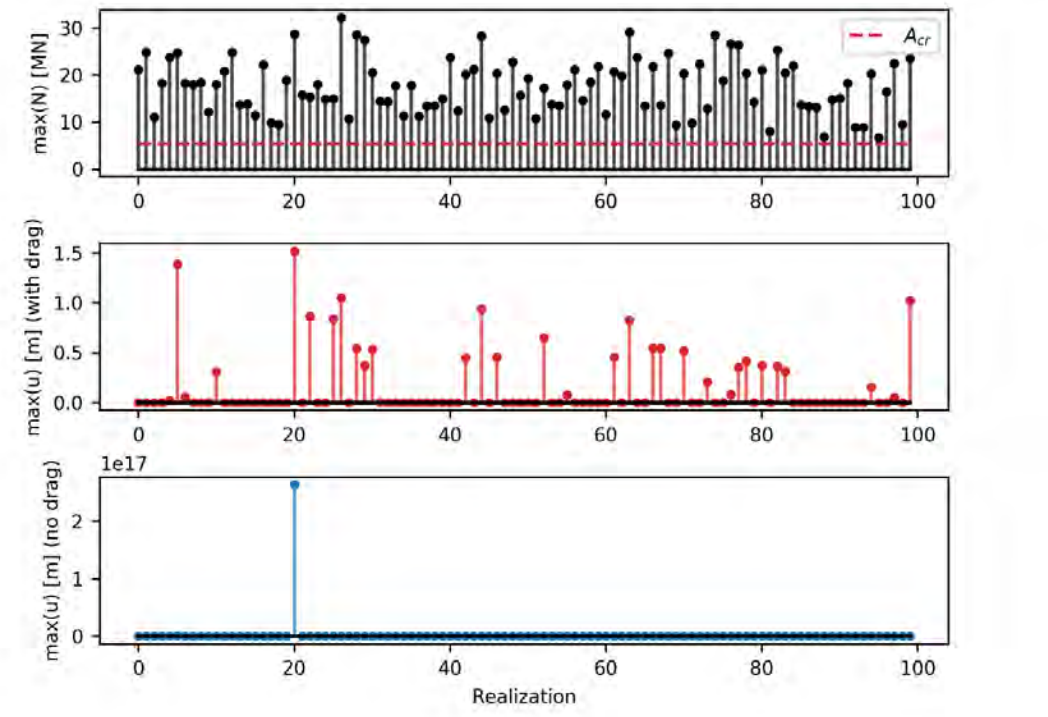

Figure 25. Maxima of axial force and displacement (with and without drag) for 100 realizations, for stochastic tri-harmonic axial force variation.

3.2 Full stochastic case

An Orcaflex-predicted spectral density of axial force variation due to a swell excitation with a peak frequency around twice the natural frequency of the SDOF system was used to simulate the response. The axial force response is resulting from a global analysis where the sea state is characterized by $T_p = 14s$, $H_s = 0.46m$ and with an unfavourable heading. The SDOF system properties were set equal to those given in Section 2.1, but the modal mass was scaled such that the damped natural frequency equalled exactly half the peak of the spectral density of the axial force ($m = 6.67 \cdot 10^7 kg$, $\omega_n = 0.225$ rad/s), keeping the critical amplitude identical. From the observations made in Section 2.1 (see Figure 3), a long simulation duration, corresponding to 1000 cycles of the mode of interest, was chosen for the analyses.

1000 realizations were run in this first study. Figure 26 show the spectral density of the Orcaflex-predicted axial force variation and the realization (of 1000) following that gives the largest axial force. The largest displacement observed is shown in Figure 27, which is 0.15 m with drag. A stem plot indicating the maximum values of all realizations are given in Figure 28. To assess the time necessary to build up large response from parametric resonance, due to a sampled stochastic excitation, Figure 29 shows the time instances where the maximum displacements occur for all realizations. This supports the fact that rather long simulation duration is required to capture the phenomenon.

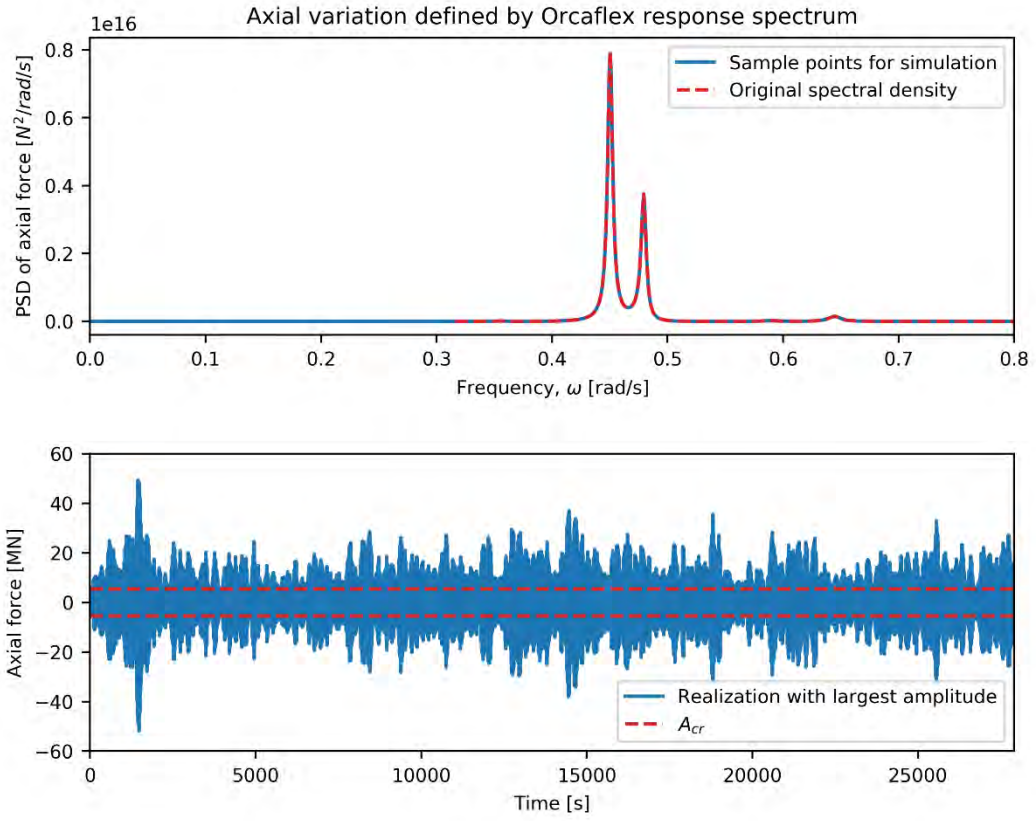

Figure 26. Spectral density of the axial force variations due to a swell sea state characterized by $T_p = 14s$, $H_s = 0.46m$ and an unfavourable heading. The corresponding axial force time history for the realization with the largest amplitude is also shown.

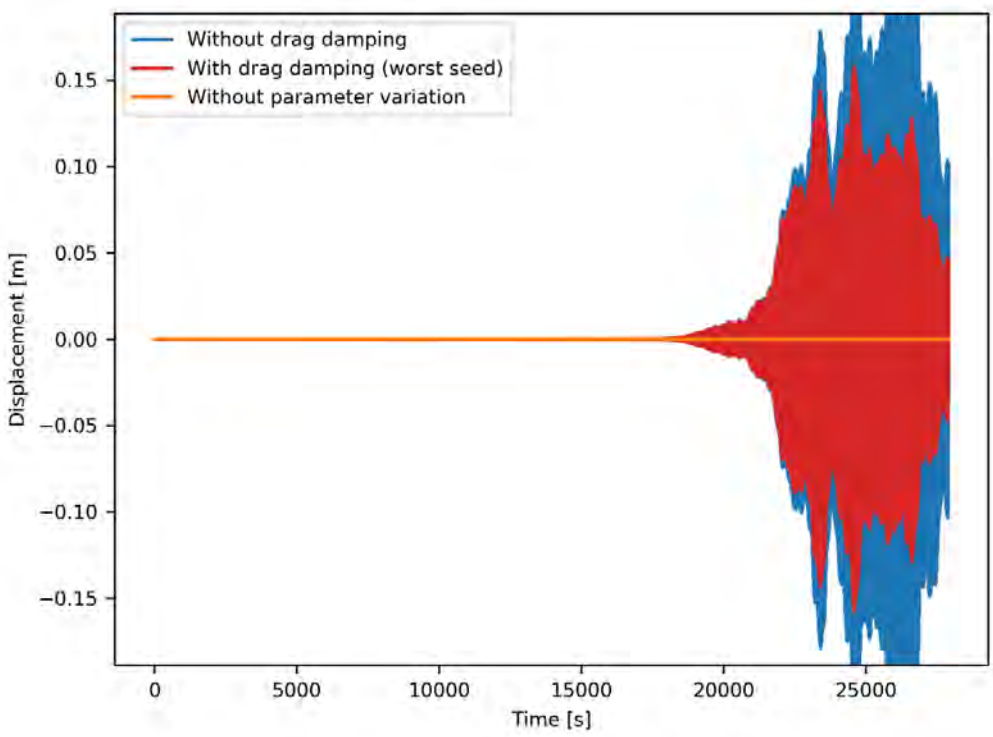

Figure 27. Largest displacement observed from all 1000 realizations due to axial force variations from a swell sea state (Figure 26).

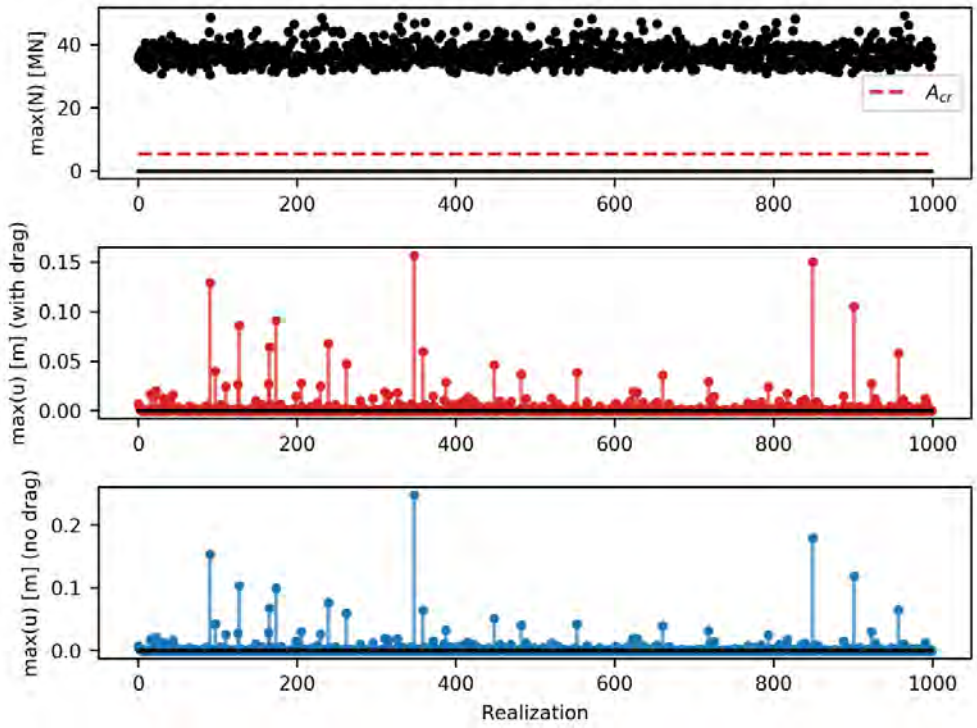

Figure 28. Maxima of axial force and displacement (with and without drag) for 100 realizations for axial force variation due to swell sea state.

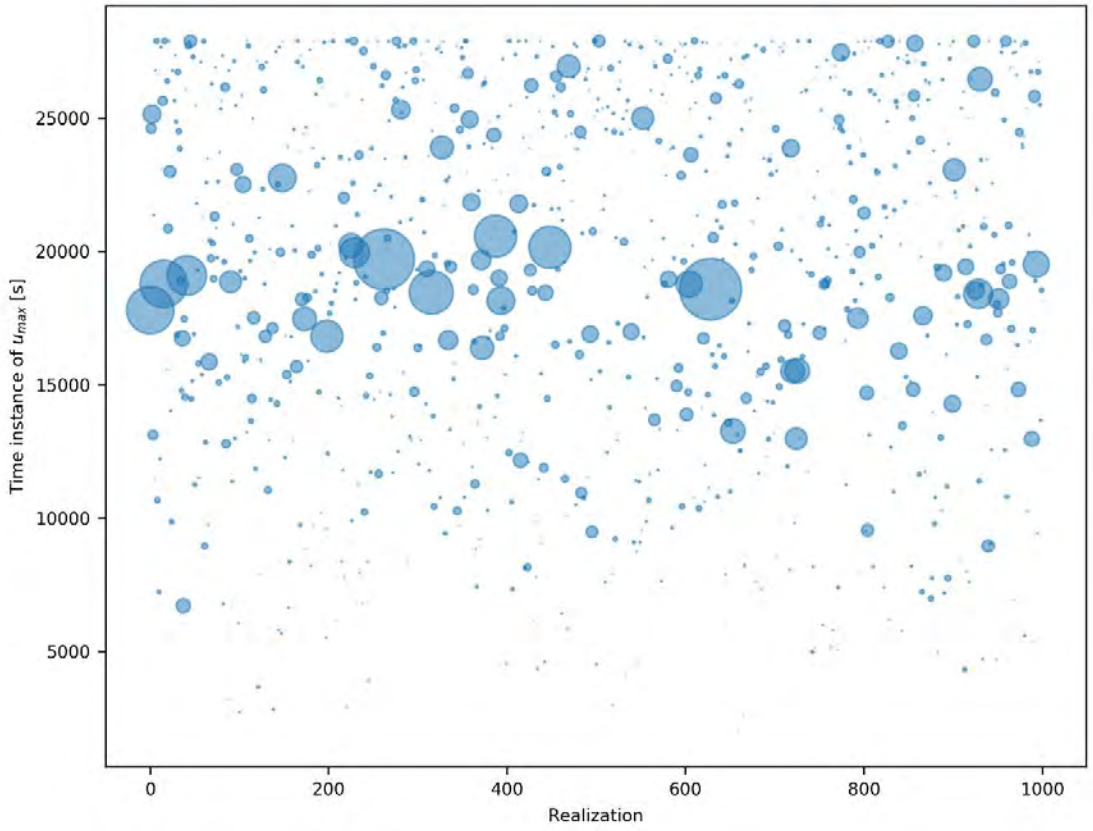

Figure 29. Time of occurrence of maximum displacement. The radius of points depends on the amplitude of the maximum displacement.

4 Concluding remarks

The most important findings in this note are summarized as follows:

- The simulation scheme set up with Newmark simulation is able to capture the parametric resonance (dynamic instability) for both SDOF and MDOF systems, exposed to harmonic parameter variation, and behaves in agreement with analytical models.
- Even for harmonic parameter variation, very long durations are required to build up response from parametric resonance (for a set ratio between applied and critical amplitude) when the excited mode has a low critical damping ratio. For stochastic parameter variation, the conclusion is the same.
- When assuming a constant maximum amplitude, bi-harmonic and tri-harmonic variation of the axial force results in lower response when the new frequency components are put away from the frequency region of parametric excitation.
- We can show that the stability of a system is restored for a system exposed to harmonic parameter variation, with quadratic drag damping, both visually and numerically (by considering eigenvalues of fundamental matrix from state space formulation). The effective damping gives a new critical amplitude such that the response reaches a terminal maximum response. This level matches the analytically computed level.
- The stochastic swell-based axial parameter variation does not induce unacceptable response, even without drag damping. Only 1000 realizations are run in this case, and a more certain conclusion would require more simulation runs. Because the response estimated is modest, the effect of the drag damping is not very large. Still, the effect of drag damping is much larger when it is needed.

5 References

[1] B. Kassteen, "Parametric roll resonance and energy transfer," *Traineesh. Report, Eindhoven Univ. Technol.*, 2010.

[2] I. Kovacic, R. Rand, and S. M. Sah, "Mathieu's Equation and Its Generalizations: Overview of Stability Charts and Their Features," *Appl. Mech. Rev.*, vol. 70, no. 2, p. 20802, 2018.

[3] O. Øiseth, B. Costa, and A. Fenerci, "Dynamic stability of elastic nonlinear systems subjected to random excitation, Report No. SBJ-32-C4-NTNU-22-RE-001." p. 47, 2018.

Concept development, floating bridge E39 Bjørnafjorden

Appendix S – Enclosure 2

Parametric excitation results

RESULTS SUMMARY - PARAMETRIC RESONANCE

****

CONCEPT: K11_07

PSD type: 100-year swell

Computed 2019-08-07 13:04:19

Analysis settings:

Parameter	Value
Bandwidth drop definition [%]	5.00
Natural frequency uncertainty [%]	20.00
N uncertainty (results with *) [%]	20.00
c_quad uncertainty (results with *) [%]	20.00
Rayleigh exceedance probability	1.0e-03
Considered frequency ratios (beta)	[0.5, 1.0, 2.0]
Considered modes	1-15

Spectral density information

				Trigger ranges		
Segment no.	std(N) [MN]	Harmonic amplitude [MN]	omega_peak [rad/s]	beta=0.5	beta=1.0	beta=2.0
1	6.6315	24.6486	0.4918	0.9566--1.0087	0.4783--0.5044	0.2392--0.2522

Modal parameters:

Mode	wd [rad/s]	Td [s]	xi0 [%]	xi w/ae [%]	m [t]	k [kN/m]	k/kg_hat [MN]	c_quad [kN/(m/s)^2]	Acr (b=2) [MN]
1	0.06	106.71	0.46	0.46	86861.19	301.18	77.90	182.65	1.44
2	0.11	57.01	0.47	0.47	50720.18	616.18	127.38	97.24	2.39
3	0.20	31.82	0.47	0.47	84224.29	3283.29	217.55	194.84	4.09
4	0.29	21.95	0.49	0.49	57026.00	4671.88	309.30	117.78	6.11
5	0.40	15.58	0.64	0.64	69969.03	11378.29	409.73	188.63	10.51
6	0.50	12.67	0.82	0.82	53488.46	13154.78	662.60	155.97	21.72
7	0.53	11.93	1.03	1.03	71046.89	19702.94	393.78	262.00	16.29
8	0.66	9.45	2.01	2.01	60209.18	26627.45	651.31	153.99	52.35
9	0.70	8.96	1.36	1.36	38002.73	18697.01	380.95	35.27	20.66

10	0.82	7.70	2.89	2.89	59522.93	39668.29	512.28	157.23	59.31
11	0.85	7.40	3.72	3.72	100935.96	72869.16	1526.06	10.13	227.38
12	0.89	7.07	2.53	2.53	97312.31	76952.29	922.08	46.54	93.33
13	0.95	6.61	15.72	15.72	6934.80	6424.24	690.12	0.00	433.93
14	0.96	6.54	2.57	2.57	56832.93	52426.12	676.49	58.75	69.54
15	0.96	6.53	12.81	12.81	9886.54	9319.53	1189.12	0.00	609.18

Harmonic results, beta = 0.5:

Mode	wd +- 20%	Matching	Chosen seg.	beta	Acr (b=0.5)	std(N)/0.4 [MN]	Onset	N [MN]	y0	y0*	Sz [MPa]	Sz* [MPa]
10	0.6528--0.9792	[1]	1	0.60	396.34	16.58	ok	24.65	nan	nan	nan	nan
11	0.6793--1.0189	[1]	1	0.58	1284.25	16.58	ok	24.65	nan	nan	nan	nan
12	0.7112--1.0668	[1]	1	0.55	682.15	16.58	ok	24.65	nan	nan	nan	nan
13	0.7604--1.1406	[1]	1	0.52	938.51	16.58	ok	24.65	nan	nan	nan	nan
14	0.7681--1.1522	[1]	1	0.51	503.05	16.58	ok	24.65	nan	nan	nan	nan
15	0.7703--1.1555	[1]	1	0.51	1510.38	16.58	ok	24.65	nan	nan	nan	nan

Harmonic results, beta = 1.0:

Mode	wd +- 20%	Matching	Chosen seg.	beta	Acr (b=1.0)	std(N)/0.4 [MN]	Onset	N [MN]	y0	y0*	Sz [MPa]	Sz* [MPa]
5	0.3226--0.4839	[1]	1	1.22	92.79	16.58	ok	24.65	nan	nan	nan	nan
6	0.3967--0.5951	[1]	1	0.99	169.67	16.58	ok	24.65	nan	nan	nan	nan
7	0.4213--0.6319	[1]	1	0.93	113.26	16.58	ok	24.65	nan	nan	nan	nan

Harmonic results, beta = 2.0:

Mode	wd +- 20%	Matching	Chosen seg.	beta	Acr (b=2.0)	std(N)/0.4 [MN]	Onset	N [MN]	y0	y0*	Sz [MPa]	Sz* [MPa]
4	0.2290--0.3435	[1]	1	1.72	6.11	16.58	fails	24.65	17.09	27.05	475.26	752.05

RESULTS SUMMARY - PARAMETRIC RESONANCE

****

CONCEPT: K11_07

PSD type: 10000-year swell

Computed 2019-08-07 13:04:19

Analysis settings:

Parameter	Value
Bandwidth drop definition [%]	5.00
Natural frequency uncertainty [%]	20.00
N uncertainty (results with *) [%]	20.00
c_quad uncertainty (results with *) [%]	20.00
Rayleigh exceedance probability	1.0e-01
Considered frequency ratios (beta)	[0.5, 1.0, 2.0]
Considered modes	1-15

Spectral density information

				Trigger ranges		
Segment no.	std(N) [MN]	Harmonic amplitude [MN]	omega_peak [rad/s]	beta=0.5	beta=1.0	beta=2.0
1	8.8758	19.0472	0.4919	0.9570--1.0089	0.4785--0.5045	0.2393--0.2522

Modal parameters:

Mode	wd [rad/s]	Td [s]	xi0 [%]	xi w/ae [%]	m [t]	k [kN/m]	k/kg_hat [MN]	c_quad [kN/(m/s)^2]	Acr (b=2) [MN]
1	0.06	106.71	0.46	0.46	86861.19	301.18	77.90	182.65	1.44
2	0.11	57.01	0.47	0.47	50720.18	616.18	127.38	97.24	2.39
3	0.20	31.82	0.47	0.47	84224.29	3283.29	217.55	194.84	4.09
4	0.29	21.95	0.49	0.49	57026.00	4671.88	309.30	117.78	6.11
5	0.40	15.58	0.64	0.64	69969.03	11378.29	409.73	188.63	10.51
6	0.50	12.67	0.82	0.82	53488.46	13154.78	662.60	155.97	21.72
7	0.53	11.93	1.03	1.03	71046.89	19702.94	393.78	262.00	16.29
8	0.66	9.45	2.01	2.01	60209.18	26627.45	651.31	153.99	52.35
9	0.70	8.96	1.36	1.36	38002.73	18697.01	380.95	35.27	20.66

10	0.82	7.70	2.89	2.89	59522.93	39668.29	512.28	157.23	59.31
11	0.85	7.40	3.72	3.72	100935.96	72869.16	1526.06	10.13	227.38
12	0.89	7.07	2.53	2.53	97312.31	76952.29	922.08	46.54	93.33
13	0.95	6.61	15.72	15.72	6934.80	6424.24	690.12	0.00	433.93
14	0.96	6.54	2.57	2.57	56832.93	52426.12	676.49	58.75	69.54
15	0.96	6.53	12.81	12.81	9886.54	9319.53	1189.12	0.00	609.18

Harmonic results, beta = 0.5:

Mode	wd +- 20%	Matching	Chosen seg.	beta	Acr (b=0.5)	std(N)/0.4 [MN]	Onset	N [MN]	y0	y0*	Sz [MPa]	Sz* [MPa]
10	0.6528--0.9792	[1]	1	0.60	396.34	22.19	ok	19.05	nan	nan	nan	nan
11	0.6793--1.0189	[1]	1	0.58	1284.25	22.19	ok	19.05	nan	nan	nan	nan
12	0.7112--1.0668	[1]	1	0.55	682.15	22.19	ok	19.05	nan	nan	nan	nan
13	0.7604--1.1406	[1]	1	0.52	938.51	22.19	ok	19.05	nan	nan	nan	nan
14	0.7681--1.1522	[1]	1	0.51	503.05	22.19	ok	19.05	nan	nan	nan	nan
15	0.7703--1.1555	[1]	1	0.51	1510.38	22.19	ok	19.05	nan	nan	nan	nan

Harmonic results, beta = 1.0:

Mode	wd +- 20%	Matching	Chosen seg.	beta	Acr (b=1.0)	std(N)/0.4 [MN]	Onset	N [MN]	y0	y0*	Sz [MPa]	Sz* [MPa]
5	0.3226--0.4839	[1]	1	1.22	92.79	22.19	ok	19.05	nan	nan	nan	nan
6	0.3967--0.5951	[1]	1	0.99	169.67	22.19	ok	19.05	nan	nan	nan	nan
7	0.4213--0.6319	[1]	1	0.93	113.26	22.19	ok	19.05	nan	nan	nan	nan

Harmonic results, beta = 2.0:

Mode	wd +- 20%	Matching	Chosen seg.	beta	Acr (b=2.0)	std(N)/0.4 [MN]	Onset	N [MN]	y0	y0*	Sz [MPa]	Sz* [MPa]
4	0.2290--0.3435	[1]	1	1.72	6.11	22.19	fails	19.05	11.93	19.30	331.67	536.66

RESULTS SUMMARY - PARAMETRIC RESONANCE

****

CONCEPT: K11_07

PSD type: 100-year wind sea

Computed 2019-08-07 13:04:18

Analysis settings:

Parameter	Value
Bandwidth drop definition [%]	10.00
Natural frequency uncertainty [%]	20.00
N uncertainty (results with *) [%]	20.00
c_quad uncertainty (results with *) [%]	20.00
Rayleigh exceedance probability	1.0e-03
Considered frequency ratios (beta)	[0.5, 1.0, 2.0]
Considered modes	1-15

Spectral density information

				Trigger ranges		
Segment no.	std(N) [MN]	Harmonic amplitude [MN]	omega_peak [rad/s]	beta=0.5	beta=1.0	beta=2.0
1	2.9840	11.0911	0.9115	1.6134--2.3207	0.8067--1.1603	0.4033--0.5802

Modal parameters:

Mode	wd [rad/s]	Td [s]	xi0 [%]	xi w/ae [%]	m [t]	k [kN/m]	k/kg_hat [MN]	c_quad [kN/(m/s)^2]	Acr (b=2) [MN]
1	0.06	106.71	0.46	4.33	86861.19	301.18	77.90	182.65	13.50
2	0.11	57.01	0.47	2.61	50720.18	616.18	127.38	97.24	13.29
3	0.20	31.82	0.47	1.72	84224.29	3283.29	217.55	194.84	14.97
4	0.29	21.95	0.49	1.31	57026.00	4671.88	309.30	117.78	16.25
5	0.40	15.58	0.64	1.22	69969.03	11378.29	409.73	188.63	20.01
6	0.50	12.67	0.82	1.15	53488.46	13154.78	662.60	155.97	30.47
7	0.53	11.93	1.03	1.41	71046.89	19702.94	393.78	262.00	22.27
8	0.66	9.45	2.01	2.30	60209.18	26627.45	651.31	153.99	59.90
9	0.70	8.96	1.36	1.61	38002.73	18697.01	380.95	35.27	24.47

10	0.82	7.70	2.89	3.11	59522.93	39668.29	512.28	157.23	63.82
11	0.85	7.40	3.72	3.82	100935.96	72869.16	1526.06	10.13	233.48
12	0.89	7.07	2.53	2.62	97312.31	76952.29	922.08	46.54	96.65
13	0.95	6.61	15.72	15.72	6934.80	6424.24	690.12	0.00	433.93
14	0.96	6.54	2.57	2.57	56832.93	52426.12	676.49	58.75	69.54
15	0.96	6.53	12.81	12.81	9886.54	9319.53	1189.12	0.00	609.18

Harmonic results, beta = 0.5:
None of the considered modes are within frequency range.

Harmonic results, beta = 1.0:

Mode	wd +- 20%	Matching	Chosen seg.	beta	Acr (b=1.0)	std(N)/0.4 [MN]	Onset	N [MN]	y0	y0*	Sz [MPa]	Sz* [MPa]
9	0.5611--0.8416	[1]	1	1.30	136.53	7.46	ok	11.09	nan	nan	nan	nan
10	0.6528--0.9792	[1]	1	1.12	255.71	7.46	ok	11.09	nan	nan	nan	nan
11	0.6793--1.0189	[1]	1	1.07	844.16	7.46	ok	11.09	nan	nan	nan	nan
12	0.7112--1.0668	[1]	1	1.03	422.19	7.46	ok	11.09	nan	nan	nan	nan
13	0.7604--1.1406	[1]	1	0.96	773.90	7.46	ok	11.09	nan	nan	nan	nan
14	0.7681--1.1522	[1]	1	0.95	306.74	7.46	ok	11.09	nan	nan	nan	nan
15	0.7703--1.1555	[1]	1	0.95	1203.65	7.46	ok	11.09	nan	nan	nan	nan

Harmonic results, beta = 2.0:

Mode	wd +- 20%	Matching	Chosen seg.	beta	Acr (b=2.0)	std(N)/0.4 [MN]	Onset	N [MN]	y0	y0*	Sz [MPa]	Sz* [MPa]
5	0.3226--0.4839	[1]	1	2.26	20.01	7.46	ok	11.09	0.00	0.00	0.00	0.00
6	0.3967--0.5951	[1]	1	1.84	30.47	7.46	ok	11.09	0.00	0.00	0.00	0.00
7	0.4213--0.6319	[1]	1	1.73	22.27	7.46	ok	11.09	0.00	0.00	0.00	0.00
8	0.5319--0.7979	[1]	1	1.37	59.90	7.46	ok	11.09	0.00	0.00	0.00	0.00
9	0.5611--0.8416	[1]	1	1.30	24.47	7.46	ok	11.09	0.00	0.00	0.00	0.00

RESULTS SUMMARY - PARAMETRIC RESONANCE

****

CONCEPT: K11_07

PSD type: 10000-year wind sea

Computed 2019-08-07 13:04:18

Analysis settings:

Parameter	Value
Bandwidth drop definition [%]	10.00
Natural frequency uncertainty [%]	20.00
N uncertainty (results with *) [%]	20.00
c_quad uncertainty (results with *) [%]	20.00
Rayleigh exceedance probability	1.0e-01
Considered frequency ratios (beta)	[0.5, 1.0, 2.0]
Considered modes	1-15

Spectral density information

				Trigger ranges		
Segment no.	std(N) [MN]	Harmonic amplitude [MN]	omega_peak [rad/s]	beta=0.5	beta=1.0	beta=2.0
1	5.3335	11.4456	0.6821	1.2978--1.4485	0.6489--0.7242	0.3244--0.3621
2	7.0266	15.0789	0.9022	1.5689--2.0751	0.7845--1.0375	0.3922--0.5188

Modal parameters:

Mode	wd [rad/s]	Td [s]	xi0 [%]	xi w/ae [%]	m [t]	k [kN/m]	k/kg_hat [MN]	c_quad [kN/(m/s)^2]	Acr (b=2) [MN]
1	0.06	106.71	0.46	5.06	86861.19	301.18	77.90	182.65	15.78
2	0.11	57.01	0.47	3.12	50720.18	616.18	127.38	97.24	15.89
3	0.20	31.82	0.47	2.01	84224.29	3283.29	217.55	194.84	17.50
4	0.29	21.95	0.49	1.50	57026.00	4671.88	309.30	117.78	18.61
5	0.40	15.58	0.64	1.35	69969.03	11378.29	409.73	188.63	22.14
6	0.50	12.67	0.82	1.21	53488.46	13154.78	662.60	155.97	32.06
7	0.53	11.93	1.03	1.49	71046.89	19702.94	393.78	262.00	23.53
8	0.66	9.45	2.01	2.37	60209.18	26627.45	651.31	153.99	61.73

9	0.70	8.96	1.36	1.67	38002.73	18697.01	380.95	35.27	25.38
10	0.82	7.70	2.89	3.16	59522.93	39668.29	512.28	157.23	64.84
11	0.85	7.40	3.72	3.96	100935.96	72869.16	1526.06	10.13	242.03
12	0.89	7.07	2.53	2.65	97312.31	76952.29	922.08	46.54	97.76
13	0.95	6.61	15.72	15.72	6934.80	6424.24	690.12	0.00	433.93
14	0.96	6.54	2.57	2.57	56832.93	52426.12	676.49	58.75	69.54
15	0.96	6.53	12.81	12.81	9886.54	9319.53	1189.12	0.00	609.18

Harmonic results, beta = 0.5:
None of the considered modes are within frequency range.

Harmonic results, beta = 1.0:

Mode	wd +- 20%	Matching	Chosen seg.	beta	Acr (b=1.0)	std(N)/0.4 [MN]	Onset	N [MN]	y0	y0*	Sz [MPa]	Sz* [MPa]
8	0.5319--0.7979	[1, 2]	2	1.36	283.56	17.57	ok	15.08	nan	nan	nan	nan
9	0.5611--0.8416	[1, 2]	2	1.29	139.06	17.57	ok	15.08	nan	nan	nan	nan
10	0.6528--0.9792	[1, 2]	2	1.11	257.75	17.57	ok	15.08	nan	nan	nan	nan
11	0.6793--1.0189	[1, 2]	2	1.06	859.47	17.57	ok	15.08	nan	nan	nan	nan
12	0.7112--1.0668	[1, 2]	2	1.01	424.60	17.57	ok	15.08	nan	nan	nan	nan
13	0.7604--1.1406	[2]	2	0.95	773.90	17.57	ok	15.08	nan	nan	nan	nan
14	0.7681--1.1522	[2]	2	0.94	306.74	17.57	ok	15.08	nan	nan	nan	nan
15	0.7703--1.1555	[2]	2	0.94	1203.65	17.57	ok	15.08	nan	nan	nan	nan

Harmonic results, beta = 2.0:

Mode	wd +- 20%	Matching	Chosen seg.	beta	Acr (b=2.0)	std(N)/0.4 [MN]	Onset	N [MN]	y0	y0*	Sz [MPa]	Sz* [MPa]
4	0.2290--0.3435	[1]	1	2.38	18.61	13.33	ok	11.45	0.00	0.00	0.00	0.00
5	0.3226--0.4839	[1, 2]	2	2.24	22.14	17.57	ok	15.08	0.00	0.00	0.00	0.00
6	0.3967--0.5951	[2]	2	1.82	32.06	17.57	ok	15.08	0.00	0.00	0.00	0.00
7	0.4213--0.6319	[2]	2	1.71	23.53	17.57	ok	15.08	0.00	0.00	0.00	0.00

RESULTS SUMMARY - PARAMETRIC EXCITATION

****

CONCEPT: K11_07

PSD type: 100-year wind

Computed 2019-05-24 07:38:48

Analysis settings:

Parameter	Value
Error margin on freqs (both in pair) [%]	10.0
Considered frequency ratios (beta)	[2.0, 1.0, 0.5]
Considered modes	1-12
Maximum Acr for listing [MN]	1000.0
Minimum std(N) for listing [MN]	0.0

Axial force information:

Mode	std(N) [MN]
1	0.00
2	1.42
3	0.00
4	0.93
5	0.00
6	2.29
7	0.00
8	0.00
9	0.94
10	0.00
11	0.78
12	0.00

Modal parameters:

Mode	wd [rad/s]	Td [s]	xi0 [%]	xi w/ae [%]	m [t]	k [kN/m]	k/kg_hat [MN]	c_quad [kN/(m/s)^2]	Acr (b=2) [MN]
1	0.06	106.71	0.46	4.38	86861.19	301.18	77.90	182.65	13.66

2	0.11	57.01	0.47	2.77	50720.18	616.18	127.38	97.24	14.11
3	0.20	31.82	0.47	1.87	84224.29	3283.29	217.55	194.84	16.28
4	0.29	21.95	0.49	1.42	57026.00	4671.88	309.30	117.78	17.62
5	0.40	15.58	0.64	1.30	69969.03	11378.29	409.73	188.63	21.32
6	0.50	12.67	0.82	1.19	53488.46	13154.78	662.60	155.97	31.53
7	0.53	11.93	1.03	1.47	71048.18	19703.30	393.79	261.97	23.22
8	0.66	9.45	2.01	2.34	60209.18	26627.45	651.31	153.99	60.95
9	0.70	8.96	1.36	1.66	37999.81	18695.57	380.89	35.24	25.23
10	0.82	7.70	2.89	3.14	59522.93	39668.29	512.28	157.23	64.44
11	0.85	7.40	3.72	3.82	100865.88	72818.56	1524.36	10.07	233.22
12	0.89	7.07	2.53	2.64	97312.31	76952.29	922.08	46.54	97.39

Harmonic results (showing results with Acr < 1000MN and std(N) > 0MN):

Axial force mode	Triggered mode	beta	xi w/aero [%]	beta for Acr	Acr	std(N)/0.4	onset
2	1	1.87	4.38	2.00	13.66	3.55	ok
6	4	1.73	1.42	2.00	17.62	5.72	ok
9	5	1.74	1.30	2.00	21.32	2.35	ok
11	5	2.11	1.30	2.00	21.32	1.95	ok
11	6	1.71	1.19	2.00	31.53	1.95	ok
2	2	1.00	2.77	1.00	59.95	3.55	ok
4	4	1.00	1.42	1.00	104.39	2.33	ok
6	6	1.00	1.19	1.00	204.41	5.72	ok
6	7	0.94	1.47	1.00	135.23	5.72	ok
9	8	1.05	2.34	1.00	281.76	2.35	ok
9	9	1.00	1.66	1.00	138.62	2.35	ok
9	10	0.86	3.14	1.00	256.94	2.35	ok
9	11	0.83	3.82	1.00	843.22	2.35	ok
11	9	1.21	1.66	1.00	138.62	1.95	ok
11	10	1.04	3.14	1.00	256.94	1.95	ok
11	11	1.00	3.82	1.00	843.22	1.95	ok
11	12	0.96	2.64	1.00	423.80	1.95	ok
2	3	0.56	1.87	0.50	145.52	3.55	ok
4	6	0.58	1.19	0.50	381.15	2.33	ok
4	7	0.54	1.47	0.50	243.30	2.33	ok
4	8	0.43	2.34	0.50	469.38	2.33	ok
6	10	0.61	3.14	0.50	407.44	5.72	ok

6	12	0.56	2.64	0.50	691.90	5.72	ok

RESULTS SUMMARY - PARAMETRIC EXCITATION

****

CONCEPT: K11_07

PSD type: 10000-year wind

Computed 2019-05-24 07:38:51

Analysis settings:

Parameter	Value
Error margin on freqs (both in pair) [%]	10.0
Considered frequency ratios (beta)	[2.0, 1.0, 0.5]
Considered modes	1-12
Maximum Acr for listing [MN]	1000.0
Minimum std(N) for listing [MN]	0.0

Axial force information:

Mode	std(N) [MN]
1	0.00
2	2.40
3	0.00
4	1.69
5	0.00
6	4.22
7	0.00
8	1.70
9	1.66
10	0.00
11	0.00
12	0.00

Modal parameters:

Mode	wd [rad/s]	Td [s]	xi0 [%]	xi w/ae [%]	m [t]	k [kN/m]	k/kg_hat [MN]	c_quad [kN/(m/s)^2]	Acr (b=2) [MN]
1	0.06	106.71	0.46	5.06	86861.19	301.18	77.90	182.65	15.78

2	0.11	57.01	0.47	3.19	50720.18	616.18	127.38	97.24	16.25
3	0.20	31.82	0.47	2.14	84224.29	3283.29	217.55	194.84	18.63
4	0.29	21.95	0.49	1.60	57026.00	4671.88	309.30	117.78	19.84
5	0.40	15.58	0.64	1.43	69969.03	11378.29	409.73	188.63	23.45
6	0.50	12.67	0.82	1.27	53488.46	13154.78	662.60	155.97	33.65
7	0.53	11.93	1.03	1.57	71048.18	19703.30	393.79	261.97	24.79
8	0.66	9.45	2.01	2.39	60209.18	26627.45	651.31	153.99	62.25
9	0.70	8.96	1.36	1.73	37999.81	18695.57	380.89	35.24	26.29
10	0.82	7.70	2.89	3.20	59522.93	39668.29	512.28	157.23	65.66
11	0.85	7.40	3.72	3.96	100865.88	72818.56	1524.36	10.07	241.76
12	0.89	7.07	2.53	2.65	97312.31	76952.29	922.08	46.54	97.76

Harmonic results (showing results with Acr < 1000MN and std(N) > 0MN):

Axial force mode	Triggered mode	beta	xi w/aero [%]	beta for Acr	Acr	std(N)/0.4	onset
2	1	1.87	5.06	2.00	15.78	6.00	ok
6	4	1.73	1.60	2.00	19.84	10.55	ok
8	4	2.32	1.60	2.00	19.84	4.25	ok
8	5	1.65	1.43	2.00	23.45	4.25	ok
9	5	1.74	1.43	2.00	23.45	4.15	ok
2	2	1.00	3.19	1.00	64.33	6.00	ok
4	4	1.00	1.60	1.00	110.79	4.22	ok
6	6	1.00	1.27	1.00	211.17	10.55	ok
6	7	0.94	1.57	1.00	139.74	10.55	ok
8	8	1.00	2.39	1.00	284.76	4.25	ok
8	9	0.95	1.73	1.00	141.52	4.25	ok
9	8	1.05	2.39	1.00	284.76	4.15	ok
9	9	1.00	1.73	1.00	141.52	4.15	ok
9	10	0.86	3.20	1.00	259.38	4.15	ok
9	11	0.83	3.96	1.00	858.51	4.15	ok
2	3	0.56	2.14	0.50	152.21	6.00	ok
4	6	0.58	1.27	0.50	389.51	4.22	ok
4	7	0.54	1.57	0.50	248.68	4.22	ok
4	8	0.43	2.39	0.50	472.70	4.22	ok
6	10	0.61	3.20	0.50	410.02	10.55	ok
6	12	0.56	2.65	0.50	692.77	10.55	ok

RESULTS SUMMARY - PARAMETRIC RESONANCE

****

CONCEPT: K12_06

PSD type: 100-year swell

Computed 2019-08-07 13:04:21

Analysis settings:

Parameter	Value
Bandwidth drop definition [%]	5.00
Natural frequency uncertainty [%]	20.00
N uncertainty (results with *) [%]	20.00
c_quad uncertainty (results with *) [%]	20.00
Rayleigh exceedance probability	1.0e-03
Considered frequency ratios (beta)	[0.5, 1.0, 2.0]
Considered modes	1-15

Spectral density information

				Trigger ranges		
Segment no.	std(N) [MN]	Harmonic amplitude [MN]	omega_peak [rad/s]	beta=0.5	beta=1.0	beta=2.0
1	4.1506	15.4273	0.4652	0.8712--1.0100	0.4356--0.5050	0.2178--0.2525

Modal parameters:

Mode	wd [rad/s]	Td [s]	xi0 [%]	xi w/ae [%]	m [t]	k [kN/m]	k/kg_hat [MN]	c_quad [kN/(m/s)^2]	Acr (b=2) [MN]
1	0.11	56.33	0.46	0.46	72341.62	899.97	271.56	1029.16	5.01
2	0.14	43.67	0.47	0.47	65155.69	1348.79	222.29	1997.42	4.16
3	0.20	31.02	0.47	0.47	61397.77	2518.65	231.43	1543.34	4.37
4	0.29	21.45	0.50	0.50	56695.90	4864.99	345.76	3010.01	6.92
5	0.37	16.87	0.58	0.58	70670.59	9805.43	362.92	301.86	8.45
6	0.47	13.38	0.82	0.82	50298.51	11087.37	737.62	1928.69	24.14
7	0.49	12.70	0.86	0.86	77397.46	18937.55	503.90	2567.94	17.33
8	0.61	10.26	1.75	1.75	62038.05	23258.08	620.75	2236.82	43.44
9	0.67	9.36	1.28	1.28	42990.14	19386.08	225.83	73.36	11.52

10	0.75	8.38	2.56	2.56	54740.63	30828.42	670.37	1445.16	68.60
11	0.81	7.74	2.97	2.97	66774.21	44081.78	929.87	466.52	110.54
12	0.84	7.44	2.90	2.90	72999.48	52135.35	770.70	840.29	89.53
13	0.90	7.00	2.95	2.95	58100.91	46847.41	693.84	344.63	81.88
14	0.91	6.89	9.34	9.34	18375.07	15413.27	1359.12	1391.72	507.56
15	0.91	6.89	9.32	9.32	14259.44	11973.47	1526.06	1066.60	568.63

Harmonic results, beta = 0.5:

Mode	wd +- 20%	Matching	Chosen seg.	beta	Acr (b=0.5)	std(N)/0.4 [MN]	Onset	N [MN]	y0	y0*	Sz [MPa]	Sz* [MPa]
10	0.6002--0.9002	[1]	1	0.62	497.74	10.38	ok	15.43	nan	nan	nan	nan
11	0.6497--0.9746	[1]	1	0.57	725.78	10.38	ok	15.43	nan	nan	nan	nan
12	0.6758--1.0137	[1]	1	0.55	596.94	10.38	ok	15.43	nan	nan	nan	nan
13	0.7180--1.0771	[1]	1	0.52	540.24	10.38	ok	15.43	nan	nan	nan	nan
14	0.7295--1.0942	[1]	1	0.51	1553.66	10.38	ok	15.43	nan	nan	nan	nan
15	0.7299--1.0948	[1]	1	0.51	1743.19	10.38	ok	15.43	nan	nan	nan	nan

Harmonic results, beta = 1.0:

Mode	wd +- 20%	Matching	Chosen seg.	beta	Acr (b=1.0)	std(N)/0.4 [MN]	Onset	N [MN]	y0	y0*	Sz [MPa]	Sz* [MPa]
5	0.2980--0.4470	[1]	1	1.25	78.30	10.38	ok	15.43	nan	nan	nan	nan
6	0.3756--0.5634	[1]	1	0.99	188.71	10.38	ok	15.43	nan	nan	nan	nan
7	0.3957--0.5936	[1]	1	0.94	132.17	10.38	ok	15.43	nan	nan	nan	nan
8	0.4898--0.7346	[1]	1	0.76	232.24	10.38	ok	15.43	nan	nan	nan	nan

Harmonic results, beta = 2.0:

Mode	wd +- 20%	Matching	Chosen seg.	beta	Acr (b=2.0)	std(N)/0.4 [MN]	Onset	N [MN]	y0	y0*	Sz [MPa]	Sz* [MPa]
3	0.1620--0.2430	[1]	1	2.30	4.37	10.38	fails	15.43	1.12	1.79	25.85	41.32
4	0.2343--0.3515	[1]	1	1.59	6.92	10.38	fails	15.43	0.27	0.46	7.98	13.59

RESULTS SUMMARY - PARAMETRIC RESONANCE

****

CONCEPT: K12_06

PSD type: 10000-year swell

Computed 2019-08-07 13:04:21

Analysis settings:

Parameter	Value
Bandwidth drop definition [%]	5.00
Natural frequency uncertainty [%]	20.00
N uncertainty (results with *) [%]	20.00
c_quad uncertainty (results with *) [%]	20.00
Rayleigh exceedance probability	1.0e-01
Considered frequency ratios (beta)	[0.5, 1.0, 2.0]
Considered modes	1-15

Spectral density information

				Trigger ranges		
Segment no.	std(N) [MN]	Harmonic amplitude [MN]	omega_peak [rad/s]	beta=0.5	beta=1.0	beta=2.0
1	5.2741	11.3180	0.4664	0.8684--1.0125	0.4342--0.5062	0.2171--0.2531

Modal parameters:

Mode	wd [rad/s]	Td [s]	xi0 [%]	xi w/ae [%]	m [t]	k [kN/m]	k/kg_hat [MN]	c_quad [kN/(m/s)^2]	Acr (b=2) [MN]
1	0.11	56.33	0.46	0.46	72341.62	899.97	271.56	1029.16	5.01
2	0.14	43.67	0.47	0.47	65155.69	1348.79	222.29	1997.42	4.16
3	0.20	31.02	0.47	0.47	61397.77	2518.65	231.43	1543.34	4.37
4	0.29	21.45	0.50	0.50	56695.90	4864.99	345.76	3010.01	6.92
5	0.37	16.87	0.58	0.58	70670.59	9805.43	362.92	301.86	8.45
6	0.47	13.38	0.82	0.82	50298.51	11087.37	737.62	1928.69	24.14
7	0.49	12.70	0.86	0.86	77397.46	18937.55	503.90	2567.94	17.33
8	0.61	10.26	1.75	1.75	62038.05	23258.08	620.75	2236.82	43.44
9	0.67	9.36	1.28	1.28	42990.14	19386.08	225.83	73.36	11.52

10	0.75	8.38	2.56	2.56	54740.63	30828.42	670.37	1445.16	68.60
11	0.81	7.74	2.97	2.97	66774.21	44081.78	929.87	466.52	110.54
12	0.84	7.44	2.90	2.90	72999.48	52135.35	770.70	840.29	89.53
13	0.90	7.00	2.95	2.95	58100.91	46847.41	693.84	344.63	81.88
14	0.91	6.89	9.34	9.34	18375.07	15413.27	1359.12	1391.72	507.56
15	0.91	6.89	9.32	9.32	14259.44	11973.47	1526.06	1066.60	568.63

Harmonic results, beta = 0.5:

Mode	wd +- 20%	Matching	Chosen seg.	beta	Acr (b=0.5)	std(N)/0.4 [MN]	Onset	N [MN]	y0	y0*	Sz [MPa]	Sz* [MPa]
10	0.6002--0.9002	[1]	1	0.62	497.74	13.19	ok	11.32	nan	nan	nan	nan
11	0.6497--0.9746	[1]	1	0.57	725.78	13.19	ok	11.32	nan	nan	nan	nan
12	0.6758--1.0137	[1]	1	0.55	596.94	13.19	ok	11.32	nan	nan	nan	nan
13	0.7180--1.0771	[1]	1	0.52	540.24	13.19	ok	11.32	nan	nan	nan	nan
14	0.7295--1.0942	[1]	1	0.51	1553.66	13.19	ok	11.32	nan	nan	nan	nan
15	0.7299--1.0948	[1]	1	0.51	1743.19	13.19	ok	11.32	nan	nan	nan	nan

Harmonic results, beta = 1.0:

Mode	wd +- 20%	Matching	Chosen seg.	beta	Acr (b=1.0)	std(N)/0.4 [MN]	Onset	N [MN]	y0	y0*	Sz [MPa]	Sz* [MPa]
5	0.2980--0.4470	[1]	1	1.25	78.30	13.19	ok	11.32	nan	nan	nan	nan
6	0.3756--0.5634	[1]	1	0.99	188.71	13.19	ok	11.32	nan	nan	nan	nan
7	0.3957--0.5936	[1]	1	0.94	132.17	13.19	ok	11.32	nan	nan	nan	nan
8	0.4898--0.7346	[1]	1	0.76	232.24	13.19	ok	11.32	nan	nan	nan	nan

Harmonic results, beta = 2.0:

Mode	wd +- 20%	Matching	Chosen seg.	beta	Acr (b=2.0)	std(N)/0.4 [MN]	Onset	N [MN]	y0	y0*	Sz [MPa]	Sz* [MPa]
3	0.1620--0.2430	[1]	1	2.30	4.37	13.19	fails	11.32	0.70	1.17	16.24	26.92
4	0.2343--0.3515	[1]	1	1.59	6.92	13.19	fails	11.32	0.14	0.27	4.12	7.81

RESULTS SUMMARY - PARAMETRIC RESONANCE

****

CONCEPT: K12_06

PSD type: 100-year wind sea

Computed 2019-08-07 13:04:21

Analysis settings:

Parameter	Value
Bandwidth drop definition [%]	10.00
Natural frequency uncertainty [%]	20.00
N uncertainty (results with *) [%]	20.00
c_quad uncertainty (results with *) [%]	20.00
Rayleigh exceedance probability	1.0e-03
Considered frequency ratios (beta)	[0.5, 1.0, 2.0]
Considered modes	1-15

Spectral density information

				Trigger ranges		
Segment no.	std(N) [MN]	Harmonic amplitude [MN]	omega_peak [rad/s]	beta=0.5	beta=1.0	beta=2.0
1	2.5415	9.4467	0.8883	1.6134--2.3951	0.8067--1.1976	0.4033--0.5988

Modal parameters:

Mode	wd [rad/s]	Td [s]	xi0 [%]	xi w/ae [%]	m [t]	k [kN/m]	k/kg_hat [MN]	c_quad [kN/(m/s)^2]	Acr (b=2) [MN]
1	0.11	56.33	0.46	2.39	72341.62	899.97	271.56	1029.16	25.97
2	0.14	43.67	0.47	2.09	65155.69	1348.79	222.29	1997.42	18.56
3	0.20	31.02	0.47	1.59	61397.77	2518.65	231.43	1543.34	14.73
4	0.29	21.45	0.50	1.24	56695.90	4864.99	345.76	3010.01	17.16
5	0.37	16.87	0.58	1.21	70670.59	9805.43	362.92	301.86	17.59
6	0.47	13.38	0.82	1.31	50298.51	11087.37	737.62	1928.69	38.60
7	0.49	12.70	0.86	1.22	77397.46	18937.55	503.90	2567.94	24.59
8	0.61	10.26	1.75	2.07	62038.05	23258.08	620.75	2236.82	51.39
9	0.67	9.36	1.28	1.53	42990.14	19386.08	225.83	73.36	13.78

10	0.75	8.38	2.56	2.80	54740.63	30828.42	670.37	1445.16	75.04
11	0.81	7.74	2.97	3.09	66774.21	44081.78	929.87	466.52	115.00
12	0.84	7.44	2.90	3.04	72999.48	52135.35	770.70	840.29	93.85
13	0.90	7.00	2.95	2.95	58100.91	46847.41	693.84	344.63	81.88
14	0.91	6.89	9.34	9.34	18375.07	15413.27	1359.12	1391.72	507.56
15	0.91	6.89	9.32	9.32	14259.44	11973.47	1526.06	1066.60	568.63

Harmonic results, beta = 0.5:
None of the considered modes are within frequency range.

Harmonic results, beta = 1.0:

Mode	wd +- 20%	Matching	Chosen seg.	beta	Acr (b=1.0)	std(N)/0.4 [MN]	Onset	N [MN]	y0	y0*	Sz [MPa]	Sz* [MPa]
10	0.6002--0.9002	[1]	1	1.18	317.18	6.35	ok	9.45	nan	nan	nan	nan
11	0.6497--0.9746	[1]	1	1.09	462.47	6.35	ok	9.45	nan	nan	nan	nan
12	0.6758--1.0137	[1]	1	1.05	380.34	6.35	ok	9.45	nan	nan	nan	nan
13	0.7180--1.0771	[1]	1	0.99	337.09	6.35	ok	9.45	nan	nan	nan	nan
14	0.7295--1.0942	[1]	1	0.97	1174.60	6.35	ok	9.45	nan	nan	nan	nan
15	0.7299--1.0948	[1]	1	0.97	1317.40	6.35	ok	9.45	nan	nan	nan	nan

Harmonic results, beta = 2.0:

Mode	wd +- 20%	Matching	Chosen seg.	beta	Acr (b=2.0)	std(N)/0.4 [MN]	Onset	N [MN]	y0	y0*	Sz [MPa]	Sz* [MPa]
5	0.2980--0.4470	[1]	1	2.38	17.59	6.35	ok	9.45	0.00	0.00	0.00	0.00
6	0.3756--0.5634	[1]	1	1.89	38.60	6.35	ok	9.45	0.00	0.00	0.00	0.00
7	0.3957--0.5936	[1]	1	1.80	24.59	6.35	ok	9.45	0.00	0.00	0.00	0.00
8	0.4898--0.7346	[1]	1	1.45	51.39	6.35	ok	9.45	0.00	0.00	0.00	0.00
9	0.5372--0.8058	[1]	1	1.32	13.78	6.35	ok	9.45	0.00	0.00	0.00	0.00

RESULTS SUMMARY - PARAMETRIC RESONANCE

****

CONCEPT: K12_06

PSD type: 10000-year wind sea

Computed 2019-08-07 13:04:20

Analysis settings:

Parameter	Value
Bandwidth drop definition [%]	10.00
Natural frequency uncertainty [%]	20.00
N uncertainty (results with *) [%]	20.00
c_quad uncertainty (results with *) [%]	20.00
Rayleigh exceedance probability	1.0e-01
Considered frequency ratios (beta)	[0.5, 1.0, 2.0]
Considered modes	1-15

Spectral density information

				Trigger ranges		
Segment no.	std(N) [MN]	Harmonic amplitude [MN]	omega_peak [rad/s]	beta=0.5	beta=1.0	beta=2.0
1	2.3096	4.9563	0.6826	1.2993--1.5752	0.6497--0.7876	0.3248--0.3938
2	6.2421	13.3954	0.8890	1.5851--2.1175	0.7926--1.0588	0.3963--0.5294

Modal parameters:

Mode	wd [rad/s]	Td [s]	xi0 [%]	xi w/ae [%]	m [t]	k [kN/m]	k/kg_hat [MN]	c_quad [kN/(m/s)^2]	Acr (b=2) [MN]
1	0.11	56.33	0.46	2.83	72341.62	899.97	271.56	1029.16	30.75
2	0.14	43.67	0.47	2.46	65155.69	1348.79	222.29	1997.42	21.85
3	0.20	31.02	0.47	1.85	61397.77	2518.65	231.43	1543.34	17.14
4	0.29	21.45	0.50	1.41	56695.90	4864.99	345.76	3010.01	19.51
5	0.37	16.87	0.58	1.36	70670.59	9805.43	362.92	301.86	19.77
6	0.47	13.38	0.82	1.42	50298.51	11087.37	737.62	1928.69	41.84
7	0.49	12.70	0.86	1.29	77397.46	18937.55	503.90	2567.94	26.00
8	0.61	10.26	1.75	2.14	62038.05	23258.08	620.75	2236.82	53.13

9	0.67	9.36	1.28	1.59	42990.14	19386.08	225.83	73.36	14.32
10	0.75	8.38	2.56	2.85	54740.63	30828.42	670.37	1445.16	76.38
11	0.81	7.74	2.97	3.11	66774.21	44081.78	929.87	466.52	115.75
12	0.84	7.44	2.90	3.07	72999.48	52135.35	770.70	840.29	94.77
13	0.90	7.00	2.95	2.95	58100.91	46847.41	693.84	344.63	81.88
14	0.91	6.89	9.34	9.34	18375.07	15413.27	1359.12	1391.72	507.56
15	0.91	6.89	9.32	9.32	14259.44	11973.47	1526.06	1066.60	568.63

Harmonic results, beta = 0.5:
None of the considered modes are within frequency range.

Harmonic results, beta = 1.0:

Mode	wd +- 20%	Matching	Chosen seg.	beta	Acr (b=1.0)	std(N)/0.4 [MN]	Onset	N [MN]	y0	y0*	Sz [MPa]	Sz* [MPa]
8	0.4898--0.7346	[1]	1	1.11	256.82	5.77	ok	4.96	nan	nan	nan	nan
9	0.5372--0.8058	[1, 2]	2	1.32	80.43	15.61	ok	13.40	nan	nan	nan	nan
10	0.6002--0.9002	[1, 2]	2	1.18	320.00	15.61	ok	13.40	nan	nan	nan	nan
11	0.6497--0.9746	[1, 2]	2	1.09	463.96	15.61	ok	13.40	nan	nan	nan	nan
12	0.6758--1.0137	[1, 2]	2	1.05	382.21	15.61	ok	13.40	nan	nan	nan	nan
13	0.7180--1.0771	[1, 2]	2	0.99	337.09	15.61	ok	13.40	nan	nan	nan	nan
14	0.7295--1.0942	[1, 2]	2	0.97	1174.60	15.61	ok	13.40	nan	nan	nan	nan
15	0.7299--1.0948	[1, 2]	2	0.97	1317.40	15.61	ok	13.40	nan	nan	nan	nan

Harmonic results, beta = 2.0:

Mode	wd +- 20%	Matching	Chosen seg.	beta	Acr (b=2.0)	std(N)/0.4 [MN]	Onset	N [MN]	y0	y0*	Sz [MPa]	Sz* [MPa]
4	0.2343--0.3515	[1]	1	2.33	19.51	5.77	ok	4.96	0.00	0.00	0.00	0.00
5	0.2980--0.4470	[1, 2]	2	2.39	19.77	15.61	ok	13.40	0.00	0.00	0.00	0.00
6	0.3756--0.5634	[1, 2]	2	1.89	41.84	15.61	ok	13.40	0.00	0.00	0.00	0.00
7	0.3957--0.5936	[2]	2	1.80	26.00	15.61	ok	13.40	0.00	0.00	0.00	0.00
8	0.4898--0.7346	[2]	2	1.45	53.13	15.61	ok	13.40	0.00	0.00	0.00	0.00

RESULTS SUMMARY - PARAMETRIC EXCITATION

****

CONCEPT: K12_06

PSD type: 100-year wind

Computed 2019-05-24 07:38:59

Analysis settings:

Parameter	Value
Error margin on freqs (both in pair) [%]	10.0
Considered frequency ratios (beta)	[2.0, 1.0, 0.5]
Considered modes	1-12
Maximum Acr for listing [MN]	1000.0
Minimum std(N) for listing [MN]	0.0

Axial force information:

Mode	std(N) [MN]
1	0.00
2	0.00
3	0.00
4	0.55
5	0.00
6	1.49
7	0.51
8	0.00
9	1.06
10	0.00
11	0.00
12	0.50

Modal parameters:

Mode	wd [rad/s]	Td [s]	xi0 [%]	xi w/ae [%]	m [t]	k [kN/m]	k/kg_hat [MN]	c_quad [kN/(m/s)^2]	Acr (b=2) [MN]
1	0.11	56.33	0.46	2.63	72341.62	899.97	271.56	1029.16	28.58

2	0.14	43.67	0.47	2.27	65155.69	1348.79	222.29	1997.42	20.16
3	0.20	31.02	0.47	1.73	61397.77	2518.65	231.43	1543.34	16.03
4	0.29	21.45	0.50	1.34	56695.90	4864.99	345.76	3010.01	18.54
5	0.37	16.87	0.58	1.30	70670.59	9805.43	362.92	301.86	18.90
6	0.47	13.38	0.82	1.38	50298.51	11087.37	737.62	1928.69	40.66
7	0.49	12.70	0.86	1.29	77397.46	18937.55	503.90	2567.94	26.00
8	0.61	10.26	1.75	2.11	62038.05	23258.08	620.75	2236.82	52.38
9	0.67	9.36	1.28	1.57	42990.14	19386.08	225.83	73.36	14.14
10	0.75	8.38	2.56	2.83	54740.63	30828.42	670.37	1445.16	75.84
11	0.81	7.74	2.97	3.10	66774.21	44081.78	929.87	466.52	115.38
12	0.84	7.44	2.90	3.05	72999.48	52135.35	770.70	840.29	94.16

Harmonic results (showing results with Acr < 1000MN and std(N) > 0MN):

Axial force mode	Triggered mode	beta	xi w/aero [%]	beta for Acr	Acr	std(N)/0.4	onset
4	2	2.04	2.27	2.00	20.16	1.38	ok
6	3	2.32	1.73	2.00	16.03	3.73	ok
7	3	2.44	1.73	2.00	16.03	1.27	ok
7	4	1.69	1.34	2.00	18.54	1.27	ok
9	4	2.29	1.34	2.00	18.54	2.65	ok
9	5	1.80	1.30	2.00	18.90	2.65	ok
12	5	2.27	1.30	2.00	18.90	1.25	ok
12	6	1.80	1.38	2.00	40.66	1.25	ok
12	7	1.71	1.29	2.00	26.00	1.25	ok
4	4	1.00	1.34	1.00	113.23	1.38	ok
6	6	1.00	1.38	1.00	244.92	3.73	ok
6	7	0.95	1.29	1.00	161.87	3.73	ok
7	6	1.05	1.38	1.00	244.92	1.27	ok
7	7	1.00	1.29	1.00	161.87	1.27	ok
9	8	1.10	2.11	1.00	255.01	2.65	ok
9	9	1.00	1.57	1.00	79.92	2.65	ok
9	10	0.90	2.83	1.00	318.87	2.65	ok
9	11	0.83	3.10	1.00	463.21	2.65	ok
12	10	1.13	2.83	1.00	318.87	1.25	ok
12	11	1.04	3.10	1.00	463.21	1.25	ok
12	12	1.00	3.05	1.00	380.96	1.25	ok
4	7	0.59	1.29	0.50	297.79	1.38	ok
4	8	0.48	2.11	0.50	432.21	1.38	ok

4	9	0.44	1.57	0.50	142.36	1.38	ok
6	11	0.58	3.10	0.50	736.22	3.73	ok
6	12	0.56	3.05	0.50	607.05	3.73	ok
7	11	0.61	3.10	0.50	736.22	1.27	ok
7	12	0.59	3.05	0.50	607.05	1.27	ok

RESULTS SUMMARY - PARAMETRIC EXCITATION

****

CONCEPT: K12_06

PSD type: 10000-year wind

Computed 2019-05-24 07:38:54

Analysis settings:

Parameter	Value
Error margin on freqs (both in pair) [%]	10.0
Considered frequency ratios (beta)	[2.0, 1.0, 0.5]
Considered modes	1-12
Maximum Acr for listing [MN]	1000.0
Minimum std(N) for listing [MN]	0.0

Axial force information:

Mode	std(N) [MN]
1	0.00
2	0.00
3	0.00
4	0.86
5	0.00
6	2.47
7	0.00
8	0.00
9	1.72
10	0.00
11	0.00
12	0.78

Modal parameters:

Mode	wd [rad/s]	Td [s]	xi0 [%]	xi w/ae [%]	m [t]	k [kN/m]	k/kg_hat [MN]	c_quad [kN/(m/s)^2]	Acr (b=2) [MN]
1	0.11	56.33	0.46	3.06	72341.62	899.97	271.56	1029.16	33.25

2	0.14	43.67	0.47	2.62	65155.69	1348.79	222.29	1997.42	23.28
3	0.20	31.02	0.47	1.98	61397.77	2518.65	231.43	1543.34	18.34
4	0.29	21.45	0.50	1.51	56695.90	4864.99	345.76	3010.01	20.89
5	0.37	16.87	0.58	1.44	70670.59	9805.43	362.92	301.86	20.93
6	0.47	13.38	0.82	1.48	50298.51	11087.37	737.62	1928.69	43.61
7	0.49	12.70	0.86	1.38	77397.46	18937.55	503.90	2567.94	27.81
8	0.61	10.26	1.75	2.19	62038.05	23258.08	620.75	2236.82	54.37
9	0.67	9.36	1.28	1.64	42990.14	19386.08	225.83	73.36	14.77
10	0.75	8.38	2.56	2.89	54740.63	30828.42	670.37	1445.16	77.45
11	0.81	7.74	2.97	3.13	66774.21	44081.78	929.87	466.52	116.49
12	0.84	7.44	2.90	3.08	72999.48	52135.35	770.70	840.29	95.08

Harmonic results (showing results with Acr < 1000MN and std(N) > 0MN):

Axial force mode	Triggered mode	beta	xi w/aero [%]	beta for Acr	Acr	std(N)/0.4	onset
4	2	2.04	2.62	2.00	23.28	2.15	ok
6	3	2.32	1.98	2.00	18.34	6.17	ok
9	4	2.29	1.51	2.00	20.89	4.30	ok
9	5	1.80	1.44	2.00	20.93	4.30	ok
12	5	2.27	1.44	2.00	20.93	1.95	ok
12	6	1.80	1.48	2.00	43.61	1.95	ok
12	7	1.71	1.38	2.00	27.81	1.95	ok
4	4	1.00	1.51	1.00	120.19	2.15	ok
6	6	1.00	1.48	1.00	253.65	6.17	ok
6	7	0.95	1.38	1.00	167.42	6.17	ok
9	8	1.10	2.19	1.00	259.80	4.30	ok
9	9	1.00	1.64	1.00	81.69	4.30	ok
9	10	0.90	2.89	1.00	322.24	4.30	ok
9	11	0.83	3.13	1.00	465.45	4.30	ok
12	10	1.13	2.89	1.00	322.24	1.95	ok
12	11	1.04	3.13	1.00	465.45	1.95	ok
12	12	1.00	3.08	1.00	382.83	1.95	ok
4	7	0.59	1.38	0.50	304.56	2.15	ok
4	8	0.48	2.19	0.50	437.60	2.15	ok
4	9	0.44	1.64	0.50	144.45	2.15	ok
6	11	0.58	3.13	0.50	738.58	6.17	ok
6	12	0.56	3.08	0.50	609.03	6.17	ok

RESULTS SUMMARY - PARAMETRIC RESONANCE

****

CONCEPT: K14_06

PSD type: 100-year swell

Computed 2019-08-07 13:04:26

Analysis settings:

Parameter	Value
Bandwidth drop definition [%]	5.00
Natural frequency uncertainty [%]	20.00
N uncertainty (results with *) [%]	20.00
c_quad uncertainty (results with *) [%]	20.00
Rayleigh exceedance probability	1.0e-03
Considered frequency ratios (beta)	[0.5, 1.0, 2.0]
Considered modes	1-15

Spectral density information

				Trigger ranges		
Segment no.	std(N) [MN]	Harmonic amplitude [MN]	omega_peak [rad/s]	beta=0.5	beta=1.0	beta=2.0
1	2.9015	10.7847	0.4720	0.8990--0.9974	0.4495--0.4987	0.2248--0.2493

Modal parameters:

Mode	wd [rad/s]	Td [s]	xi0 [%]	xi w/ae [%]	m [t]	k [kN/m]	k/kg_hat [MN]	c_quad [kN/(m/s)^2]	Acr (b=2) [MN]
1	0.15	41.36	0.46	0.46	75735.72	1748.25	1321.87	2755.44	24.45
2	0.18	35.02	0.47	0.47	63357.40	2039.19	283.72	1590.61	5.30
3	0.25	25.16	0.48	0.48	53416.85	3332.12	353.96	1868.90	6.78
4	0.29	21.86	0.49	0.49	43959.29	3632.77	319.98	424.81	6.31
5	0.38	16.35	0.62	0.62	45033.99	6649.96	417.06	1260.65	10.28
6	0.47	13.27	0.79	0.79	52941.77	11874.69	654.13	1672.15	20.71
7	0.56	11.22	1.00	1.00	76370.06	23950.49	2088.84	8773.11	83.40
8	0.62	10.15	1.84	1.84	55092.24	21123.99	843.73	4428.21	62.16
9	0.71	8.89	1.57	1.57	32951.65	16463.41	1744.45	281.35	109.23

10	0.75	8.38	2.76	2.76	49313.52	27736.31	867.14	2953.10	95.79
11	0.82	7.69	2.23	2.23	99456.16	66360.63	534.39	302.59	47.74
12	0.89	7.05	3.69	3.69	39585.63	31503.38	1323.71	154.82	195.15
13	0.90	6.99	10.06	10.06	8068.28	6588.06	1217.69	3105.46	490.23
14	0.91	6.91	3.22	3.22	36487.41	30218.90	1119.27	490.70	143.98
15	0.91	6.89	9.33	9.33	10344.82	8676.38	1583.63	1658.98	590.93

Harmonic results, beta = 0.5:

Mode	wd +- 20%	Matching	Chosen seg.	beta	Acr (b=0.5)	std(N)/0.4 [MN]	Onset	N [MN]	y0	y0*	Sz [MPa]	Sz* [MPa]
10	0.5997--0.8996	[1]	1	0.63	660.46	7.25	ok	10.78	nan	nan	nan	nan
11	0.6533--0.9800	[1]	1	0.58	379.23	7.25	ok	10.78	nan	nan	nan	nan
12	0.7132--1.0698	[1]	1	0.53	1110.03	7.25	ok	10.78	nan	nan	nan	nan
13	0.7192--1.0788	[1]	1	0.52	1427.29	7.25	ok	10.78	nan	nan	nan	nan
14	0.7277--1.0915	[1]	1	0.52	896.90	7.25	ok	10.78	nan	nan	nan	nan
15	0.7295--1.0942	[1]	1	0.52	1809.82	7.25	ok	10.78	nan	nan	nan	nan

Harmonic results, beta = 1.0:

Mode	wd +- 20%	Matching	Chosen seg.	beta	Acr (b=1.0)	std(N)/0.4 [MN]	Onset	N [MN]	y0	y0*	Sz [MPa]	Sz* [MPa]
5	0.3074--0.4611	[1]	1	1.23	92.60	7.25	ok	10.78	nan	nan	nan	nan
6	0.3789--0.5683	[1]	1	1.00	164.61	7.25	ok	10.78	nan	nan	nan	nan
7	0.4480--0.6720	[1]	1	0.84	590.27	7.25	ok	10.78	nan	nan	nan	nan
8	0.4953--0.7429	[1]	1	0.76	323.88	7.25	ok	10.78	nan	nan	nan	nan

Harmonic results, beta = 2.0:

Mode	wd +- 20%	Matching	Chosen seg.	beta	Acr (b=2.0)	std(N)/0.4 [MN]	Onset	N [MN]	y0	y0*	Sz [MPa]	Sz* [MPa]
3	0.1998--0.2997	[1]	1	1.89	6.78	7.25	fails	10.78	0.19	0.37	5.76	11.09
4	0.2300--0.3450	[1]	1	1.64	6.31	7.25	fails	10.78	0.85	1.58	30.31	56.17

RESULTS SUMMARY - PARAMETRIC RESONANCE

****

CONCEPT: K14_06

PSD type: 10000-year swell

Computed 2019-08-07 13:04:26

Analysis settings:

Parameter	Value
Bandwidth drop definition [%]	5.00
Natural frequency uncertainty [%]	20.00
N uncertainty (results with *) [%]	20.00
c_quad uncertainty (results with *) [%]	20.00
Rayleigh exceedance probability	1.0e-01
Considered frequency ratios (beta)	[0.5, 1.0, 2.0]
Considered modes	1-15

Spectral density information

				Trigger ranges		
Segment no.	std(N) [MN]	Harmonic amplitude [MN]	omega_peak [rad/s]	beta=0.5	beta=1.0	beta=2.0
1	3.2089	6.8863	0.4633	0.8682--1.1330	0.4341--0.5665	0.2170--0.2832

Modal parameters:

Mode	wd [rad/s]	Td [s]	xi0 [%]	xi w/ae [%]	m [t]	k [kN/m]	k/kg_hat [MN]	c_quad [kN/(m/s)^2]	Acr (b=2) [MN]
1	0.15	41.36	0.46	0.46	75735.72	1748.25	1321.87	2755.44	24.45
2	0.18	35.02	0.47	0.47	63357.40	2039.19	283.72	1590.61	5.30
3	0.25	25.16	0.48	0.48	53416.85	3332.12	353.96	1868.90	6.78
4	0.29	21.86	0.49	0.49	43959.29	3632.77	319.98	424.81	6.31
5	0.38	16.35	0.62	0.62	45033.99	6649.96	417.06	1260.65	10.28
6	0.47	13.27	0.79	0.79	52941.77	11874.69	654.13	1672.15	20.71
7	0.56	11.22	1.00	1.00	76370.06	23950.49	2088.84	8773.11	83.40
8	0.62	10.15	1.84	1.84	55092.24	21123.99	843.73	4428.21	62.16
9	0.71	8.89	1.57	1.57	32951.65	16463.41	1744.45	281.35	109.23

10	0.75	8.38	2.76	2.76	49313.52	27736.31	867.14	2953.10	95.79
11	0.82	7.69	2.23	2.23	99456.16	66360.63	534.39	302.59	47.74
12	0.89	7.05	3.69	3.69	39585.63	31503.38	1323.71	154.82	195.15
13	0.90	6.99	10.06	10.06	8068.28	6588.06	1217.69	3105.46	490.23
14	0.91	6.91	3.22	3.22	36487.41	30218.90	1119.27	490.70	143.98
15	0.91	6.89	9.33	9.33	10344.82	8676.38	1583.63	1658.98	590.93

Harmonic results, beta = 0.5:

Mode	wd +- 20%	Matching	Chosen seg.	beta	Acr (b=0.5)	std(N)/0.4 [MN]	Onset	N [MN]	y0	y0*	Sz [MPa]	Sz* [MPa]
10	0.5997--0.8996	[1]	1	0.62	660.46	8.02	ok	6.89	nan	nan	nan	nan
11	0.6533--0.9800	[1]	1	0.57	379.23	8.02	ok	6.89	nan	nan	nan	nan
12	0.7132--1.0698	[1]	1	0.52	1110.03	8.02	ok	6.89	nan	nan	nan	nan
13	0.7192--1.0788	[1]	1	0.52	1427.29	8.02	ok	6.89	nan	nan	nan	nan
14	0.7277--1.0915	[1]	1	0.51	896.90	8.02	ok	6.89	nan	nan	nan	nan
15	0.7295--1.0942	[1]	1	0.51	1809.82	8.02	ok	6.89	nan	nan	nan	nan

Harmonic results, beta = 1.0:

Mode	wd +- 20%	Matching	Chosen seg.	beta	Acr (b=1.0)	std(N)/0.4 [MN]	Onset	N [MN]	y0	y0*	Sz [MPa]	Sz* [MPa]
5	0.3074--0.4611	[1]	1	1.21	92.60	8.02	ok	6.89	nan	nan	nan	nan
6	0.3789--0.5683	[1]	1	0.98	164.61	8.02	ok	6.89	nan	nan	nan	nan
7	0.4480--0.6720	[1]	1	0.83	590.27	8.02	ok	6.89	nan	nan	nan	nan
8	0.4953--0.7429	[1]	1	0.75	323.88	8.02	ok	6.89	nan	nan	nan	nan
9	0.5654--0.8481	[1]	1	0.66	617.33	8.02	ok	6.89	nan	nan	nan	nan

Harmonic results, beta = 2.0:

Mode	wd +- 20%	Matching	Chosen seg.	beta	Acr (b=2.0)	std(N)/0.4 [MN]	Onset	N [MN]	y0	y0*	Sz [MPa]	Sz* [MPa]
3	0.1998--0.2997	[1]	1	1.85	6.78	8.02	fails	6.89	0.00	0.09	0.15	2.67
4	0.2300--0.3450	[1]	1	1.61	6.31	8.02	fails	6.89	0.11	0.46	3.88	16.52

RESULTS SUMMARY - PARAMETRIC RESONANCE

****

CONCEPT: K14_06

PSD type: 100-year wind sea

Computed 2019-08-07 13:04:25

Analysis settings:

Parameter	Value
Bandwidth drop definition [%]	10.00
Natural frequency uncertainty [%]	20.00
N uncertainty (results with *) [%]	20.00
c_quad uncertainty (results with *) [%]	20.00
Rayleigh exceedance probability	1.0e-03
Considered frequency ratios (beta)	[0.5, 1.0, 2.0]
Considered modes	1-15

Spectral density information

				Trigger ranges		
Segment no.	std(N) [MN]	Harmonic amplitude [MN]	omega_peak [rad/s]	beta=0.5	beta=1.0	beta=2.0
1	3.0440	11.3144	0.9476	1.6896--2.4128	0.8448--1.2064	0.4224--0.6032

Modal parameters:

Mode	wd [rad/s]	Td [s]	xi0 [%]	xi w/ae [%]	m [t]	k [kN/m]	k/kg_hat [MN]	c_quad [kN/(m/s)^2]	Acr (b=2) [MN]
1	0.15	41.36	0.46	1.71	75735.72	1748.25	1321.87	2755.44	90.54
2	0.18	35.02	0.47	1.65	63357.40	2039.19	283.72	1590.61	18.69
3	0.25	25.16	0.48	1.46	53416.85	3332.12	353.96	1868.90	20.66
4	0.29	21.86	0.49	1.26	43959.29	3632.77	319.98	424.81	16.17
5	0.38	16.35	0.62	1.14	45033.99	6649.96	417.06	1260.65	18.95
6	0.47	13.27	0.79	1.17	52941.77	11874.69	654.13	1672.15	30.65
7	0.56	11.22	1.00	1.28	76370.06	23950.49	2088.84	8773.11	106.80
8	0.62	10.15	1.84	2.12	55092.24	21123.99	843.73	4428.21	71.61
9	0.71	8.89	1.57	1.85	32951.65	16463.41	1744.45	281.35	128.77

10	0.75	8.38	2.76	2.97	49313.52	27736.31	867.14	2953.10	103.07
11	0.82	7.69	2.23	2.31	99456.16	66360.63	534.39	302.59	49.45
12	0.89	7.05	3.69	3.84	39585.63	31503.38	1323.71	154.82	203.09
13	0.90	6.99	10.06	10.06	8068.28	6588.06	1217.69	3105.46	490.23
14	0.91	6.91	3.22	3.22	36487.41	30218.90	1119.27	490.70	143.98
15	0.91	6.89	9.33	9.33	10344.82	8676.38	1583.63	1658.98	590.93

Harmonic results, beta = 0.5:
None of the considered modes are within frequency range.

Harmonic results, beta = 1.0:

Mode	wd +- 20%	Matching	Chosen seg.	beta	Acr (b=1.0)	std(N)/0.4 [MN]	Onset	N [MN]	y0	y0*	Sz [MPa]	Sz* [MPa]
9	0.5654--0.8481	[1]	1	1.34	670.27	7.61	ok	11.31	nan	nan	nan	nan
10	0.5997--0.8996	[1]	1	1.26	422.79	7.61	ok	11.31	nan	nan	nan	nan
11	0.6533--0.9800	[1]	1	1.16	229.90	7.61	ok	11.31	nan	nan	nan	nan
12	0.7132--1.0698	[1]	1	1.06	733.25	7.61	ok	11.31	nan	nan	nan	nan
13	0.7192--1.0788	[1]	1	1.05	1092.66	7.61	ok	11.31	nan	nan	nan	nan
14	0.7277--1.0915	[1]	1	1.04	567.72	7.61	ok	11.31	nan	nan	nan	nan
15	0.7295--1.0942	[1]	1	1.04	1368.08	7.61	ok	11.31	nan	nan	nan	nan

Harmonic results, beta = 2.0:

Mode	wd +- 20%	Matching	Chosen seg.	beta	Acr (b=2.0)	std(N)/0.4 [MN]	Onset	N [MN]	y0	y0*	Sz [MPa]	Sz* [MPa]
5	0.3074--0.4611	[1]	1	2.47	18.95	7.61	ok	11.31	0.00	0.00	0.00	0.00
6	0.3789--0.5683	[1]	1	2.00	30.65	7.61	ok	11.31	0.00	0.00	0.00	0.00
7	0.4480--0.6720	[1]	1	1.69	106.80	7.61	ok	11.31	0.00	0.00	0.00	0.00
8	0.4953--0.7429	[1]	1	1.53	71.61	7.61	ok	11.31	0.00	0.00	0.00	0.00
9	0.5654--0.8481	[1]	1	1.34	128.77	7.61	ok	11.31	0.00	0.00	0.00	0.00
10	0.5997--0.8996	[1]	1	1.26	103.07	7.61	ok	11.31	0.00	0.00	0.00	0.00

RESULTS SUMMARY - PARAMETRIC RESONANCE

****

CONCEPT: K14_06

PSD type: 10000-year wind sea

Computed 2019-08-07 13:04:25

Analysis settings:

Parameter	Value
Bandwidth drop definition [%]	10.00
Natural frequency uncertainty [%]	20.00
N uncertainty (results with *) [%]	20.00
c_quad uncertainty (results with *) [%]	20.00
Rayleigh exceedance probability	1.0e-01
Considered frequency ratios (beta)	[0.5, 1.0, 2.0]
Considered modes	1-15

Spectral density information

				Trigger ranges		
Segment no.	std(N) [MN]	Harmonic amplitude [MN]	omega_peak [rad/s]	beta=0.5	beta=1.0	beta=2.0
1	5.1643	11.0824	0.7099	1.3373--1.5379	0.6686--0.7690	0.3343--0.3845
2	6.4128	13.7617	0.9389	1.6658--2.1382	0.8329--1.0691	0.4165--0.5345

Modal parameters:

Mode	wd [rad/s]	Td [s]	xi0 [%]	xi w/ae [%]	m [t]	k [kN/m]	k/kg_hat [MN]	c_quad [kN/(m/s)^2]	Acr (b=2) [MN]
1	0.15	41.36	0.46	1.98	75735.72	1748.25	1321.87	2755.44	104.82
2	0.18	35.02	0.47	1.91	63357.40	2039.19	283.72	1590.61	21.64
3	0.25	25.16	0.48	1.67	53416.85	3332.12	353.96	1868.90	23.63
4	0.29	21.86	0.49	1.42	43959.29	3632.77	319.98	424.81	18.22
5	0.38	16.35	0.62	1.26	45033.99	6649.96	417.06	1260.65	20.96
6	0.47	13.27	0.79	1.25	52941.77	11874.69	654.13	1672.15	32.75
7	0.56	11.22	1.00	1.35	76370.06	23950.49	2088.84	8773.11	112.64
8	0.62	10.15	1.84	2.18	55092.24	21123.99	843.73	4428.21	73.64

9	0.71	8.89	1.57	1.86	32951.65	16463.41	1744.45	281.35	129.47
10	0.75	8.38	2.76	3.01	49313.52	27736.31	867.14	2953.10	104.46
11	0.82	7.69	2.23	2.33	99456.16	66360.63	534.39	302.59	49.88
12	0.89	7.05	3.69	3.81	39585.63	31503.38	1323.71	154.82	201.50
13	0.90	6.99	10.06	10.06	8068.28	6588.06	1217.69	3105.46	490.23
14	0.91	6.91	3.22	3.22	36487.41	30218.90	1119.27	490.70	143.98
15	0.91	6.89	9.33	9.33	10344.82	8676.38	1583.63	1658.98	590.93

Harmonic results, beta = 0.5:
None of the considered modes are within frequency range.

Harmonic results, beta = 1.0:

Mode	wd +- 20%	Matching	Chosen seg.	beta	Acr (b=1.0)	std(N)/0.4 [MN]	Onset	N [MN]	y0	y0*	Sz [MPa]	Sz* [MPa]
7	0.4480--0.6720	[1]	1	1.27	686.00	12.91	ok	11.08	nan	nan	nan	nan
8	0.4953--0.7429	[1]	1	1.15	352.50	12.91	ok	11.08	nan	nan	nan	nan
9	0.5654--0.8481	[1, 2]	2	1.33	672.08	16.03	ok	13.76	nan	nan	nan	nan
10	0.5997--0.8996	[1, 2]	2	1.25	425.63	16.03	ok	13.76	nan	nan	nan	nan
11	0.6533--0.9800	[1, 2]	2	1.15	230.90	16.03	ok	13.76	nan	nan	nan	nan
12	0.7132--1.0698	[1, 2]	2	1.05	730.38	16.03	ok	13.76	nan	nan	nan	nan
13	0.7192--1.0788	[1, 2]	2	1.04	1092.66	16.03	ok	13.76	nan	nan	nan	nan
14	0.7277--1.0915	[1, 2]	2	1.03	567.72	16.03	ok	13.76	nan	nan	nan	nan
15	0.7295--1.0942	[1, 2]	2	1.03	1368.08	16.03	ok	13.76	nan	nan	nan	nan

Harmonic results, beta = 2.0:

Mode	wd +- 20%	Matching	Chosen seg.	beta	Acr (b=2.0)	std(N)/0.4 [MN]	Onset	N [MN]	y0	y0*	Sz [MPa]	Sz* [MPa]
4	0.2300--0.3450	[1]	1	2.47	18.22	12.91	ok	11.08	0.00	0.00	0.00	0.00
5	0.3074--0.4611	[1, 2]	2	2.44	20.96	16.03	ok	13.76	0.00	0.00	0.00	0.00
6	0.3789--0.5683	[1, 2]	2	1.98	32.75	16.03	ok	13.76	0.00	0.00	0.00	0.00
7	0.4480--0.6720	[2]	2	1.68	112.64	16.03	ok	13.76	0.00	0.00	0.00	0.00
8	0.4953--0.7429	[2]	2	1.52	73.64	16.03	ok	13.76	0.00	0.00	0.00	0.00

RESULTS SUMMARY - PARAMETRIC EXCITATION

****

CONCEPT: K14_06

PSD type: 100-year wind

Computed 2019-05-24 07:38:58

Analysis settings:

Parameter	Value
Error margin on freqs (both in pair) [%]	10.0
Considered frequency ratios (beta)	[2.0, 1.0, 0.5]
Considered modes	1-12
Maximum Acr for listing [MN]	1000.0
Minimum std(N) for listing [MN]	0.0

Axial force information:

Mode	std(N) [MN]
1	0.00
2	0.00
3	0.00
4	0.00
5	0.49
6	0.67
7	0.57
8	0.00
9	0.66
10	0.00
11	0.00
12	0.00

Modal parameters:

Mode	wd [rad/s]	Td [s]	xi0 [%]	xi w/ae [%]	m [t]	k [kN/m]	k/kg_hat [MN]	c_quad [kN/(m/s)^2]	Acr (b=2) [MN]
1	0.15	41.36	0.46	1.88	75735.72	1748.25	1321.87	2755.44	99.53

2	0.18	35.02	0.47	1.87	63357.40	2039.19	283.72	1590.61	21.19
3	0.25	25.16	0.48	1.65	53416.85	3332.12	353.96	1868.90	23.35
4	0.29	21.86	0.49	1.40	43959.29	3632.77	319.98	424.81	17.96
5	0.38	16.35	0.62	1.24	45033.99	6649.96	417.06	1260.65	20.62
6	0.47	13.27	0.79	1.24	52941.77	11874.69	654.13	1672.15	32.49
7	0.56	11.22	1.00	1.28	76370.06	23950.49	2088.84	8773.11	106.80
8	0.62	10.15	1.84	2.17	55092.24	21123.99	843.73	4428.21	73.30
9	0.71	8.89	1.57	1.85	32951.65	16463.41	1744.45	281.35	128.77
10	0.75	8.38	2.76	3.01	49313.52	27736.31	867.14	2953.10	104.46
11	0.82	7.69	2.23	2.40	99456.16	66360.63	534.39	302.59	51.38
12	0.89	7.05	3.69	3.84	39585.63	31503.38	1323.71	154.82	203.09

Harmonic results (showing results with Acr < 1000MN and std(N) > 0MN):

Axial force mode	Triggered mode	beta	xi w/aero [%]	beta for Acr	Acr	std(N)/0.4	onset
5	2	2.14	1.87	2.00	21.19	1.23	ok
6	3	1.90	1.65	2.00	23.35	1.68	ok
6	4	1.65	1.40	2.00	17.96	1.68	ok
7	3	2.24	1.65	2.00	23.35	1.43	ok
7	4	1.95	1.40	2.00	17.96	1.43	ok
9	5	1.84	1.24	2.00	20.62	1.65	ok
5	5	1.00	1.24	1.00	131.15	1.23	ok
6	6	1.00	1.24	1.00	206.16	1.68	ok
6	7	0.85	1.28	1.00	667.95	1.68	ok
7	6	1.18	1.24	1.00	206.16	1.43	ok
7	7	1.00	1.28	1.00	667.95	1.43	ok
7	8	0.90	2.17	1.00	351.70	1.43	ok
9	8	1.14	2.17	1.00	351.70	1.65	ok
9	9	1.00	1.85	1.00	670.27	1.65	ok
9	10	0.94	3.01	1.00	425.63	1.65	ok
9	11	0.87	2.40	1.00	234.33	1.65	ok
5	10	0.51	3.01	0.50	679.82	1.23	ok
5	11	0.47	2.40	0.50	388.61	1.23	ok
6	11	0.58	2.40	0.50	388.61	1.68	ok

RESULTS SUMMARY - PARAMETRIC EXCITATION

****

CONCEPT: K14_06

PSD type: 10000-year wind

Computed 2019-05-24 07:38:57

Analysis settings:

Parameter	Value
Error margin on freqs (both in pair) [%]	10.0
Considered frequency ratios (beta)	[2.0, 1.0, 0.5]
Considered modes	1-12
Maximum Acr for listing [MN]	1000.0
Minimum std(N) for listing [MN]	0.0

Axial force information:

Mode	std(N) [MN]
1	0.00
2	0.00
3	0.00
4	0.00
5	1.22
6	1.69
7	0.00
8	0.00
9	1.63
10	0.00
11	0.00
12	0.00

Modal parameters:

Mode	wd [rad/s]	Td [s]	xi0 [%]	xi w/ae [%]	m [t]	k [kN/m]	k/kg_hat [MN]	c_quad [kN/(m/s)^2]	Acr (b=2) [MN]
1	0.15	41.36	0.46	2.25	75735.72	1748.25	1321.87	2755.44	119.09

2	0.18	35.02	0.47	2.18	63357.40	2039.19	283.72	1590.61	24.71	
3	0.25	25.16	0.48	1.90	53416.85	3332.12	353.96	1868.90	26.89	
4	0.29	21.86	0.49	1.60	43959.29	3632.77	319.98	424.81	20.52	
5	0.38	16.35	0.62	1.37	45033.99	6649.96	417.06	1260.65	22.79	
6	0.47	13.27	0.79	1.33	52941.77	11874.69	654.13	1672.15	34.84	
7	0.56	11.22	1.00	1.35	76370.06	23950.49	2088.84	8773.11	112.64	
8	0.62	10.15	1.84	2.25	55092.24	21123.99	843.73	4428.21	76.00	
9	0.71	8.89	1.57	1.91	32951.65	16463.41	1744.45	281.35	132.96	
10	0.75	8.38	2.76	3.05	49313.52	27736.31	867.14	2953.10	105.85	
11	0.82	7.69	2.23	2.34	99456.16	66360.63	534.39	302.59	50.10	
12	0.89	7.05	3.69	3.81	39585.63	31503.38	1323.71	154.82	201.50	

Harmonic results (showing results with Acr < 1000MN and std(N) > 0MN):

Axial force mode	Triggered mode	beta	xi w/aero [%]	beta for Acr	Acr	std(N)/0.4	onset
5	2	2.14	2.18	2.00	24.71	3.05	ok
6	3	1.90	1.90	2.00	26.89	4.22	ok
6	4	1.65	1.60	2.00	20.52	4.22	ok
9	5	1.84	1.37	2.00	22.79	4.08	ok
5	5	1.00	1.37	1.00	137.88	3.05	ok
6	6	1.00	1.33	1.00	213.50	4.22	ok
6	7	0.85	1.35	1.00	686.00	4.22	ok
9	8	1.14	2.25	1.00	358.11	4.08	ok
9	9	1.00	1.91	1.00	681.08	4.08	ok
9	10	0.94	3.05	1.00	428.45	4.08	ok
9	11	0.87	2.34	1.00	231.39	4.08	ok
5	10	0.51	3.05	0.50	682.82	3.05	ok
5	11	0.47	2.34	0.50	385.35	3.05	ok
6	11	0.58	2.34	0.50	385.35	4.22	ok

AAS-JAKOBSEN COWI Multiconsult

JOHS HOLT AkerSolutions entail NGI DISSING+WEITLING architecture a|s mossmaritime

Concept development, floating bridge E39 Bjørnafjorden

Appendix S – Enclosure 3

10205546-11-NOT-186

Verification of modal interpretation of drag damping

MEMO

PROJECT	Concept development, floating bridge E39 Bjørnafjorden	DOCUMENT CODE	10205546-11-NOT-186
CLIENT	Statens vegvesen	ACCESSIBILITY	Restricted
SUBJECT	Verification of modal interpretation of drag damping	PROJECT MANAGER	Svein Erik Jakobsen
TO	Statens vegvesen	PREPARED BY	Knut Andreas Kvåle
COPY TO		RESPONSIBLE UNIT	AMC

SUMMARY

To assess the bridge concepts' robustness against parametric excitation, single-degree-of-freedom (SDOF) analyses of their modes are used as a key tool. A major aspect of the modal analyses is the establishment of a modal quadratic damping, representing the nonlinear damping originating from pontoons and mooring lines. The validity of the simplified approach applied to establish this modal damping is discussed herein.

0	15.08.2019	Final issue	K. A. Kvåle	R. M. Larssen	S. E. Jakobsen
REV.	DATE	DESCRIPTION	PREPARED BY	CHECKED BY	APPROVED BY

1 Description of methodology

The linearized system damping due to a motion described by the pure oscillation of mode n could be established as follows:

$$\left[C_{quad_{lin}}\right] = \left[C_{quad}\right]\{|\dot{u}|\} \cdot \frac{8}{3\pi} = \left[C_{quad}\right]\{|\phi_n|\}\left|\dot{y}_{n,0}\right| \frac{8}{3\pi} \tag{1}$$

Here, $\left[C_{quad}\right]$ is the quadratic damping coefficient matrix, $\{|\dot{u}|\}$ is the absolute values of all degrees of interest (DOFs) of interest placed in a finite element method (FEM) format, $\{\phi_n\}$ is mode n for the corresponding DOFs and $\dot{y}_{n,0}$ is the generalized velocity of mode n.

By conducting a full modal analysis, as described in Appendix F, the corresponding linear modal damping of mode n can be established by solving the following eigenvalue problem:

$$\left(-\lambda^2 \cdot \left(\left[\, M_s \,\right] + [M_h(\omega)]\right) + i\lambda \cdot \left([C_s] + \left[C_{quad_{lin}}\right] + [C_h(\omega)]\right) + \left([K_s] + [K_h]\right)\right)\{\phi_n\} = \{0\}$$

$$\xi_{n,eq} = -\frac{Re(\lambda_n)}{|\lambda_n|} \tag{2}$$

where $\xi_{n,eq}$ is the linearized critical damping ratio of mode n, and λ_n is the complex eigenvalue of mode n.

This approach provides the true behaviour of the system due to the added damping, in a linear sense, and the modal properties will reflect the fact that the modes (including the mode shapes) might change due to the extra non-classical damping. The downside is that the results are only valid for the mode under investigation, and the full modal analysis has to be conducted for all modes of interest. Due to this, a much neater and more naïve approach has been applied throughout the assessments conducted in the concept development. By assuming that the modes of the system are independent of the quadratic damping contributions (not strictly true), they can be used directly to estimate the generalized (modal) damping as follows (see Appendix S):

$$c_{quad,n} = \{\phi_n\}^T \left[C_{quad}\right] diag(\{|\phi_n|\})\{\phi_n\} \tag{3}$$

Furthermore, this can be linearized about the generalized velocity $\left|\dot{y}_{n,0}\right|$ as follows:

$$c_{quad,n,eq} = c_{quad,n}\left|\dot{y}_{n,0}\right| \cdot \frac{8}{3\pi}$$

$$\xi_{n,eq} = \frac{c_{quad,n,eq} + c_{lin}}{2\sqrt{mk}} \tag{4}$$

Here, m describes the modal mass, k the modal stiffness, c_{lin} the modal linear damping and $c_{quad,n,eq}$ the equivalent linearized quadratic damping of mode n. The following section compare the resulting linearized damping from the two approaches for important modes of the concepts K11, K12 and K14.

2 Results and discussion

2.1 K11

The results of the full modal analysis based on linearized damping contribution defined by 20 m generalized displacement of mode 4 on K11 are depicted in Figure 2-1. The linearized full damping established for mode 4 using the naïve approach given in Equations 3 and 4 is also shown in the figure. The corresponding mode phase collinearity (MPC) is given in Figure 2-2. The MPC is described more in detail in Appendix F, but in essence it describes how valid the diagonalization of the system matrices is. In other words, the MPC is useful for the validation of the SDOF assumption.

Damping ratios and MPC corresponding to a displacement of 50m of mode 4 are given in Figure 2-3 and Figure 2-4, respectively. Even though 50 meters does not represent feasible displacements, the results are useful as a reference for the evaluation of the simplified approach's validity.

The simplified approach provides excellent agreement with the full modal analysis results, both for 20m and 50m displacement.

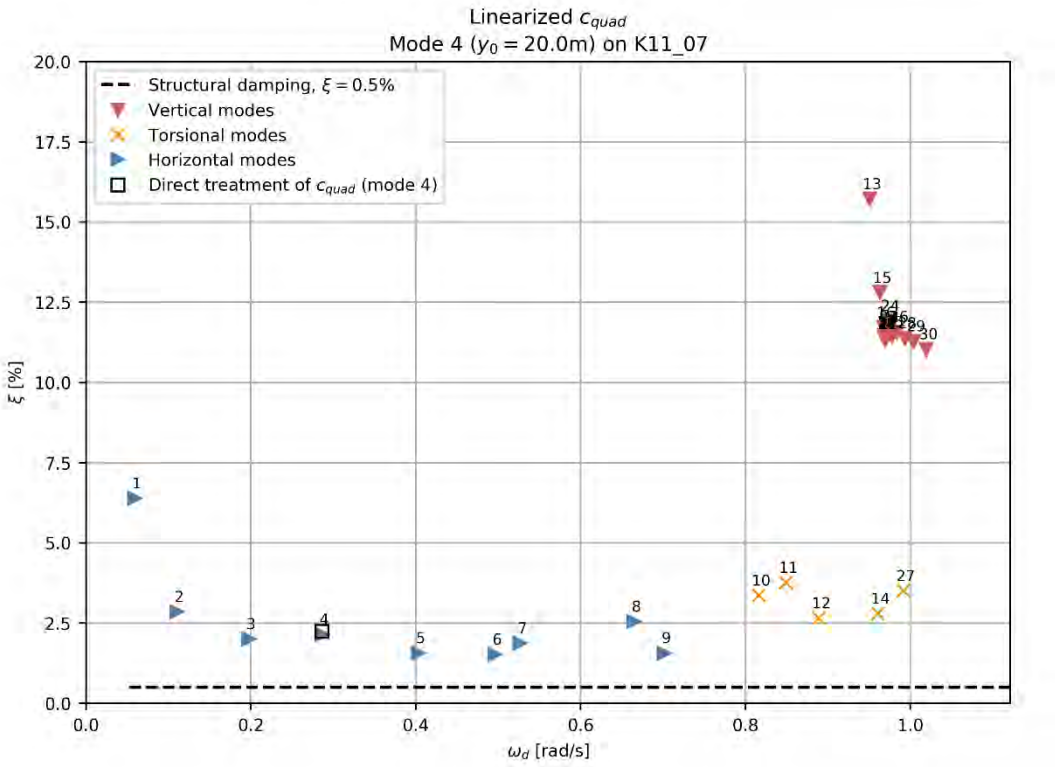

Figure 2-1. Critical damping ratios of the first 30 modes of K11_07 due to linearized quadratic damping from a generalized displacement of 20 m of mode 4.

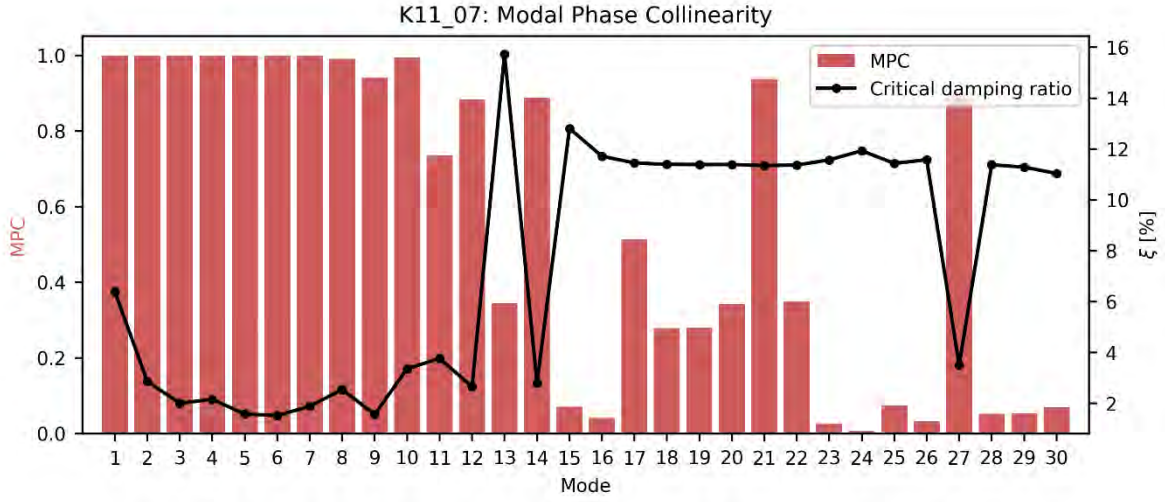

Figure 2-2. Mode phase collinearities of the 30 first modes of K11_07 due to linearized quadratic damping from a generalized displacement of 20 m of mode 4.

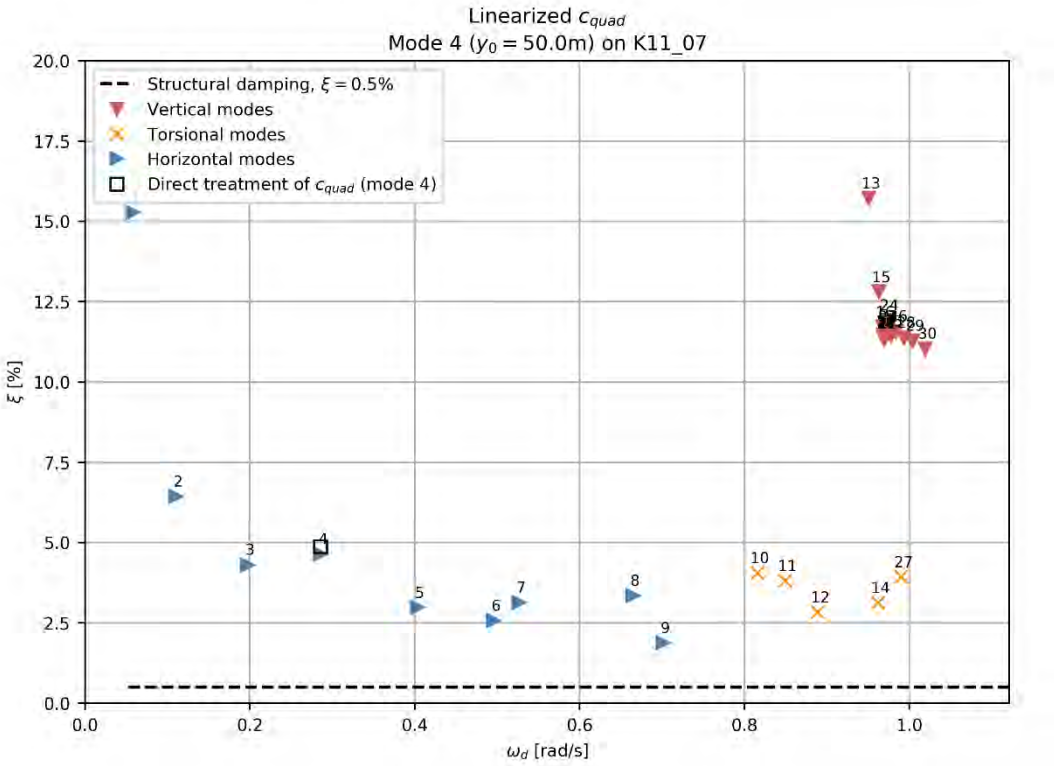

Figure 2-3. Critical damping ratios of the first 30 modes of K11_07 due to linearized quadratic damping from a generalized displacement of 50 m of mode 4.

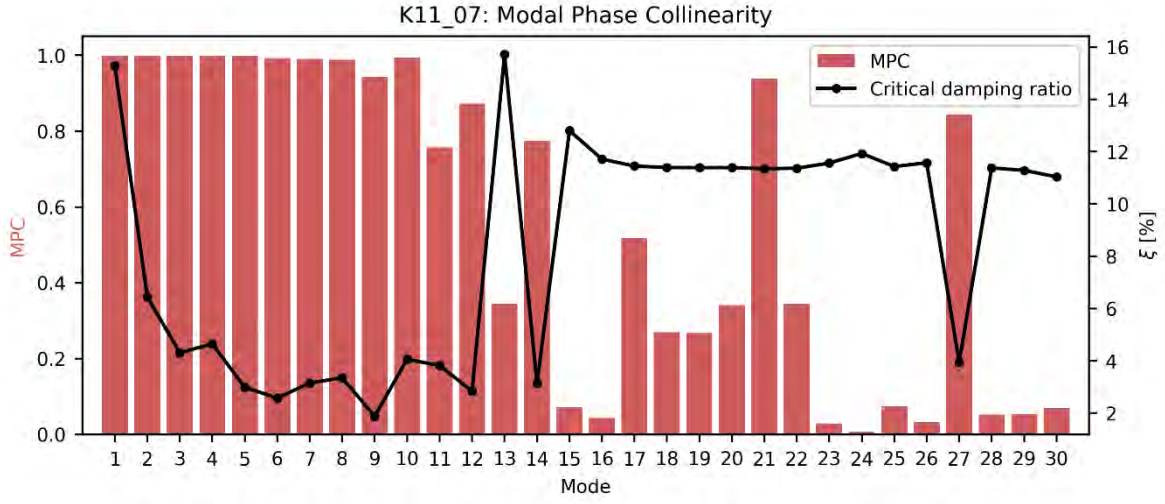

Figure 2-4. Mode phase collinearities of the 30 first modes of K11_07 due to linearized quadratic damping from a generalized displacement of 50 m of mode 4.

2.2 K12

2.2.1 Mode 3

The critical damping ratios from a full modal analysis including linearized drag damping and the corresponding MPC, for 5m generalized displacement of mode 3 on K12, are given in Figure 2-5 and Figure 2-6, respectively. All results support the usage of the simplified approach.

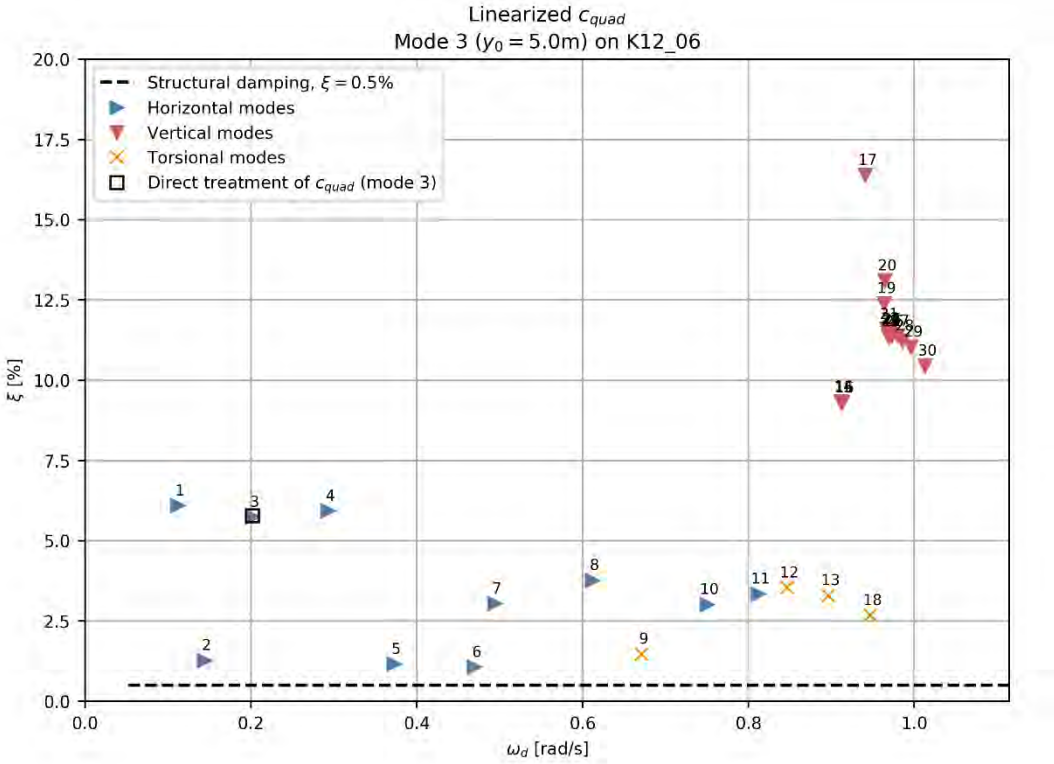

Figure 2-5. Critical damping ratios of the first 30 modes of K12_06 due to linearized quadratic damping from a generalized displacement of 5 m of mode 3.

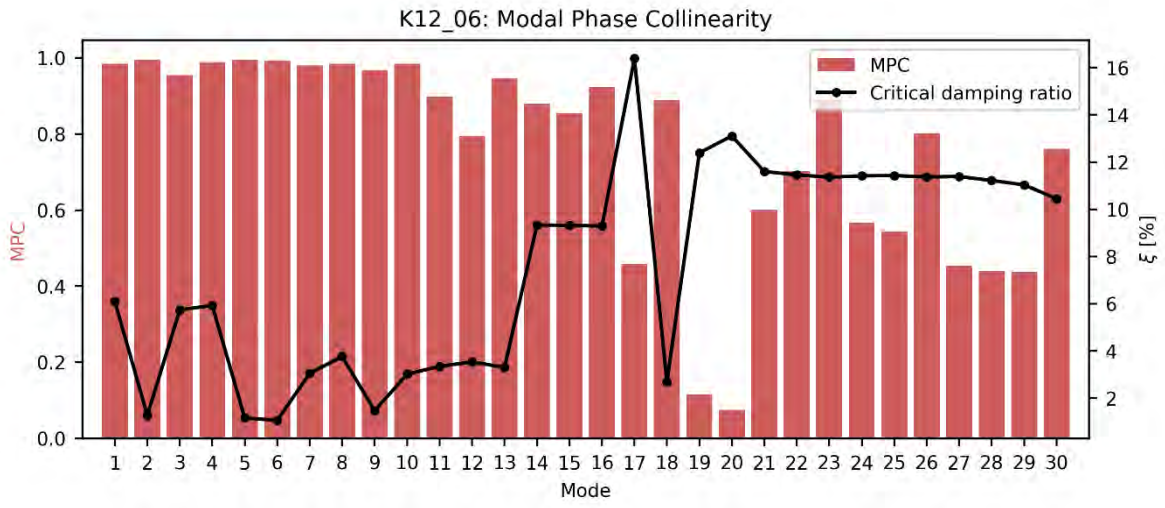

Figure 2-6. Mode phase collinearities of the first 30 modes of K12_06 due to linearized quadratic damping from a generalized displacement of 5 m of mode 3.

2.2.2 Mode 4

The critical damping ratios from a full modal analysis including linearized drag damping and the corresponding MPC, for 5m generalized displacement of mode 4 on K12, are given in Figure 2-7 and Figure 2-8, respectively. All results support the usage of the simplified approach.

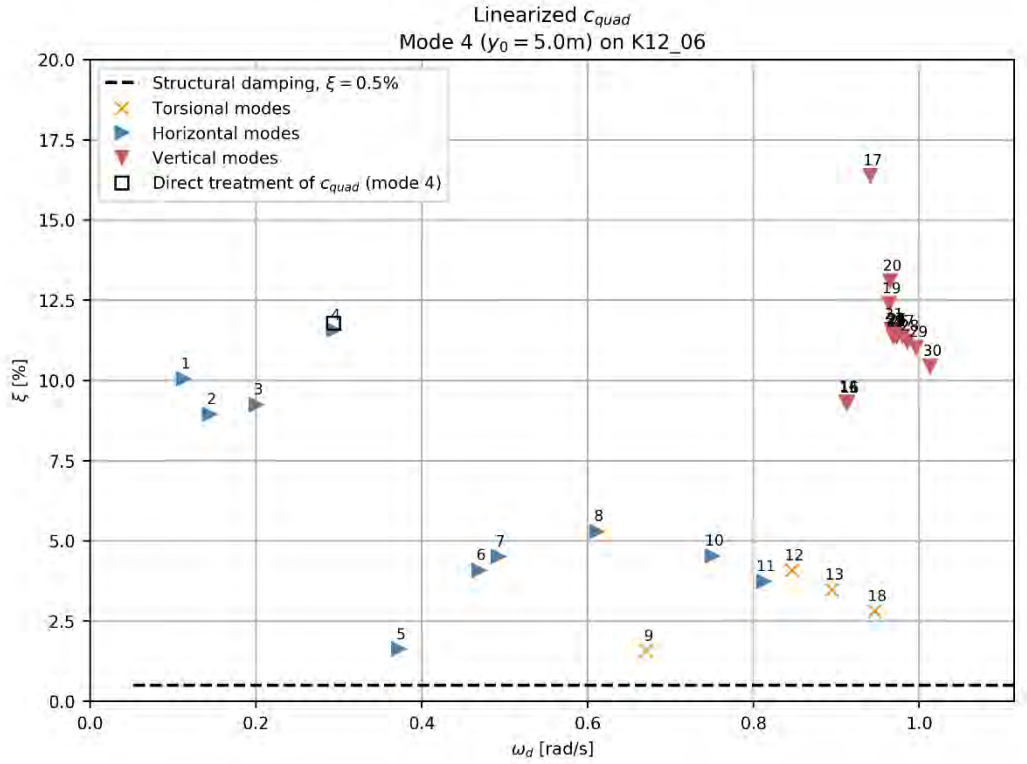

Figure 2-7. Critical damping ratios of the first 30 modes of K12_06 due to linearized quadratic damping from a generalized displacement of 5 m of mode 4.

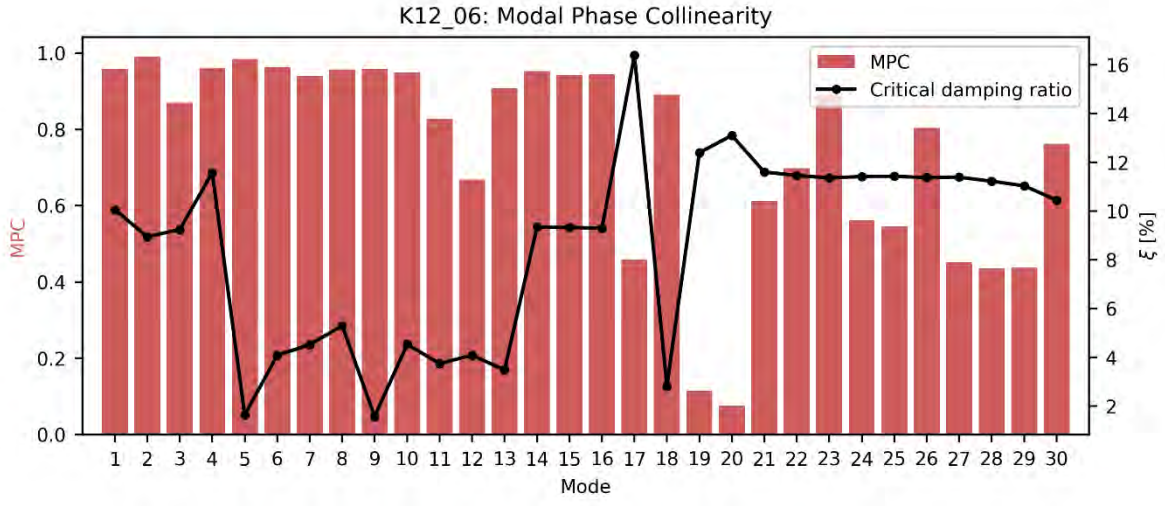

Figure 2-8. Mode phase collinearities of the first 30 modes of K12_06 due to linearized quadratic damping from a generalized displacement of 5 m of mode 3.

2.3 K14

The critical damping ratios from a full modal analysis including linearized drag damping and the corresponding MPC, for 5m generalized displacement of mode 4 on K14, are given in Figure 2-9 and Figure 2-10, respectively. All results support the usage of the simplified approach.

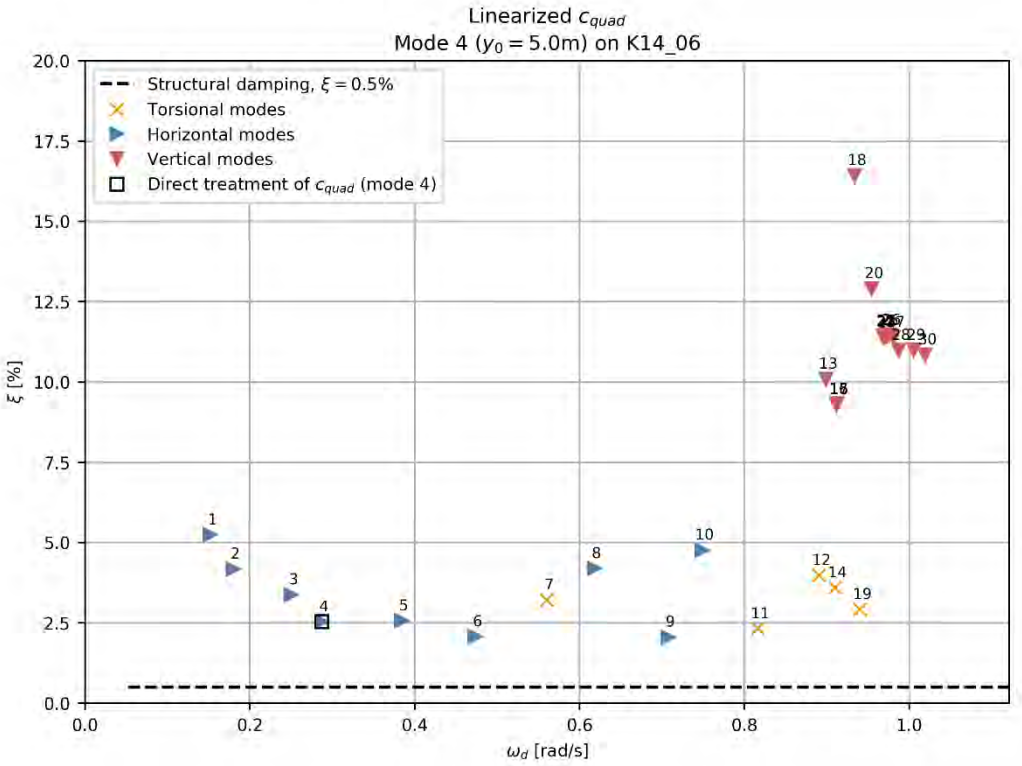

Figure 2-9. Critical damping ratios of the first 30 modes of K14_06 due to linearized quadratic damping from a generalized displacement of 5 m of mode 4.

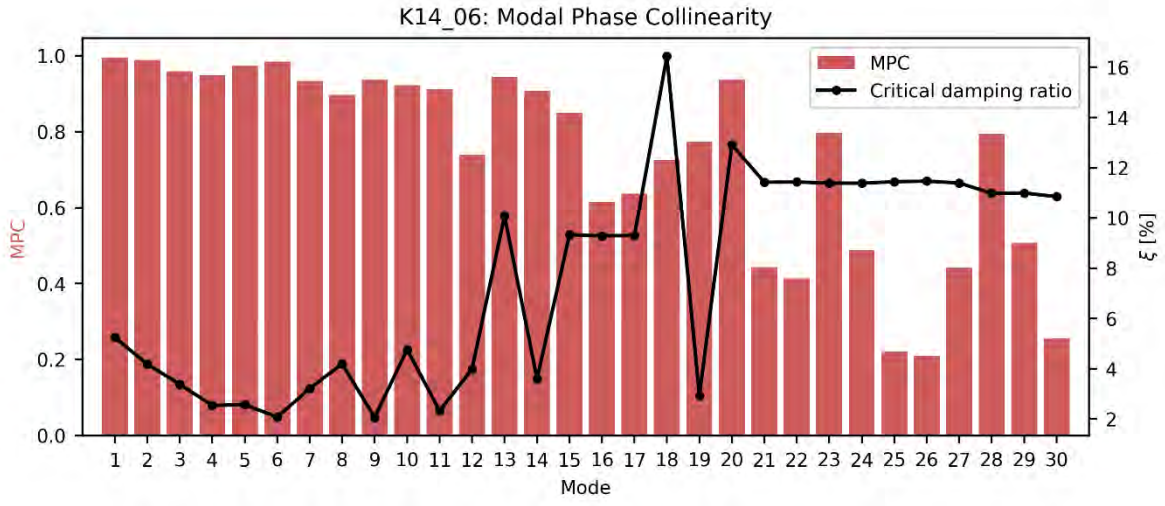

Figure 2-10. Mode phase collinearities of the first 30 modes of K14_06 due to linearized quadratic damping from a generalized displacement of 5 m of mode 4.

3 Concluding remarks

A close-to perfect agreement between linearized quadratic drag damping established with a full modal analysis and using a simplified approach was found for all modes investigated, for all concepts (not including K13). Also, the single-degree-of-freedom assumption appears to be reasonable for the amplitudes considered (50m on K11, 5m on K12, 5m on K14), under the assumption of linear behaviour.

AAS-JAKOBSEN COWI Multiconsult

JOHS HOLT AkerSolutions entail NGI DISSING+WEITLING architecture a|s mossmaritime

Concept development, floating bridge E39 Bjørnafjorden

Appendix S – Enclosure 4

10205546-11-NOT-187

Effect of KC-dependent drag coefficient on parametric excitation

MEMO

PROJECT	Concept development, floating bridge E39 Bjørnafjorden	DOCUMENT CODE	10205546-11-NOT-187
CLIENT	Statens vegvesen	ACCESSIBILITY	Restricted
SUBJECT	Effect of KC-dependent drag coefficient on parametric excitation	PROJECT MANAGER	Svein Erik Jakobsen
TO	Statens vegvesen	PREPARED BY	Knut Andreas Kvåle
COPY TO		RESPONSIBLE UNIT	AMC

SUMMARY

Drag coefficients are known to vary based on amplitude and velocity of the oscillation, typically characterized by the normalized quantity known as K_c-number. The quadratic drag damping crucial for the limitation of the response due to parametric excitation is fully controlled by the drag coefficients for the end-supported K11. Herein, the effect of including the K_c-dependency on the parametric excitation of mode 4 on K11 is assessed in a single-degree-of-freedom manner.

0	15.08.2019	Final issue	K. A. Kvåle	R. M. Larssen	S. E. Jakobsen
REV.	DATE	DESCRIPTION	PREPARED BY	CHECKED BY	APPROVED BY

1 Interpretation of CFD analyses

The K_c-number is defined as follows [1]:

$$K_c = \frac{VT}{L}$$

where T is the oscillation period, V is the velocity, and L is a characteristic length chosen for the normalization. For a fixed oscillation period $T = 2\pi/\omega_d$, this can be rewritten as follows:

$$K_c = \frac{2\pi}{\omega_d} \cdot \frac{\omega_d u}{L} = \frac{2\pi u}{L}$$

Here, u and ω_d are introduced as the displacement and damped natural frequency of a mode considered, respectively. The drag coefficients and different K_c-numbers obtained in the CFD analyses are shown in Figure 1-1. As indicated in the figure, a curve fit was conducted based on the most credible data points, and an assumed maximum drag coefficient of 1 was furthermore applied. Details regarding the CFD analyses are found in Appendix H.

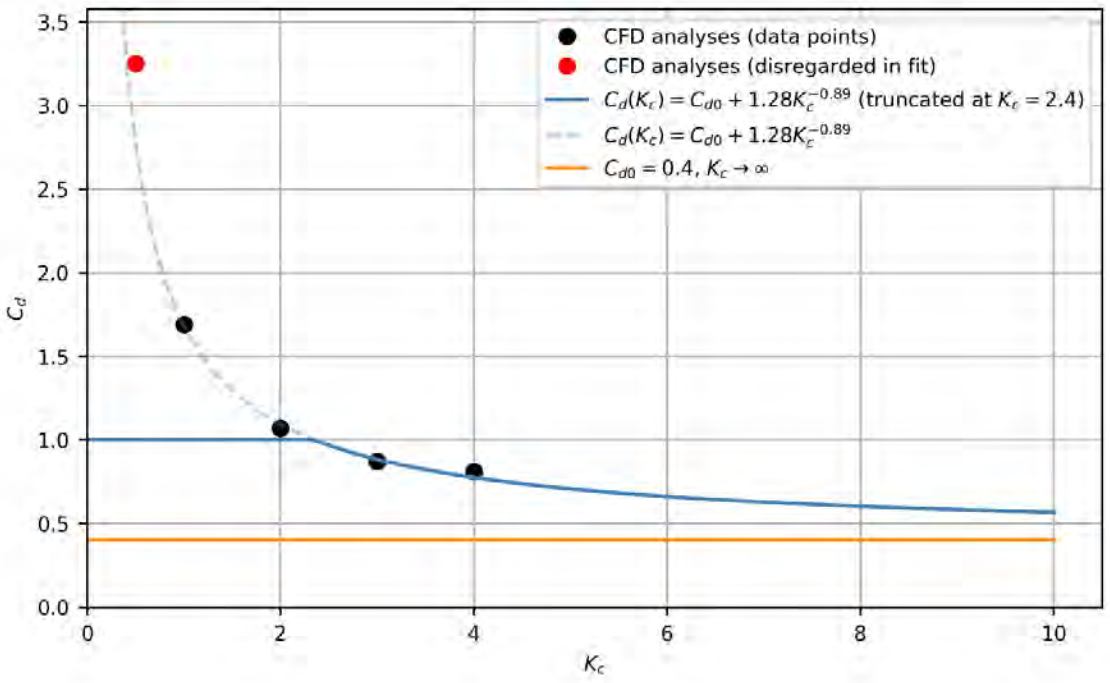

Figure 1-1. CFD-predicted and curve fitted relationship between K_c and C_d.

2 Effective modal quadratic damping coefficient

For a given modal response y_0, the displacements of all relevant degrees of freedom (DOFs) on all pontoons are given as follows:

$$\{u\} = \{|\phi_n|\}y_0$$

where $\{\phi_n\}$ represents the mode shape of mode n for the relevant DOFs, stacked in a finite element method (FEM) format. The K_c-number corresponding to all the relevant DOFs i can thus be established straightforwardly as $K_{c,i} = 2\pi u/L$. Based on the curve fit, the drag coefficient is established from $C_{d,i} = \hat{C}_d(K_{c,i})$. Based on this, the diagonal of the coefficient matrix $[C_{quad}]$ is established from the following well-known expression:

$$C_{quad,ii} = \frac{1}{2}\rho \cdot A_i \cdot C_{d,i}$$

As described in the main part of Appendix S, the generalized (modal) quadratic damping can then finally be established as follows:

$$c_{quad,n} = \{\phi_n\}^T [C_{quad}] \text{diag}(\{|\phi_n|\}) \{\phi_n\}$$

By applying the equation above, the effective modal quadratic damping was established for mode 4 on K11_07, as shown in Figure 2-1. As indicated in the figure, c_{quad} is dependent on the generalized displacement through the dependency to the K_c-number. The quadratic damping established by using fixed damping coefficients of 0.3, 0.4 and 1.0 are also given in the figure, for reference.

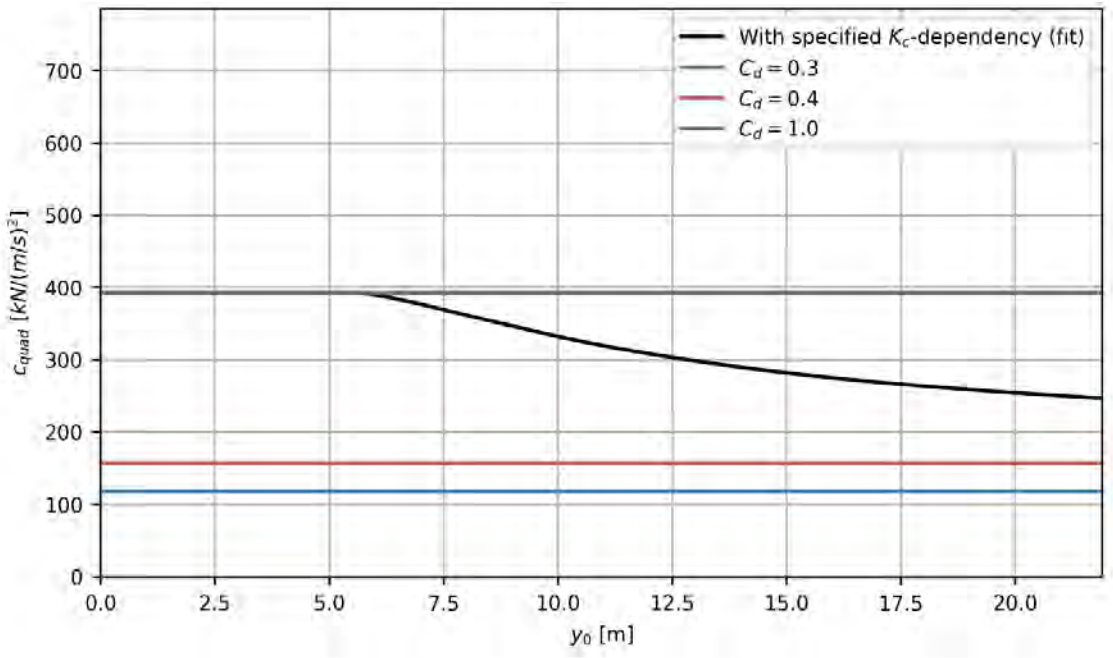

Figure 2-1. Effective modal quadratic damping for different modal response values of mode 4 on K11_07.

3 Iterative procedure to estimate terminal displacement

As seen in Figure 2-1, the quadratic damping can be interpreted as a function of the stationary generalized displacement. For the estimation of the terminal displacement introduced in Appendix S, the following expression is used:

$$y_0 = 3\pi \frac{N \cdot \hat{k}_g - 2c_{lin}\omega_n}{16 c_{quad} \omega_n^2}$$

such that, in fact, the stationary (terminal) displacement is also a function of the quadratic damping. This fact makes iteration necessary to estimate the terminal displacement when assuming that the drag coefficient is K_c-dependent. The resulting iteration is given in Figure 3-1, whereas the values of C_d used for each pontoon are depicted in Figure 3-2. For the iteration, the following parameters were used: $N = 24.65MN$, $\omega_n = 0.28623 rad/s$ ($T_n = 21.95s$), and $\hat{k}_g = 15.1 \cdot 10^{-3} m^{-1}$.

The iteration was initiated with the stationary value of the drag coefficient, defined as $C_{d0} = 0.4$ in Figure 1-1, such that the 0th iteration of the displacement and damping are based on the stationary drag coefficient. As Figure 3-2 indicates, the ceiling value of $C_d = 1.0$ is relatively quickly reached. At the same iteration, the quadratic damping and terminal displacement have converged to their final values of $c_{quad} = 392.6 kN/\left(\frac{m}{s}\right)^2$ and $y_0 = 5.13\ m$. Using the stationary value $C_{d0} = 0.4$, $y_0 = 12.8\ m$ is obtained.

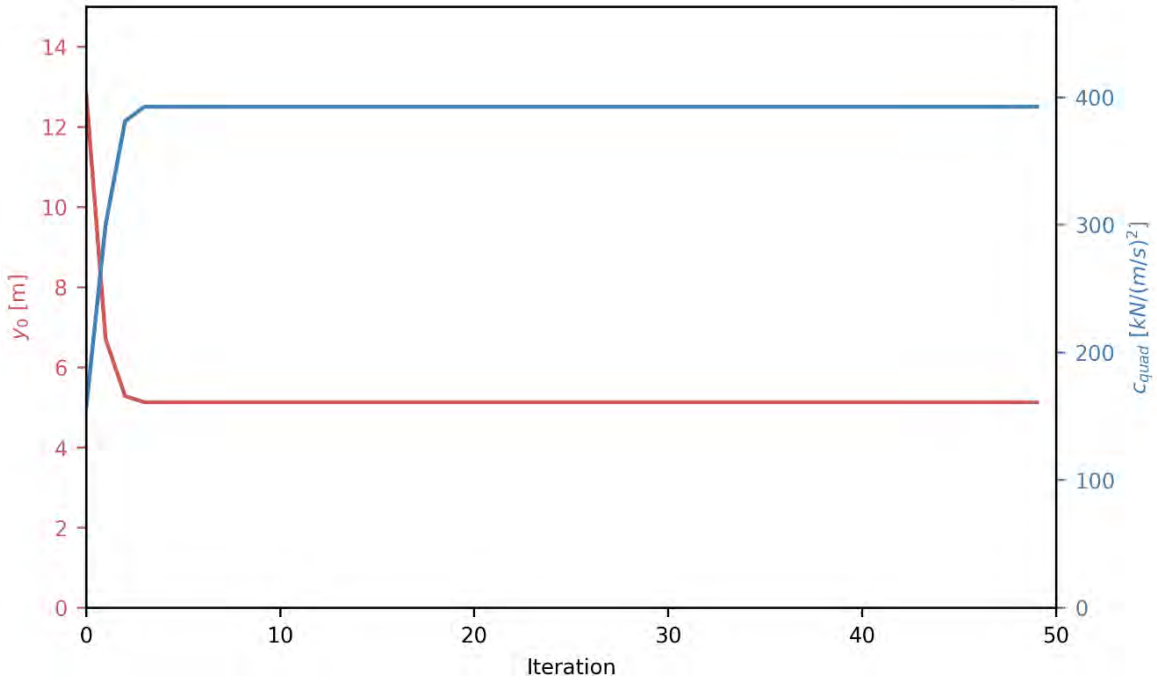

Figure 3-1. Terminal response due to K_c-dependent C_d, on mode 4 of K11_07. The response due to the stationary drag coefficient $C_d = C_{d0} = 0.4$ is used as the starting point for the iteration and is therefore indicated at iteration 0 on the plot.

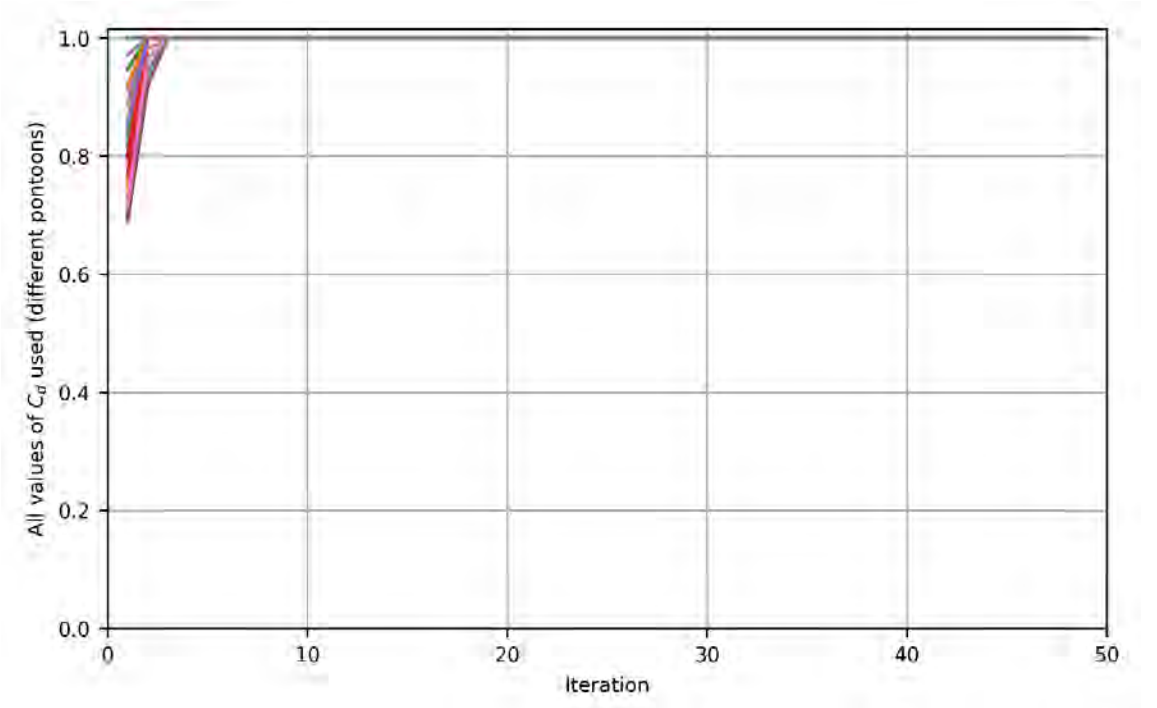

Figure 3-2. Used drag coefficients (values for all pontoons are plotted).

4 Concluding remarks

The CFD-analyses indicate a significantly larger damping than what has been assumed, both with respect to stationary values and, in particular, for lower oscillation amplitudes (or low K_c-numbers). The observed effects of K_c-number (describing velocity and oscillation period) on the drag coefficient C_d from the CFD-analyses were included in the evaluation of terminal displacement of mode 4 on K11, through a curve fit and a defined maximum threshold value of drag coefficient of 1.0. The effect observed on the terminal response is significant (reduction of 60%).

5 References

[1] «DNV-RP-C205 : Environmental conditions and environmental loads,» DNV, 2010.

Concept development, floating bridge E39 Bjørnafjorden

Appendix S – Enclosure 5

10205546-11-NOT-188

Assessment of risk of parametric excitation of mooring cables

AAS-JAKOBSEN COWI Multiconsult

JOHS HOLT AkerSolutions entail NGI DISSING+WEITLING architecture a|s mossmaritime

MEMO

PROJECT	Concept development, floating bridge E39 Bjørnafjorden	DOCUMENT CODE	10205546-11-NOT-188
CLIENT	Statens vegvesen	ACCESSIBILITY	Restricted
SUBJECT	Assessment of risk of parametric excitation of mooring cables	PROJECT MANAGER	Svein Erik Jakobsen
TO	Statens vegvesen	PREPARED BY	Knut Andreas Kvåle
COPY TO		RESPONSIBLE UNIT	AMC

SUMMARY

Herein, the response on the mooring cables on K12 due to parametric excitation is assessed in a simplified manner. The results are based on analytical expressions of the modal parameters that are used as input to the same methodology applied to evaluation of the bridge girder. The response caused by parametric excitation is not deemed to be a problem for the mooring lines, as it is highly limited (at most approximately 2.5 cm along the cable).

0	15.08.2019	Final issue	K. A. Kvåle	R. M. Larssen	S. E. Jakobsen
REV.	DATE	DESCRIPTION	PREPARED BY	CHECKED BY	APPROVED BY

1 Introduction

The evaluation of parametric excitation has thus far been solely concerned with effects on the bridge girder. In principle, it should be assessed for the mooring cables of the moored concepts as well. The phenomenon of parametric excitation of cables was discussed by Cantero et al. in [1] [2], applied on submerged floating tunnels.

The following assessment is based on the model set-up given in [3] [4]. The model is otherwise treated identically as the bridge girder and is relying on a modal approach.

2 Simplified analytical approach

2.1 Model set-up

Irvine's non-dimensional sag parameter λ can be established through the following expression:

$$\lambda^2 = \frac{E}{\sigma_s}\left(\frac{\gamma L}{\sigma_s}\right)^2$$

Here, E is the Young's modulus, σ_s is the static normal stress (equal to axial force divided by area, i.e., N/A), L is the length of the cable, and the weight normal to the cable axis, γ can be established as follows:

$$\gamma = \rho_{eff} g \cos\theta$$

with $\rho_{eff} = \rho_c - \rho_w$ introduced as the effective density of the cable material accounting for buoyancy, and ρ_c and ρ_w are the densities of the cable itself and the water, respectively; g is the gravitational constant; and θ the slope of the cable ($\theta = 0$ corresponds to a horizontal cable). As a result, [2] obtains the following natural frequency of the first out-of-plane mode:

$$\omega_{y1} = \frac{\pi}{L}\sqrt{\frac{\sigma_s}{\rho_{eff}}}$$

Furthermore, the natural frequencies of the following out-of-plane modes can be computed from the following expression:

$$\omega_{yn} = n\omega_{y1}$$

From a low-sag approximation, the following natural frequency for the in-plane modes can be determined:

$$\omega_{zn} \approx n\omega_1(1 + \kappa_n)$$

$$\kappa_n = \frac{\lambda^2}{\pi^4 n^4}(1 + (-1)^{n+1})^2$$

The corresponding mode shapes are represented by the following function:

$$\psi(x) = \sin\frac{\pi n x}{L}$$

By imposing the parameters given in Table 2-1, the natural periods of the first ten in-plane and out-of-plane modes were calculated. The results are given in Figure 2-1.

Table 2-1. Parameters for evaluation.

Parameter	Value
Drag coefficient, C_d	1.2
Water density, ρ_w	1025 kg/m^3
Cable diameter, d	147 mm
Cable length, L	900 m
Angle, θ	45°
Cable density (steel), ρ_c	7800 kg/m^3
Static axial force, N_0	1.0 MN
Dynamic axial force ampltiude, N	2.0 MN
Linear critical damping ratio, ξ	0.5%
Young's modulus, E	210GPa

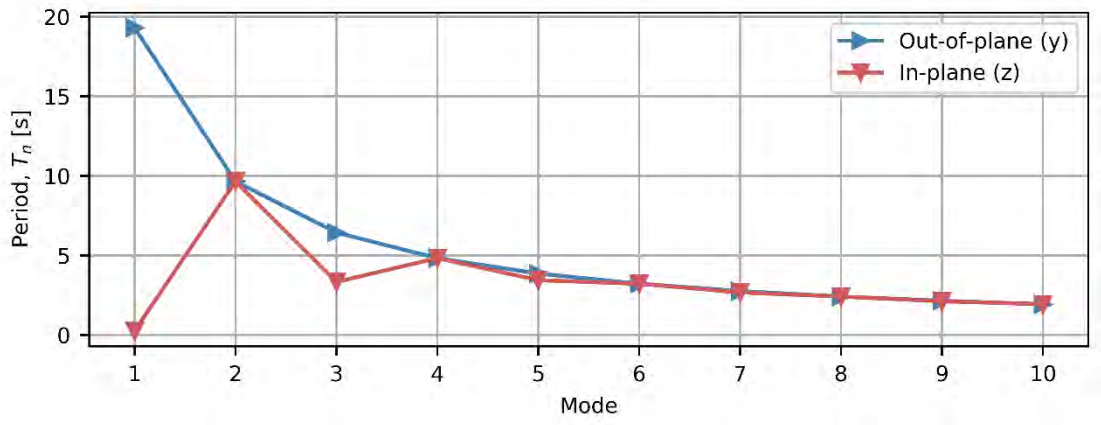

Figure 2-1. The natural periods of the first ten out-of-plane and in-plane modes.

2.2 Modal quadratic damping

The contribution from the drag forces on an infinitesimal segment of the mooring line can be described as follows:

$$df(x,t) = C_{quad} \cdot |\dot{u}(x)|\dot{u}(x)dx$$

By decomposing the response into vibration modes, $\dot{u}(x,t) = \psi(x)\dot{y}(t)$, this can be rewritten as follows:

$$\begin{aligned} df(x,t) &= f(x,t)dx \\ &= C_{quad} \cdot |\psi(x)\dot{y}(t)|\psi(x)\dot{y}(t)dx \\ &= C_{quad} \cdot |\psi(x)|\psi(x)dx \cdot |\dot{y}(t)|\dot{y}(t) \end{aligned} \quad (2)$$

Furthermore, the modal drag force can be established through:

$$f(t)^* = c_{quad}|\dot{y}|\dot{y} \quad (3)$$

This can be rewritten as follows:

$$\begin{aligned} f(t)^* &= \int_0^L f(x,t)\,\psi(x)dx \\ &= \int_0^L C_{quad}|\psi(x)|\psi(x)^2\,dx|\dot{y}|\dot{y} \end{aligned} \quad (4)$$

Finally, by comparing the Equations 3 and 4, the following expression is established for the modal quadratic damping coefficient:

$$c_{quad} = C_{quad}\int_0^L |\psi(x)^3|dx \quad (5)$$

The quadratic damping for the first 10 modes is depicted in Figure 2-2. The values correspond to a mode shape scaling with maximum displacement 1.

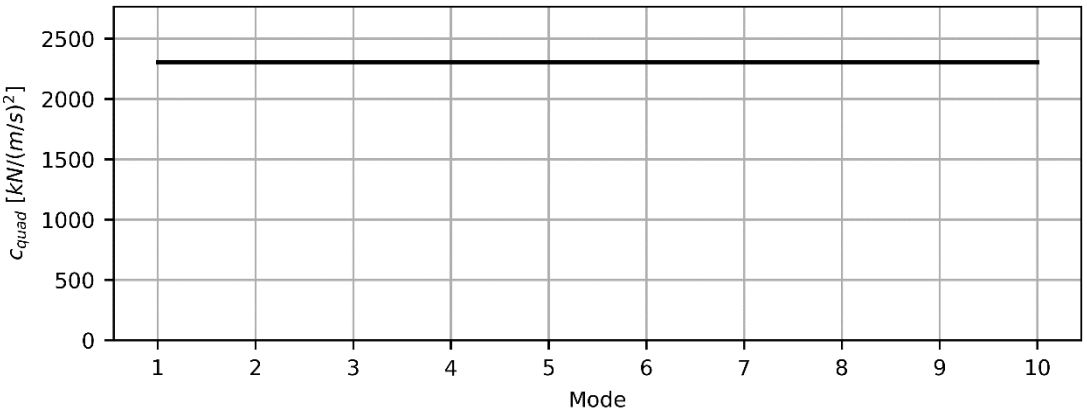

Figure 2-2. The quadratic damping is identical for all modes.

2.3 Critical ampltiude and terminal response

The modal parameter $\hat{k}_g$ was established based on the following expression:

$$k_g = \int_0^L \psi'(x)^2 \, N(x) dx$$

$$\hat{k}_g = \int_0^L \psi'(x)^2 \, dx, \qquad N(x) = 1$$

The critical amplitude of the 10 first modes, both out-of-plane and in-plane, were calculated based on the predicted ratios $k/\hat{k}_g$ and critical damping ratios for an assumed frequency ratio (excitation to mode) of 2.0. The results are depicted in Figure 2-3. The figure reveals very low critical amplitudes, such that parametric excitation is likely to be initiated by the applied axial forces acting on them. The consequence of the exceedance of the critical amplitude, by assuming a harmonic axial force equal the maximum dynamic value observed during the worst-case 10000-year condition, was assessed by the computation of the terminal response. The resulting terminal generalized response is given in Figure 2-4 for the first 10 modes (both in-plane and out-of-plane). The corresponding displacement along the cable is depicted in Figure 2-5 for modes 1–4.

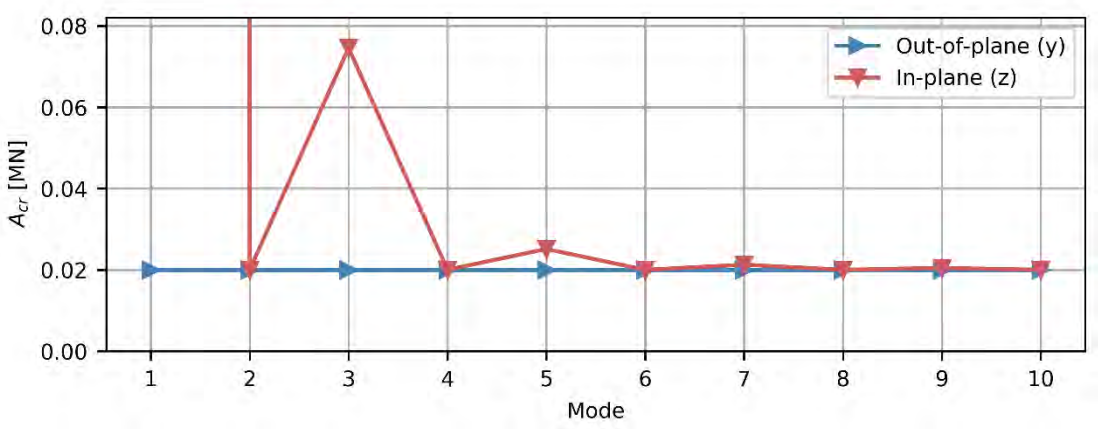

Figure 2-3. The critical axial force amplitude for all modes.

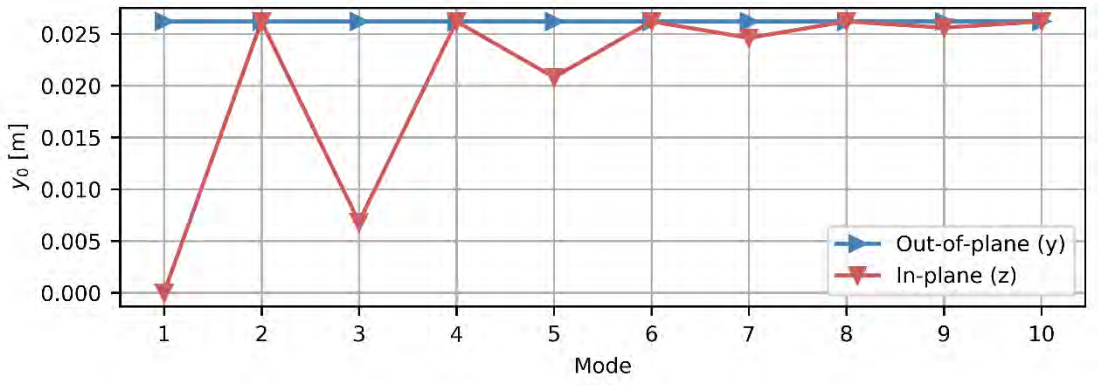

Figure 2-4. Generalized (modal) terminal response for modes 1–10 due to applied harmonic axial force of 2.0MN, with an assumed frequency ratio of 2.0 to all modes.

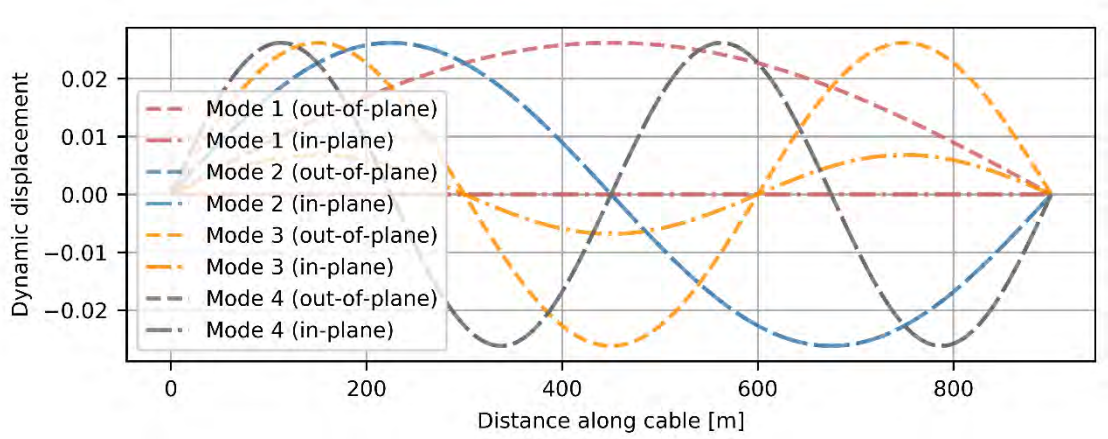

Figure 2-5. The physical displacements of modes 1–4 resulting from the generalized responses depicted in Figure 2-4.

3 Concluding remarks

The critical amplitude of the mooring cables is drastically exceeded, due to the low stiffness of the cables. However, due to the large quadratic damping, the resulting response, i.e., roughly 2.5 cm at most, is not deemed problematic.

4 References

[1] D. Cantero, A. Rønnquist og A. Naess, «Recent Studies of Parametrically Excited Mooring Cables for Submerged Floating Tunnels,» *Procedia Engineering,* pp. 99-106, 2016.

[2] D. Cantero, A. Rønnquist og A. Naess, «Tension during parametric excitation in submerged vertical taut tethers,» *Applied Ocean Research,* pp. 279-289, 2017.

[3] J. Macdonald, «Multi-modal vibration amplitudes of taut inclined cables due to direct and/or parametric excitation,» *Journal of Sound and Vibration,* pp. 473-494, 2016.

[4] J. Macdonald, M. Dietz, S. Neild, A. Gonzalez-Buelga, A. Crewe og D. Wagg, «Generalised modal stability of inclined cables subjected to support excitations,» *Journal of Sound and Vibration,* pp. 4515-4533, 2010.

[5] M. H. Patel og H. I. Park, «Dynamics of tension leg platform tethers at low tension. Part I-Mathieu stability at large parameters,» *Marine structures,* pp. 257-273, 1991.

[6] N. Perkins, «Modal interactions in the non-linear response of elastic cables under parametric/external excitation,» *International Journal of Non-Linear Mechanics,* pp. 233-250, 1992.

Concept development, floating bridge E39 Bjørnafjorden

Appendix S – Enclosure 6

10205546-11-NOT-189

Effect of static forces on K12

MEMO

PROJECT	Concept development, floating bridge E39 Bjørnafjorden	DOCUMENT CODE	10205546-11-NOT-189
CLIENT	Statens vegvesen	ACCESSIBILITY	Restricted
SUBJECT	Effect of static forces on K12	PROJECT MANAGER	Svein Erik Jakobsen
TO	Statens vegvesen	PREPARED BY	Knut Andreas Kvåle
COPY TO		RESPONSIBLE UNIT	AMC

SUMMARY

The effects on parametric excitation from static forces has thus far only been assessed in a preliminary manner, by comparing the amplitude of the static axial force with the ratio $k/\hat{k}_g$. To better evaluate the prioritized concept's robustness against the phenomenon, a more complete assessment is given herein.

0	15.08.2019	Final issue	K. A. Kvåle	R. M. Larssen	S. E. Jakobsen
REV.	DATE	DESCRIPTION	PREPARED BY	CHECKED BY	APPROVED BY

1 Introduction

By introducing relevant static forces in the finite element model, a new reference state is established, and a following modal analysis will reveal the effects of the static forces compared to a statically unloaded model. Only the effects on the girder due to current and static wind, corresponding to 100-year and 10000-year conditions, are considered. Effects due to temperature and due to the static displacement (offset) of the mooring lines are outside the scope of this assessment.

The following effects are considered to be relevant due to the effects of static forces:

1. Downward shift of natural frequencies due to the added negative geometric stiffness, implying that other modes might be relevant for parametric excitation. In principle, an upward shift due to tension forces should also be considered. However, due to the small effects observed on the natural frequencies, as seen in the next section, this is not considered.
2. Reduction of the ratio $k/\hat{k}_g$, directly leading to a reduction of the robustness against parametric excitation; A_{cr} is proportionally reduced.
3. Change of reference state or base configuration due to the deformation might change the system behaviour. This is an effect of the nonlinear behaviour of the structure, which is not considered herein. It might be wise to evaluate this effect in later stages of the project.

2 Effect on modal solution

The static analyses are based on the environmental parameters specified in Table 2-1. All static forces are applied to yield a net compression in the arch, i.e., are assumed to approach the bridge from east. The results from the modal analyses based on the static analyses are depicted in Figure 1, Figure 2, and Figure 3, for no static forces, static forces corresponding to the listed 100-year conditions, and static forces corresponding to the listed 10000-year conditions, respectively. Note that no aerodynamic contributions are considered, and the following does therefore not represent fully realistic scenarios. The figures indicate that the resulting natural frequencies and critical damping ratios are not highly affected by the applied static forces.

The effects on the ratio $k/\hat{k}_g$, damped natural circular frequency, critical axial force amplitude, critical damping ratio, and stiffness are shown for modes 1–10 in Figure 4, Figure 5, Figure 6, Figure 7, and Figure 8, respectively. The results, which are based on what is considered highly conservative assumptions, indicate that the critical amplitude is only slightly affected by the static forces (at most approximately 5% reduction for the critical mode 4). They also indicate that the reductions are direct consequences of the reduced values of the ratio $k/\hat{k}_g$, as the critical damping ratio is more or less unaffected by the static forces. Furthermore, as also indicated in Figure 1, Figure 2, and Figure 3, the damped natural frequencies are barely affected by the static forces (5% and 2.3% reduction of modes 3 and 4, respectively).

Table 2-1. Environmental conditions.

	Mean wind velocity	Current	Drag coefficient, C_d (including safety factor 2)
100-year conditions	29.6 m/s	1.76 m/s	0.8
10000-year conditions	35.9 m/s	1.85 m/s	0.8

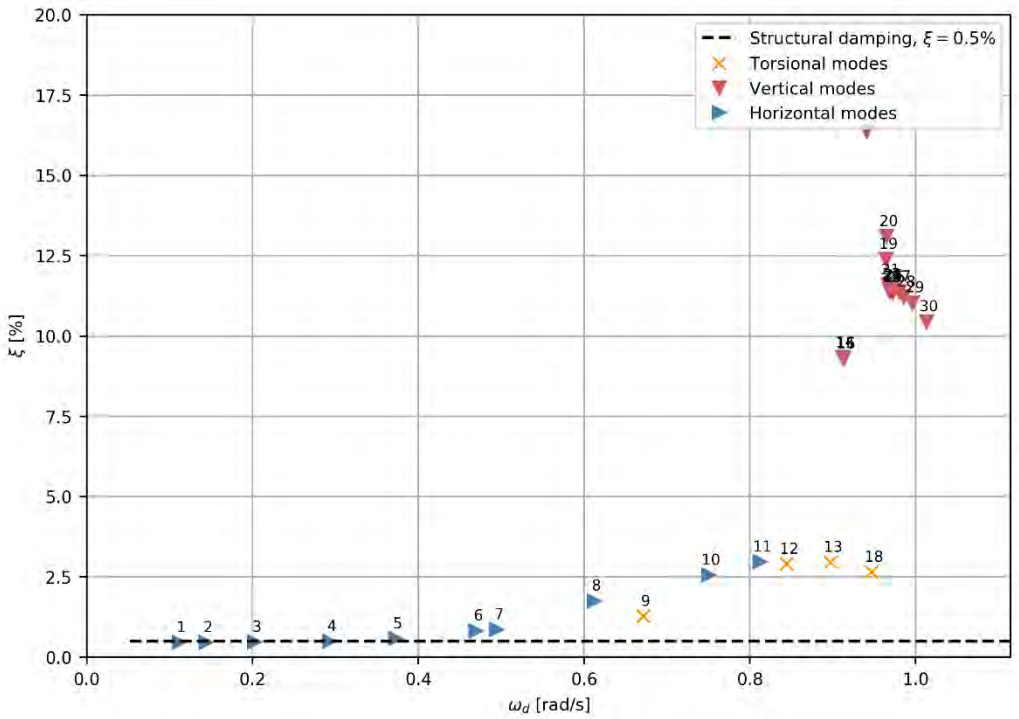

Figure 1. No static wind or current loads.

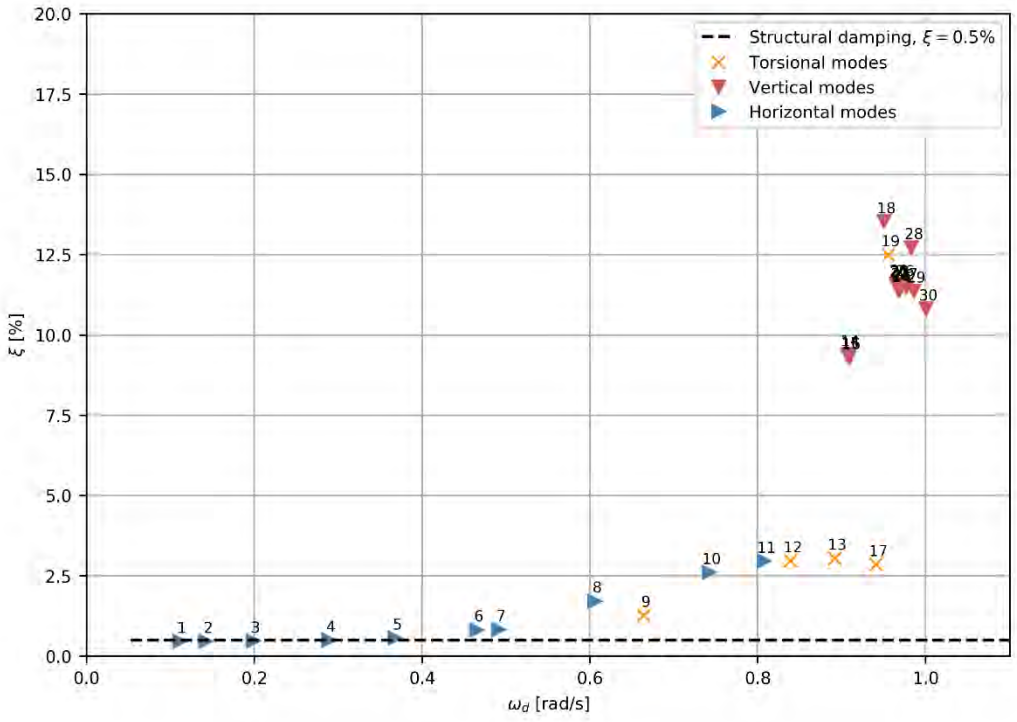

Figure 2. 100-year static wind or current loads from east.

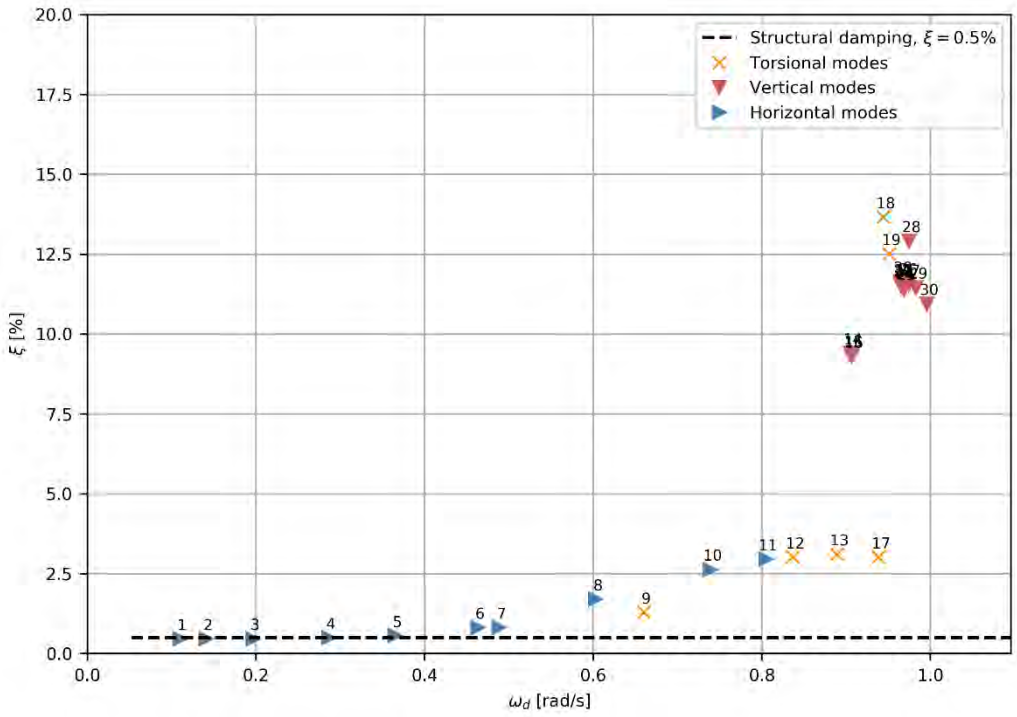

Figure 3. 10000-year static wind or current loads from east.

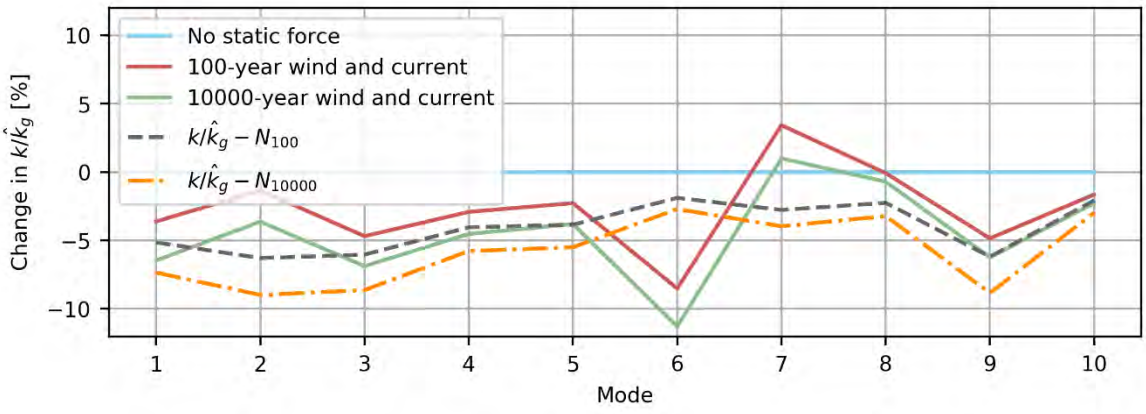

Figure 4. Effect on ratio $k/\hat{k}_g$ due to 100-year (100E) and 10000-year (10000E) static wind and current loads.

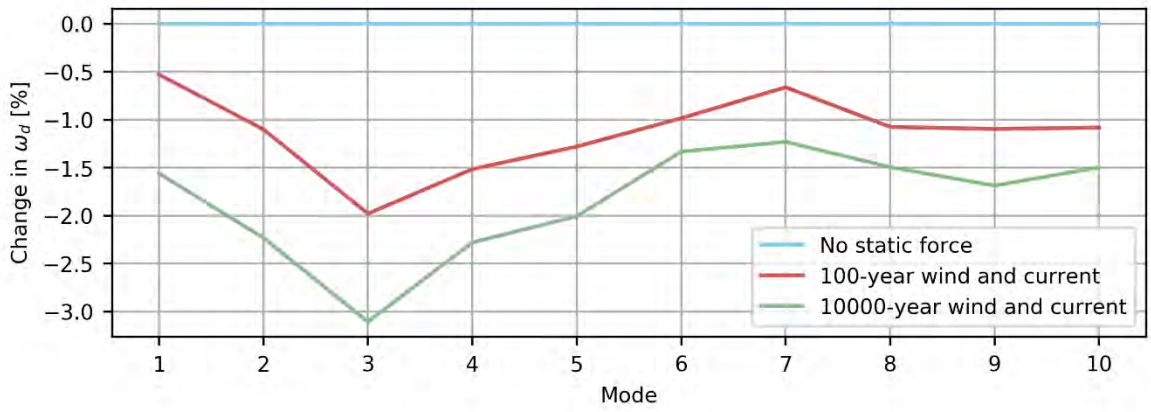

Figure 5. Effect on ratio ω_d due to 100-year (100E) and 10000-year (10000E) static wind and current loads.

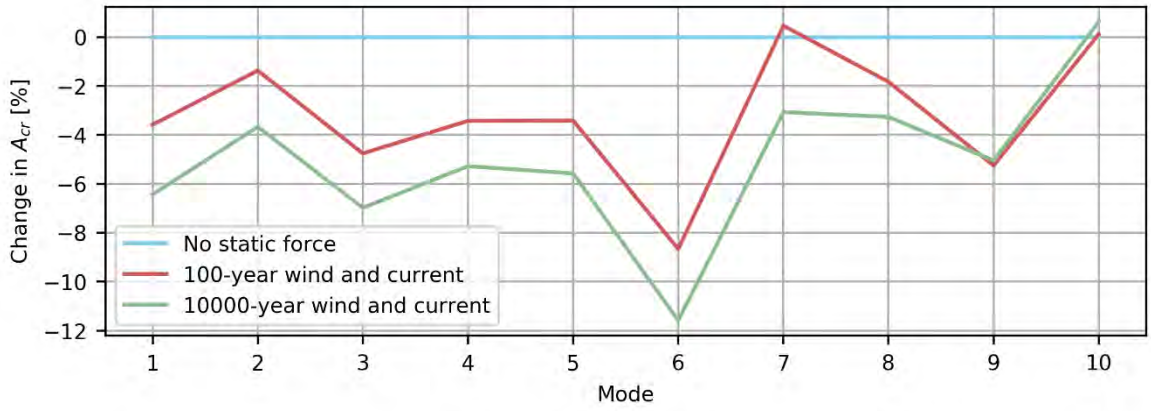

Figure 6. Effect on critical axial force amplitude A_{cr} due to 100-year (100E) and 10000-year (10000E) static wind and current loads.

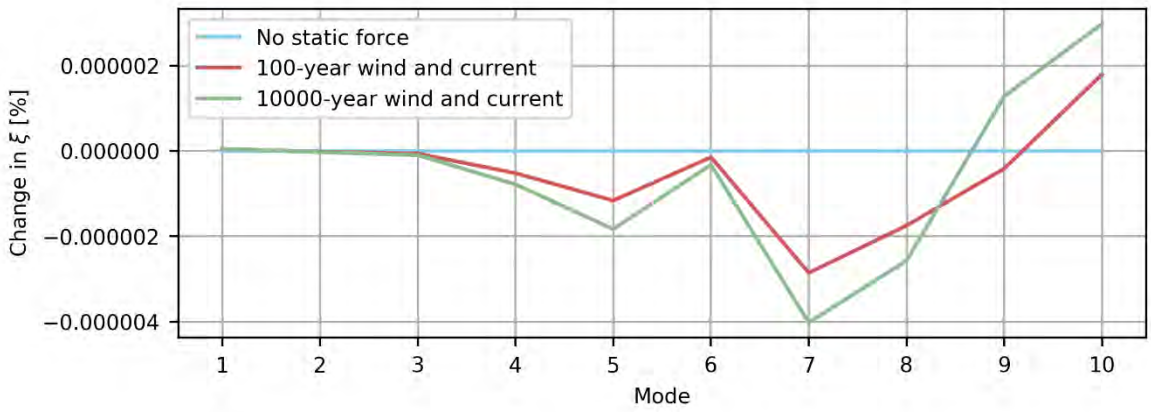

Figure 7. Only insignificant effects to critical damping ratios are observed due to the static loads.

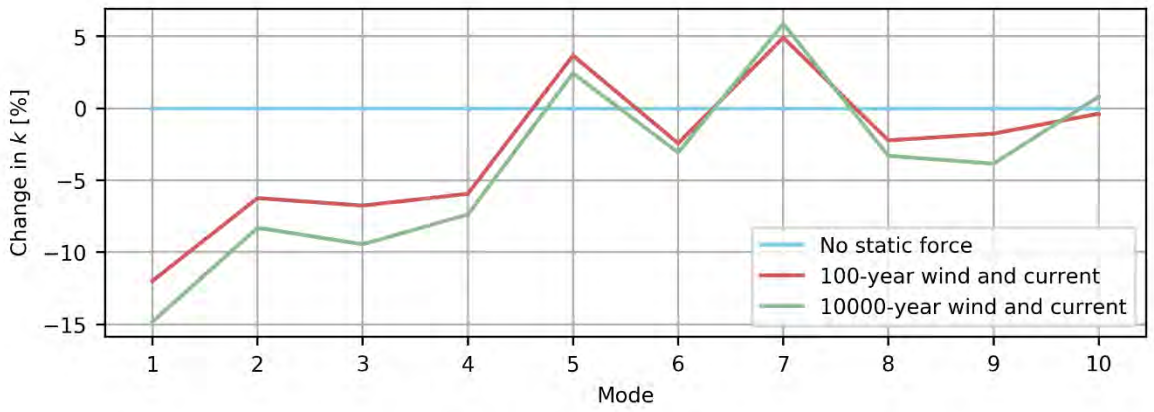

Figure 8. Change in stiffness due to static forces.

3 Concluding remarks

By applying static forces corresponding to 100-year and 10000-year mean wind and current, the effect on parametric excitation is studied. Based on conservative assumptions, the critical amplitude is only seen to be slightly affected by static forces: approximately 5% reduction for the critical mode 4. The reduction is a direct effect of the reduced ratio $k/\hat{k}_g$. Natural frequencies are also only barely affected by static forces.